

SINGLET MOLECULAR OXYGEN MEDIATED ELECTRONIC  
ENERGY TRANSFER

Dissertation for the Degree of Ph. D.  
MICHIGAN STATE UNIVERSITY  
REX DONAL KENNER  
1976



This is to certify that the

thesis entitled

SINGLET MOLECULAR OXYGEN MEDIATED ELECTRONIC

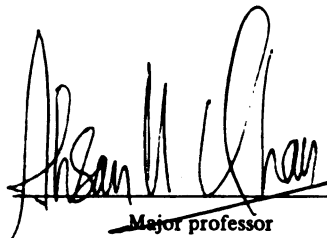
ENERGY TRANSFER

presented by

REX DONAL KENNER

has been accepted towards fulfillment  
of the requirements for

Ph. D. degree in Chemistry

  
Major professor

Date June 9, 1976



615117

## ABSTRACT

### SINGLET MOLECULAR OXYGEN MEDIATED ELECTRONIC ENERGY TRANSFER

By

Rex Donal Kenner

The reversible quenching of luminescence by molecular oxygen is a well known phenomenon. One system, 12:56 dibenzanthracene in an organic polymer matrix, has been reported to show an increased fluorescence in the presence of molecular oxygen. This observation was not explained. In this thesis, this system and a number of other aromatic hydrocarbons in several different polymer matrices are investigated. The amount of increase in the fluorescence in the presence of molecular oxygen is studied as a function of the organic molecule, pressure of oxygen, intensity of exciting radiation, and polymer matrix.

To provide a molecular basis for interpretation of the dependences observed for the oxygen enhancement of the fluorescence, the singlet oxygen feedback mechanism is proposed. This mechanism states: if the energetic requirements are met, electronic energy transfer from singlet molecular oxygen to the triplet state of the



acceptor molecule can generate the excited singlet state of the acceptor molecule.

Cross beam experiments were performed to determine the contribution of ground state depopulation to the oxygen enhanced fluorescence. The ground state depopulation in the absence of oxygen was determined by using triplet-triplet absorption and was compared to the amount of fluorescence enhancement observed under the same excitation conditions upon the addition of atmospheric air. It was found that the amount of fluorescence enhancement is much larger than the amount of ground state depopulation.

In a photostationary experiment, a number of processes contribute to the observed oxygen enhancement of fluorescence. These include ground state depopulation, the inner filter effect, reabsorption of the fluorescence by the triplet manifold of the organic acceptor molecule, intermolecular energy transfer to the triplet manifold, and the singlet oxygen feedback mechanism. The magnitudes of the processes not actively involving molecular oxygen is discussed but no quantitative conclusion is reached as to the relative importance of these processes and singlet oxygen feedback in a photostationary system.

The discovery of singlet oxygen-triplet organic molecule annihilation fluorescence produced by the singlet oxygen feedback mechanism is reported. It was found that the singlet oxygen feedback mechanism can lead to observable emission from the first excited singlet state of the organic acceptor for those molecules where the energy gap between the first excited singlet state and



the first triplet state is small enough, for example chrysene ( $S_1-T_1 = 7700 \text{ cm}^{-1}$ ) and 12:56 dibenzanthracene ( $S_1-T_1 = 7000 \text{ cm}^{-1}$ ). For pyrene ( $S_1-T_1 = 10000 \text{ cm}^{-1}$ ), the singlet oxygen feedback mechanism leads to a specific sensitization of the pyrene singlet excimer. For naphthalene ( $S_1-T_1 = 10900 \text{ cm}^{-1}$ ), the singlet oxygen feedback process leads to direct emission from the exciplex formed from naphthalene ( $T_1$ ) and molecular oxygen ( $^1\Delta_g$ ).

The theoretical analysis of the singlet oxygen feedback mechanism is reported. The "Golden Rule" formula was used to evaluate the rates of the intramolecular radiationless transitions in the molecular oxygen-organic molecule complex. It was found that the predicted rates are consistent with the observed singlet oxygen-triplet organic molecule annihilation fluorescence.

Nanosecond time resolved spectroscopy was used in an attempt to find the expected oxygen dependent fluorescence lifetime in a system equilibrated with oxygen. The systems investigated include biacetyl in the gas phase and solution, and aromatic hydrocarbons in polymer matrices. No evidence for the oxygen dependent fluorescence was found.

SINGLET MOLECULAR OXYGEN MEDIATED  
ELECTRONIC ENERGY TRANSFER

By

Rex Donald Kenner

A DISSERTATION

Submitted to  
Michigan State University  
in partial fulfillment of the requirements  
for the degree of

DOCTOR OF PHILOSOPHY

DEPARTMENT OF CHEMISTRY

1976

## ACKNOWLEDGMENTS

This writer would like to acknowledge the assistance, guidance, and encouragement of Dr. A. U. Khan, which is almost entirely responsible for the completion of this project.

In addition, this writer would like to acknowledge the financial assistance from The Research Corporation and Michigan State University Department of Chemistry.

## TABLE OF CONTENTS

	Page
LIST OF TABLES . . . . .	v
LIST OF FIGURES . . . . .	vii
 Chapter	
I. INTRODUCTION . . . . .	1
Rationale Behind Selection of the Topic . . . . .	1
Preview of Contents . . . . .	2
II. A SURVEY OF PERTINENT LITERATURE . . . . .	4
Introduction . . . . .	4
Spectroscopic Properties of Molecular Oxygen . . . . .	5
Simultaneous Transitions Involving Molecular Oxygen . . . . .	5
Environmental Interactions Affecting the Lifetime of Singlet Oxygen . . . . .	6
Methods for Generation of Singlet Molecular Oxygen . . . . .	9
Methods for Detection of Singlet Oxygen . . . . .	10
Photophysical Properties of Aromatic Molecules . . . . .	10
Photophysical Processes Involving Molecular Oxygen and Organic Molecules . . . . .	13
Intermolecular Electronic Energy Transfer . . . . .	14
Simultaneous Transitions Not Involving Molecular Oxygen . . . . .	15
Polymers as Rigid Matrices . . . . .	15
III. PHOTOSTATIONARY EXPERIMENTS CHARACTERIZING THE OXYGEN ENHANCED FLUORESCENCE . . . . .	17
Introduction . . . . .	17
Experimental . . . . .	18
General Observations of Oxygen Enhanced Fluorescence . . . . .	22
Pressure Studies . . . . .	28
Singlet Molecular Oxygen Feedback Mechanism . . . . .	31
Correlations of Observations with Predictions . . . . .	36
Microscopic Mechanism . . . . .	37

Chapter	Page
IV. A QUANTITATIVE COMPARISON OF GROUND STATE DEPOPULATION AND FLUORESCENCE ENHANCEMENT . . . . .	38
Introduction . . . . .	38
Experimental . . . . .	40
Results and Discussion . . . . .	43
V. FLUORESCENCE ENHANCEMENT NOT ACTIVELY INVOLVING MOLECULAR OXYGEN . . . . .	48
Introduction . . . . .	48
Processes Which Reduce the Fluorescence Intensity . . . . .	48
Simulated Quenching Experiments . . . . .	53
Interpretation of the Simulated Quenching Experiments . . . . .	56
VI. SINGLET OXYGEN-TRIPLET ORGANIC MOLECULE ANNIHILATION LUMINESCENCE . . . . .	61
Introduction . . . . .	61
Experimental . . . . .	62
Materials and Sample Preparation . . . . .	68
General Results . . . . .	69
Chrysene . . . . .	77
12:56 Dibenzanthracene . . . . .	82
12 Benzanthracene . . . . .	84
Pyrene . . . . .	91
Napthalene . . . . .	97
Other Molecules . . . . .	101
Discussion . . . . .	101
VII. THEORETICAL ANALYSIS OF THE SINGLET OXYGEN FEEDBACK MECHANISM . . . . .	103
Theoretical Approach . . . . .	103
Rates of the Singlet Oxygen Feedback . . . . .	106
Oxciplex Emission . . . . .	116
Conclusions . . . . .	116
VIII. SUMMARY . . . . .	118
APPENDIX . . . . .	122
BIBLIOGRAPHY . . . . .	128

## LIST OF TABLES

Table	Page
1. Spectroscopic Parameters (in $\text{cm}^{-1}$ ) for Some States of Molecular Oxygen . . . . .	5
2. Energies of Molecular Oxygen Double Molecule States . .	6
3. Rates of Quenching of Singlet Oxygen by Some Molecules of Interest . . . . .	8
4. Molecular Electronic Transition f-number Scale . . .	12
5. Characteristics of Some Energy Transfer Mechanisms . .	15
6. Simultaneous Transitions Not Involving Molecular Oxygen . . . . .	16
7. Solute Molecules and Polymer Matrices Investigated . .	21
8. Percent Fluorescence Increase for 0.1 M 12:56 Dibenanthracene in Various Polymers as a Function of the Relative Excitation Intensity . . . . .	27
9. Percent of Fluorescence Intensity Increase . . . . .	29
10. Comparison of the Amount of Ground State Depopulation to the Amount of Fluorescence Enhancement . . . .	44
11. % Fluorescence Enhancement as a Function of % Triplets for Chrysene $5 \times 10^{-3}$ M in Pst . . . . .	55
12. Relative Spectral Intensity as a Function of Experimental Conditions . . . . .	57
13. Summary of Results for Singlet Oxygen-Triplet Organic Molecule Annihilation Luminescence . . . . .	78
14. Electronic Matrix Elements for Processes Involving Oxygen and Alternant Aromatic Hydrocarbons . . . .	107
15. Coefficients of Atomic Orbitals in the Wavefunction of the Highest and Second Highest Bonding Molecular Orbitals . . . . .	108



Table	Page
16. Root-Mean Square Average of Terms in Atomic Orbital Coefficients for Aromatic Hydrocarbons of Interest . . .	111
17. Values of Electronic Matrix Elements and Franck-Condon Factors for Aromatic Hydrocarbons of Interest . . .	114
18. Rate of Intramolecular Radiationless Transitions Between the States of the Complex in $\text{sec}^{-1}$ . . . . .	115

## LIST OF FIGURES

Figure	Page
1. Unimolecular Photophysical Processes in Organic Molecules . . . . .	11
2. Usual Configuration of Equipment for Photostationary Oxygen Induced Fluorescence Enhancement Experiments . .	23
3. Emission Spectra for Chrysene in Polystyrene at Various Pressures, Showing Fluorescence Enhancement and Phosphorescence Quenching . . . . .	24
4. Plot of % Fluorescence Enhancement and % Phosphorescence Quenching as a Function of Log (Pressure of Air), for Chrysene $5 \times 10^{-3}$ M in Polystyrene . . . . .	30
5. Plot of % Fluorescence Enhancement and % Phosphorescence Quenching as a Function of Log (Pressure of Air), for Chrysene 0.01 M in Polystyrene . . . . .	32
6. Schematic Representation of the Singlet Molecular Oxygen Feedback Mechanism . . . . .	34
7. Schematic of Cross-Beam Apparatus: (A) Detection System, (B) Quartz Fiber Optics, (C) Opaque Cell Covering, (D) Sample, (E) Cell, (F) Excitation Source, Filter and Lens, (G) Mechanical Light Chopper, (H) Light Source for Absorption Measurements . . . . .	41
8. Triplet-Triplet Absorption Spectrum for Chrysene in Polystyrene at Room Temperature . . . . .	46
9. Apparatus for Simulated Quenching Experiments: (A) Detection System, (B) Phosphorescope, (C) Cell, (D) Sample, (E) Auxiliary Excitation Source and Filter, (F) Excitation Monochromator, (G) Main Excitation Source . . . . .	54
10. Apparatus for Detection of Singlet Oxygen-Triplet Organic Molecule Annihilation Fluorescence: Mechanical and Optical Systems . . . . .	63
11. Apparatus for Detection of Singlet Oxygen-Triplet Organic Molecule Annihilation Fluorescence: Vacuum System . . . . .	64

Figure	Page
12. Phosphorescence Decay and Oxygen Induced Fluorescence of Chrysene ( $10^{-2}\text{M}$ ) in Polystyrene Fluffs . . . . .	70
13. Total Emission Showing Oxygen Induced Fluorescence Burst for 12:56 DBA ( $10^{-2}\text{M}$ ) . . . . .	74
14. Plot of Log (Singlet Oxygen-Triplet Organic Molecule Annihilation Fluorescence Intensity) vs Log (Phosphorescence Intensity) for Chrysene- $\text{d}_{12}$ 0.01 M in Deuterated Polystyrene . . . . .	75
15. Electronic Energy Level Diagram for Chrysene, Including Possible Singlet Oxygen Feedback States . . . . .	79
16. Spectrum of Oxygen Induced Fluorescence of Chrysene $10^{-2}\text{M}$ in Polystyrene Fluffs . . . . .	80
17. Electronic Energy Level Diagram for 12:56 Dibenzanthracene, Including Possible Singlet Oxygen Feedback Complex States . . . . .	83
18. Spectrum of Oxygen Induced Fluorescence in 12:56 DBA $10^{-2}\text{M}$ in Polystyrene Fluffs . . . . .	85
19. Electronic Energy Level Diagram for 12 Benzanthracene, Including Possible Singlet Oxygen Feedback Complex States . . . . .	86
20. Fluorescence Spectrum of 12 Benzanthracene 0.01 M in Polystyrene . . . . .	87
21. Spectrum of Oxygen Induced Luminescence of Pyrene $10^{-2}\text{M}$ in Polystyrene Fluffs . . . . .	92
22. Spectrum of Oxygen Induced Luminescence for Pyrene $10^{-1}\text{M}$ in Polystyrene Fluffs . . . . .	93
23. Electronic Energy Level Diagram for Pyrene, Including Possible Singlet Oxygen Feedback Complex States . . . . .	95
24. Absorption and Emission Spectra of Napthalene ( $\text{T}_1$ ) - Molecular Oxygen ( $^1\Delta$ ) Oxciplex . . . . .	99
25. Electronic Energy Level Diagram for Napthalene, Including Possible Singlet Oxygen Feedback Complex States . . . . .	100
26. Molecular Oxygen - Organic Molecule Complex States . . . . .	104

## CHAPTER I

### INTRODUCTION

#### Rationale Behind Selection of the Topic

Reversible quenching of luminescence from organic molecules by molecular oxygen is a well known phenomenon. In most studies of molecular luminescence, efforts are made to exclude molecular oxygen to prevent this interference. It was therefore most unusual when it was reported that for 12:56 dibenzanthracene (DBA) in polymer matrices, the fluorescence intensity was reversibly increased in the presence of molecular oxygen, whereas the phosphorescence showed the normal quenching (138). 12:56 DBA shows the usual quenching in solution. The observed fluorescence increase in the polymer matrix was not explained.

The current investigation was undertaken to determine (i) the generality of the oxygen induced fluorescence increase and (ii) to explore possible mechanisms for its interpretation.

The singlet molecular oxygen feedback mechanism was proposed to provide a molecular basis for the explanation of the enhanced fluorescence. Due to the possible applications of mechanisms similar to singlet oxygen feedback to (i) chemiluminescence, (ii) photosynthesis, (iii) other biological systems, an investigation of the proposed singlet oxygen-triplet organic molecule annihilation step was undertaken.

### Preview of Contents

Chapter I is an introduction to this work. In Chapter II, pertinent background literature is discussed including (i) singlet molecular oxygen, (ii) photophysical properties of organic molecules and their interactions with oxygen, (iii) electronic energy transfer and simultaneous transitions, and (iv) the use of polymers as inert matrices for the study of the properties of organic guest molecules.

Chapter III presents the photostationary experiments investigating oxygen induced fluorescence enhancement. These experiments determine the occurrence of this phenomenon and its dependence on (i) the organic guest molecule, (ii) the polymer matrix, (iii) the excitation intensity, and (iv) the partial pressure of oxygen. The singlet molecular oxygen feedback mechanism is presented and its predictions are correlated with the experimental results.

Chapter IV describes experiments which quantitatively compare the amount of fluorescence enhancement observed with the triplet population in the evacuated sample to test the ground state depopulation mechanism. It is concluded that this trivial mechanism does not account for the observed oxygen induced fluorescence increase.

In Chapter V a number of mechanisms which reduce the guest fluorescence intensity in the presence of a high organic triplet population are presented. The magnitude of the enhancement caused by these mechanisms is then compared with the results of simulated triplet quenching experiments in the absence of molecular oxygen.

In Chapter VI, the discovery of singlet oxygen-triplet organic molecule annihilation fluorescence is reported. A study of this

luminescence for a number of guest molecules was conducted. The observation of singlet oxygen sensitization of latent excimers in pyrene and of oxiplex emission in naphthalene are reported.

Chapter VII presents a theoretical method which has been used to determine the rates of radiationless transitions. The results of the application of this method to the processes in feedback mechanism are presented.

Chapter VIII is a summary of this work.

## CHAPTER II

### A SURVEY OF PERTINENT LITERATURE

#### Introduction

Since molecular oxygen is intimately involved in all living processes, any interaction involving this molecule is of interest. To a great extent, the special nature of oxygen chemistry is due to the existence of two low lying electronically excited singlet states,  $^1\Delta_g$  and  $^1\Sigma_g^+$ . The long lifetimes and favorable energy dispositions of these two states give molecular oxygen a unique versatility. The range of phenomenon in which singlet molecular oxygen is involved or is suspected of involvement is large. These include (1) quenching of excited state molecules, (2) photo-oxidations, (3) some chemiluminescence reactions, (4) photodynamic effects, (5) photochemical smog generation, and (6) photocarcinogenicity.

In this chapter the literature pertinent to this investigation is briefly reviewed. The topics of interest include (1) spectroscopic properties of molecular oxygen, (2) the double molecule transitions involving molecular oxygen, (3) the effect of the environment on the lifetime of singlet oxygen, (4) methods of generation and (5) detection of singlet oxygen, (6) the photophysical properties of organic molecules and (7) their interactions with molecular oxygen, (8) intermolecular electronic energy transfer, and (9) polymers as inert matrices for the study of the properties of the guest molecule.

### Spectroscopic Properties of Molecular Oxygen

The electronic structure and spectra of molecular oxygen have been studied in detail (1-3). The spectroscopic properties of some of the states of molecular oxygen are summarized in Table 1. Of particular interest are the two low energy singlet states,  $^1\Delta_g$  and  $^1\Sigma_g^+$ .

TABLE 1.--Spectroscopic Parameters (in  $\text{cm}^{-1}$ ) for Some States of Molecular Oxygen.

State	$T_e$	$w_e$	$w_e x_e$	$v_{00}$	$\tau(\text{sec})$
X $^3\Sigma_g^-$	0	1580.36	12.07		
a $^1\Delta_g$	7918.1	1509	12	7882.3	3876 (4,5)
b $^1\Sigma_g^+$	13195.2	1432.69	13.95	13120.95	6.9(6,7) 11.8(8)
A $^3\Sigma_g^+$	36096	819	22.5		
B $^3\Sigma_g^-$	49802.1	700.36	8.002		

### Simultaneous Transitions Involving Molecular Oxygen

Simultaneous transitions as a one photon two molecule process were first invoked as an idea by Ellis and Kneser in the interpretation of liquid oxygen absorption spectra (9). They may be described as a transition for a pair of atomic or molecular species to an algebraically additive composite state. The simultaneous transitions for molecular oxygen have been observed in absorption of high pressure gaseous oxygen (10-15), solutions under high



pressure oxygen (16,17), and in emission in gas discharge and chemiluminescent systems (10,18-21). The various transitions and their energies are given in Table 2.

TABLE 2.--Energies of Molecular Oxygen Double Molecule States.

Complex State	$\nu_{00}$ in Å
$(^1\Delta_g, ^3\Sigma_g^-)$	12700
$(^1\Sigma_g^+, ^3\Sigma_g^-)$	7620
$(^1\Delta_g, ^1\Delta_g)$	6334
$(^1\Delta_g, ^1\Sigma_g^+)$	4773
$(^1\Sigma_g^+, ^1\Sigma_g^+)$	3612

A theoretical treatment of these transitions and the collisionally induced single molecule transitions have been given by Robinson (22), Rettschnick and Hoytink (23), Krishna (24,25), and others (26,27). They have shown that the forbidden single molecule transitions can acquire enhanced transition probability in the collision complex by borrowing intensity from an allowed transition usually assumed to be the Schuman-Runge band system. The borrowing is made possible by the electron exchange between the two oxygen molecules during the collision.

#### Environmental Interactions Affecting the Lifetime of Singlet Oxygen

Introduction: Since the radiative lifetimes of the two lowest singlet states of molecular oxygen are extremely long, the

observed lifetimes are controlled by the rates of non-radiative quenching processes and consequently considerable effort has been put into determining these quenching rate constants (28-33).

Gas Phase: The rate constants for the quenching of  $^1\Sigma$  by inert (physical) quenchers is often three or four orders of magnitude larger than for quenching  $^1\Delta$ . See Table 3 for a list of rate constants for molecules of interest in this work. For a more comprehensive list see D. R. Kearns (232).

The deactivation of vibrationally excited singlet oxygen has been investigated (35,39,40) and it is found that the deactivation of oxygen in the first vibrationally excited level of the  $^1\Delta$  state is slower than that of the zero vibrational level (35).

Condensed Phases: If the gas phase rate constants are used to estimate the predicted lifetime of singlet oxygen in solution, values of  $10^{-11}$  seconds for  $^1\Sigma$  and  $2 \times 10^{-5}$  seconds for  $^1\Delta$  are obtained (232). There have been a number of indirect determinations of the lifetime of  $^1\Delta$  in solution using chemical detection techniques (41-45). It is found that the lifetime is solvent dependent (46-48) and a semi-empirical equation has been derived to predict the lifetime of  $^1\Delta$  in solution from the intensities of near I.R. absorption (37,38).

In addition to quenching of singlet oxygen by the solvent, quenching by a number of solutes has been investigated, including amino acids and proteins (49), organic solutes (50-53), and metal chelates (36,54). Much attention has been paid to the quenching of  $^1\Delta$  by carotenoids, especially beta-carotene (36,41,55-57).

TABLE 3.--Rates of Quenching of Singlet Oxygen by Some Molecules of Interest.

Quencher	$^1\Sigma_g^+$ ( $1\text{ m}^{-1}\text{s}^{-1}$ )	$^1\Delta_g$ ( $1\text{ m}^{-1}\text{s}^{-1}$ )	Reference
$\text{N}_2$	$1.2 \times 10^6$		28-30, 32
		$6.0 \times 10$	31
$\text{O}_2$	$9 \times 10^4$		28-30, 32
		$1.4 \times 10^3 (v=0)$	31
		$5 \times 10^2 (v=1)$	35
$\text{H}_2\text{O}$	$2 \times 10^9$		32, 33
		$9 \times 10^3$	31
$\text{CO}_2$	$1.8 \times 10^8$		28, 30, 32
		$2.3 \times 10^3$	31
Napthalene (triplet		$9 \times 10^{10}$	34
Beta carotene		$1.3 \times 10^{10}$	in benzene, 36
Polystyrene- $\text{h}_8$		$4 \times 10^{-5}\text{sec}$	lifetime estimated using equation of
Polystyrene- $\text{d}_8$		$2 \times 10^{-5}\text{sec}$	Merkel, <u>et al.</u> , 37, 38

Beta-carotene quenches by energy transfer (36) and may be important in protecting biological systems from the effects of singlet oxygen (41).

### Methods for Generation of Singlet Molecular Oxygen

The techniques used to generate singlet molecular oxygen can be classified as either physical or chemical methods.

1. Physical methods: (a) direct optical excitation, Two sources have been used extensively for the direct optical excitation of singlet molecular oxygen; (i) He-Ne laser (6328 Å) which excites the 0,0 transition of  $2(^3\Sigma) \rightarrow 2(^1\Delta)$  (58), and (ii) Nd(YAG) laser (1.065 microns) which excites  $^3\Sigma_{v=0} \rightarrow ^1\Delta_{v=1}$  (1.067 microns) (35,39, 40,49,50,59).

(b) Energy Transfer, the singlet states of molecular oxygen can be formed by energy from a variety of species, organic triplet states (60-64), excited singlet states (65), inorganic molecules (66,67), and atomic species (68).

(c) Gas Discharge, Radiofrequency discharge tubes have been used extensively to generate singlet oxygen (69,70).

2. Chemical Methods: In addition to physical techniques, various chemical techniques are available for the generation of singlet oxygen. These include decomposition of hydrogen peroxide (20,21,71,72), ozonides (73-75), endoperoxides (76,77), superoxide ion (78,79), potassium perchromate (80,81), basic hydrolysis of peroxyacetylnitrates (82), and enzymatic reactions (83-85).

### Methods for Detection of Singlet Oxygen

One of the central problems in singlet oxygen research is the difficulty in the detection of the singlet molecular oxygen. A number of techniques have been used. For the gas phase the methods used include: emission spectroscopy (20,62,86,87), paramagnetic resonance spectroscopy (64,88-90), photoionization and mass spectroscopy (66,91-95), and calorimetry (20,96,97). In condensed phases it is usually necessary to use chemical methods for detecting singlet oxygen (42,46,98-100). These methods should be used with caution (232). For a discussion of the above techniques and the difficulties associated with each see the review by R. P. Wayne (230).

A new technique which combines the specificity of chemical techniques with the sensitivity of optical detection has been recently reported (233).

### Photophysical Properties of Aromatic Molecules (215-226)

The discussion here will be limited to those aspects of the photophysical properties of aromatic hydrocarbons which are considered important in the current investigation. The low lying states of the aromatic hydrocarbons can be described by considering only the  $\pi$  electron system (101). The lowest transitions usually involve the transfer of an electron from a  $\pi$ -bonding to a  $\pi$ -antibonding orbital (102). The transitions of interest are summarized in Figure 1. The approximate rates of the optical transitions for  $\pi \rightarrow \pi^*$  and  $n \rightarrow \pi^*$  transitions are summarized in Table 4.

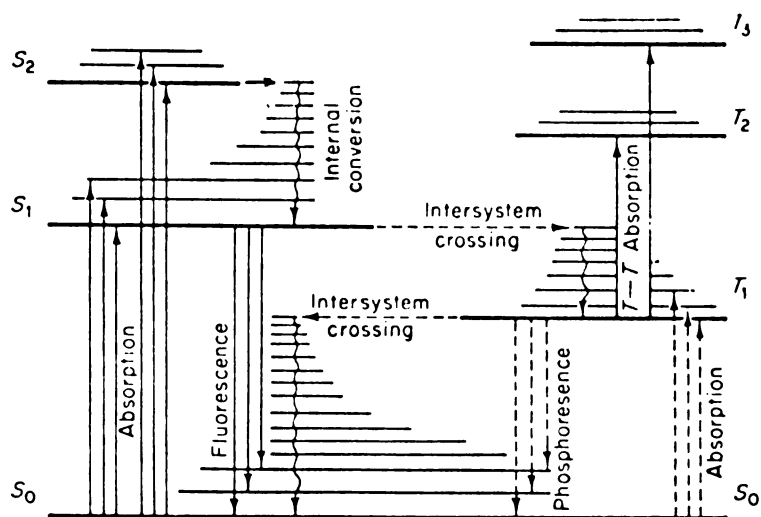


**Figure 1.--Unimolecular Photophysical Processes in Organic Molecules.** Solid lines are spin-allowed transitions; dashed lines are spin forbidden transitions; wavy lines are vibrational relaxation. (Adapted from S. P. McGlynn, T. Azumi, and M. Kinoshito, "Molecular Spectroscopy of the Triplet State," Prentice-Hall, Englewood Cliffs, N.J., 1969, p. 2.

TABLE 4.--Molecular Electronic Transition f-number Scale (103).

$\log \epsilon_{\max}$	$\log f$	$\log \tau_0$	$\pi - \pi^*$	$n - \pi^*$
singlet-singlet				
5	0	-9	allowed	
		-8		
4	-1	-7	forbidden	allowed
		-6		
2	-3	-5		forbidden
1	-4	-4		
singlet-triplet				
0	-5	-3		allowed
-1	-6	-2	allowed	
-2	-7	-1		forbidden
-3	-8	0	forbidden	
-4	-9	1		

\* Adapted from M. Kasha, Proc. International Conf. on Lumin. (1966), p. 167.

The  $\pi$ -electronic states of aromatic hydrocarbons can be classified using the perimeter free electron orbital model (PFE0) introduced by Platt (101). The lowest excited singlet state for the aromatic hydrocarbons are either  $^1L_a$  or  $^1L_b$  and transitions to these states from the ground state ( $^1A$ ) are symmetry forbidden (218). This reduces the intensity of the absorption to these states by a factor of 10 for  $^1L_a$  and  $10^2 - 10^3$  for  $^1L_b$  (104).

The bimolecular processes of interest are not included in Figure 1 for simplification. The interaction of an excited molecule and a ground state molecule can lead to the formation of a complex. These complexes are usually dissociative in the ground state and are called excimers (105,106). The interaction of two molecules in their excited triplet states can lead to energy transfer and P-type delayed fluorescence (triplet-triplet annihilation fluorescence) (107,108). In addition there are a number of bimolecular process involving molecular oxygen which are presented in the next section.

#### Photophysical Processes Involving Molecular Oxygen and Organic Molecules

The interactions between molecular oxygen and organic molecules can be divided into several groups depending on the photophysical process being affected and the initial state of molecular oxygen involved. The observed effects involving ground state oxygen include the following:

1. Contact charge transfer absorption (109,110)
2. Enhanced  $S_0 - T_1$  absorption (109,111-113)



3. Cooperative absorption (simultaneous transitions) (114-116)
4. Fluorescence quenching (215-217)
5. Phosphorescence quenching (215-217).

Those processes involving singlet molecular oxygen include:

6. Sensitized emission (18,71,117,118)
7. Singlet oxygen-triplet organic molecule annihilation luminescence (119,120)
8. Cooperative emission (this work).

#### Intermolecular Electronic Energy Transfer (221,222,234-236)

The mechanisms for transfer of electronic energy from one molecule to another can be classified as either (1) radiative or (2) non-radiative. Radiative energy transfer is a two step process involving the emission and subsequent absorption of a photon. This mechanism has been referred to as the trivial mechanism (121,122).

The non-radiative mechanisms can be further subdivided depending on the type of interaction between the molecules. At distances greater than molecular diameters the coupling is through the interaction of the electric dipoles and spectral overlap of the emission and absorption spectra of the donor and acceptor is required (123). This is referred to as Forster or dipole-dipole resonance transfer (234,236).

At very small intermolecular distances the orbitals of the two molecules begin to overlap and the electron exchange

interaction is important (124,125). The characteristics of each of these mechanisms is summarized in Table 5.

TABLE 5.--Characteristics of Some Energy Transfer Mechanisms.\*

	Radiative	Foster	Collisional
Increasing viscosity	No effect	Slightly decreased	Decreased
Donor lifetime	Unchanged	Decreased	Decreased
Donor emission spectrum	Changed	Unchanged	Unchanged
Donor absorption spectrum	Unchanged	Unchanged	Unchanged
Increasing volume	Increased	No effect	No effect

\* Adapted from A. A. Lamola in "Energy Transfer and Organic Photochemistry, Vol. XIV, Techniques of Organic Chemistry" (A. Weissberger, ed.) p. 17, Wiley, New York, 1969.

#### Simultaneous Transitions Not Involving Molecular Oxygen

Some systems not involving molecular oxygen for which simultaneous transitions have been observed are listed in Table 6. A general theory for the simultaneous absorption of light by neighboring ions in a crystal has been presented by Dexter (126).

#### Polymers as Rigid Matrices

Organic polymers have been used as rigid matrices in a number of studies. It is assumed that the polymer electronic states do not interact with those of the solute but this may not always be true (134). Polymers have been used for luminescence

TABLE 6.--Simultaneous Transitions Not Involving Molecular Oxygen.

Energy Type	Example	Comment and Reference
vibration-rotation	$\text{H}_2 + \text{CO}$ $\text{H}_2$	127 130
vibration-vibration	$\text{CO}_2 + (\text{N}_2, \text{O}_2, \text{ or } \text{H}_2)$  $\text{CS}_2 + (\text{I}_2, \text{Br}_2)$	high pressure gas absorption 128 liquid absorption, 129
electronic-electronic	$\text{Pr}^{+3} + \text{Pr}^{+3}$    $\text{YbPO}_4$	in $\text{LaCl}_3$ crystal, excitation spectrum 131 in solution, absorption 132  powdered, emission 133

studies (135-140), especially as a function of temperature (134, 141-143) and/or pressure (144-146). The interaction of the solute and the matrix has been investigated using electron spin resonance spectroscopy (147). Bimolecular processes including excimer formation (134,148-150) and electronic energy transfer (134,151-157) have been studied. Oxygen diffusion (136,138,158) and photochemical reactions (159) in polymers have been reported. Polymer supported substrates have also been used for the generation (160) and detection of singlet molecular oxygen (233).

## CHAPTER III

### PHOTOSTATIONARY EXPERIMENTS CHARACTERIZING THE OXYGEN ENHANCED FLUORESCENCE

#### Introduction

Reversible quenching of luminescence by molecular oxygen is well documented. Phosphorescence quenching is complete in the presence of even small concentrations of oxygen; whereas fluorescence intensity is generally only relatively reduced (215-217). In 1968 Geacintov et al., using 12:56 dibenzanthracene (DBA) dissolved in a polyvinyl acetate matrix, reported a 10% increase of fluorescence from the film when equilibrated in air as compared to the evacuated system (138). This fluorescence enhancement is particularly striking because on admission of air the phosphorescence exhibits normal quenching, and 12:56 DBA in fluid solvents exhibits the normal quenching of fluorescence and phosphorescence by molecular oxygen.

A number of solutes dissolved in each of several different polymer matrices have been investigated to establish the generality of the oxygen enhanced fluorescence and to explore possible mechanisms to explain these observations. A careful study of the amount of fluorescence enhancement for a given solute-polymer system as a function of partial pressure of oxygen was also undertaken.

In this chapter, the method used to determine the fluorescence enhancement is described. The results of the experiments

are then discussed and finally the singlet molecular oxygen feedback mechanism is presented.

### Experimental

An accurate measurement of both intensity and spectral features of the emission as a function of the partial pressure of oxygen constitute the goal of these experiments. In order to quantitatively compare the results of measurements at different pressures, a method of normalization with respect to the excitation intensity is necessary. The instrument used in these experiments permitted the spectrum recorded at different pressures to be stored in the memory of a signal averaging computer which enables one to normalize, subtract and integrate the spectra.

The apparatus used consisted of a Warner and Swasey Model 501 Rapid Scanning Spectrometer with a Fabritek Model 1072 Instrument computer. The model 501 has a double-pass Czerny-Turner monochromator with a set of rotating corner mirrors which cause the spectrum to be scanned passed the exit slits at selectable speeds between 1.25 and 125 milliseconds per scan (161). Only the slowest speed was used which allowed eight spectra per second to be collected and averaged in the computer. The model 501 is fitted with dual detectors, each recording half the spectrum which allows the photomultipliers to be selected to give the maximum spectral sensitivity. For most of the work reported here, an RCA 1-P28HV (a selected 1-P28) was used in the spectral region from 200-400 nm, and an RCA 4473 was used in the 400-600 nm region. A dual input

analog to digital converter was used in conjunction with the computer, one input for each photomultiplier.

The collection optics of the model 501 are Cassegrainian spherical mirrors which allows the sample to be viewed at distances of ten centimeters to infinity from the monochromator. This allowed the sample to be connected to a vacuum line at a distance during the experiments so that the pressure in the cell could be varied without altering the position of the sample with respect to the excitation and the detection optics.

For a typical experiment, the cell containing the sample was connected to the vacuum line and evacuated. The position and focus of the model 501 and the excitation source were then optimized to (i) maximize the observed luminescence intensity and (ii) to adjust the detected intensity of the scattered light to be comparable to the luminescence intensity. Both the emission spectrum and the scattered exciting light peak were collected by averaging a known number of scans, usually 1024. The spectrum was automatically stored in the memory of the computer.

The pressure in the cell was then increased and another spectrum collected and stored in the memory of the signal averager. The relative intensity of the two stored spectra could be changed and was adjusted until the integrated intensity of the two scattered light peaks were equal. It was assumed that the fraction of the exciting light detected as scattered light remains constant throughout the experiment and therefore the differences between the normalized spectra are not due to changes in the excitation intensity. The

evacuated spectrum was subtracted from the higher pressure one which leaves an increased intensity with pressure as positive and a decreased intensity as negative. The evacuated spectrum and the difference spectrum were plotted with the aid of an X-Y recorder and digitally integrated. From the height of the integration curve, the relative areas could be found and the change in the fluorescence expressed as a percent change with respect to the integrated evacuated intensity.

Many different combinations of excitation sources and filters were used but the usual one was a 75 watt xenon lamp (PEK) with a 340 nm interference filter. It is important that the scattered exciting radiation not have a significant spectral overlap with the fluorescence since the normalization procedure then becomes very uncertain.

The samples used in these experiments were organic solutes in thin polymer films. The solutes and polymers used are listed in Table 7. The films were prepared by the solvent casting technique (138) which involved dissolving the appropriate amount of the polymer in a small amount of an appropriate solvent and adding the required amount of the solute. The solution was then poured into a casting dish which was floated on mercury and evaporated slowly to dryness. The film was left adhering to the bottom of the casting dish and was removed by floating it with distilled water. Some problems were encountered with the polyvinyl acetate films which tended to soften in the water and become sticky. Polystyrene was the easiest to work with and was by far the most frequently used matrix in these experiments.

TABLE 7.--Solute Molecules and Polymer Matrices Investigated.

Solute Molecules	Matrices
Napthalene	Polystyrene (Pst)
Anthracene	Polyvinyl Acetate (Pvac)
12 Benzanthracene	Polyvinyl Chloride (Pvc)
34 Benzpyrene	Polycarbonate (Pc)
Phenanthrene	Polymethylmethacrylate (Pmma)
Chrysene	
12:34 Dibenanthracene	
Fluoranthene	
12:56 Dibenanthracene	
Benzophenone	

Once the film was removed from the casting dish, it was dried with paper towels and placed in a vacuum desiccator and kept under vacuum for two or three days to remove all traces of the solvent. The solvent must be completely removed from the film to prevent noticable photodecomposition during the excitation periods used in these experiments. In a properly dried sample there was no noticable decomposition and the same film could be reused many times. The final films were usually stored in the dark and pieces of the films could be cut and used as needed.

The concentration of the solutes in the films in this work is reported in moles of solute per liter of polymer assuming a density of 1.1 grams per milliliter for all the polymers.

The amount of light scattered from the surface of the films was large and the samples were light and easily moved by the pressure



gradients involved in changing the pressure in the cell. A triangular cell was designed to minimize these problems. The sample film was cut to fit the wide face of the triangular cell and was held in place by the back faces. The cell was connected to the vacuum line by a ground glass joint so it could be demounted to load the sample. The backside excitation configuration was found to reduce the scattered light peak to an intensity comparable to that of the fluorescence. The normal configuration of the instrumentation and the cell is shown in Figure 2. The cell is not shown to scale.

Most of the solutes used in this research were obtained from Aldrich Chemical Company and were used as received except as indicated below. Chrysene, Aldrich, vacuum sublimed; 12:56 DBA, Aldrich, recrystallized from glacial acetic acid; 12:34 DBA and 34 Benzpyrene, Nutritional Biochemicals, used as received; and benzophenone, Baker, recrystallized from cyclohexane. The polymers were obtained from the Polyscience Company and were purified as indicated by Geacintov, et al. (138).

#### General Observations of Oxygen Enhanced Fluorescence

The results of a typical experiment described in the last section for chrysene 0.01 M in polystyrene is shown in Figure 3. The bottom trace is the emission of the evacuated sample. The trace is in two parts, one from each photomultiplier and the two overlap somewhat in the middle as indicated by the wavelength scale. The longer wavelength spectrum is recorded at a much higher

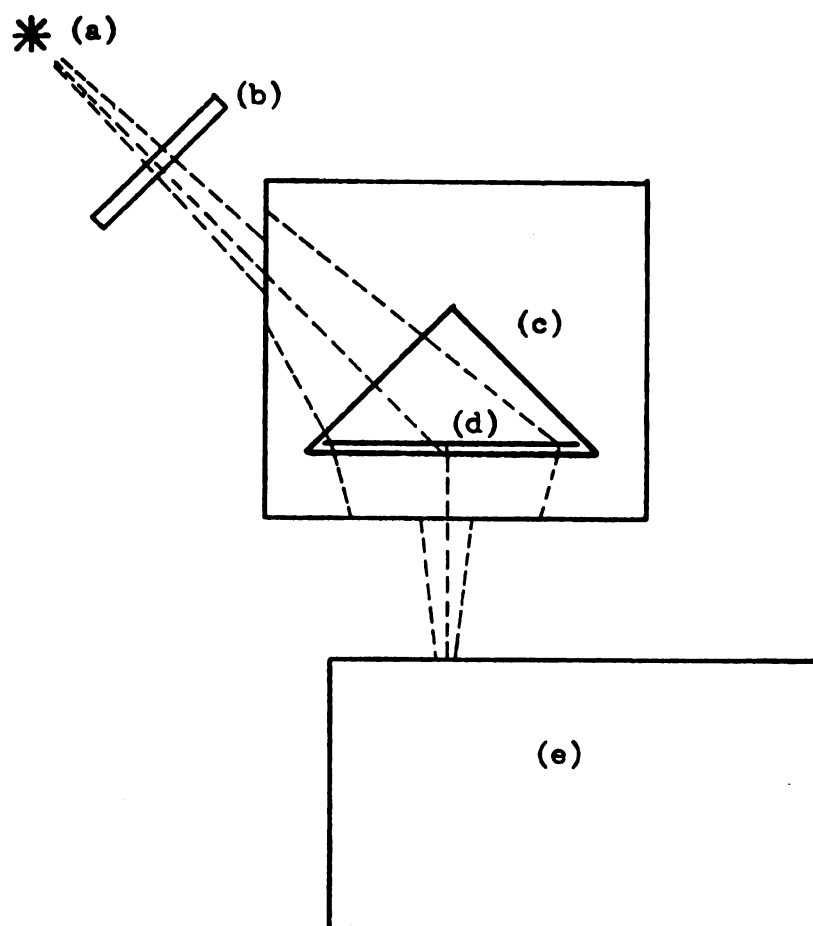


Figure 2.--Usual configuration of equipment for photostationary oxygen induced fluorescence enhancement experiments. (a) excitation source, (b) filter, (c) triangular quartz cell, (d) sample, (e) detection monochromator.

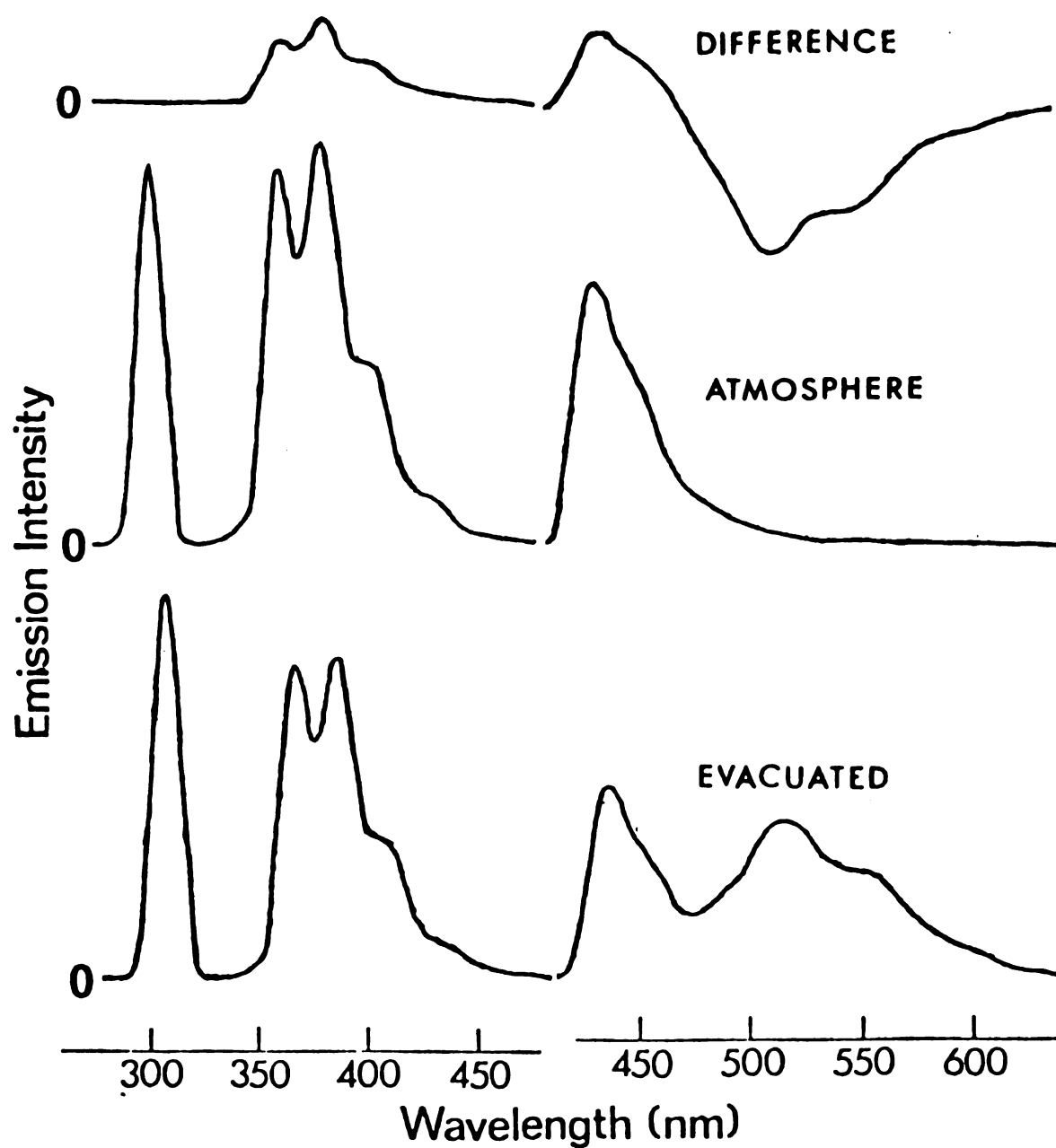


Figure 3.--Emission spectra for chrysene in polystyrene at various pressures, showing fluorescence enhancement and phosphorescence quenching.

sensitivity and the apparent peak at 450 nm is a repeat of the tail of the fluorescence shown in the short wavelength spectrum. A glass cut-off filter is used in front of the long wavelength photomultiplier to prevent the observation of the second order spectrum. This cut-off filter is the cause of the sharp rise at the beginning of the long wavelength spectrum.

The peak at about 330 nm is the scattered exciting radiation. The structured band between 360 and 450 nm is the chrysene fluorescence and the band at 500 nm is the chrysene phosphorescence.

The pair of spectra in the middle trace are the sample luminescence in atmospheric pressure of air. These spectra are normalized to match the area of the scattered light peak under atmospheric conditions to the scattered light peak of the evacuated sample. Qualitatively one can easily see that the intensity of the fluorescence has increased while the intensity of the phosphorescence has decreased.

The difference spectrum was obtained and clearly shows the increase in the fluorescence region and the decrease in the phosphorescence region. The enhanced fluorescence spectrum shows the same vibrational structure as the prompt fluorescence but a somewhat different Franck-Condon envelope. More will be said about this later. The integration of the evacuated and the difference spectra gives a value of thirty percent for the amount of fluorescence enhancement with complete quenching of the phosphorescence.

Listed in Table 7 are the solute molecules which have been tested to determine whether they show the oxygen induced fluorescence

enhancement. Each has been tested in one or more of the polymer matrices listed. It was observed that under the appropriate experimental conditions each of the samples could exhibit the effect except benzophenone which has an extremely low fluorescence efficiency. The requirements for observation of the oxygen induced fluorescence enhancement are that (i) the molecule have a fluorescing state, (ii) the excitation source have a high enough intensity and (iii) oxygen is able to diffuse into the matrix.

The measured value for the fluorescence enhancement is given by:

$$\% F = (F_p - F_0)/F_0 \times 100$$

where  $F_0$  and  $F_p$  are the fluorescence intensities for the evacuated sample and the sample at a higher pressure, respectively. This value depends on a large number of experimental variables. These include (1) the excitation intensity, (2) the wavelength of excitation, (3) the relative positions of the excitation systems, (4) the partial pressure of oxygen and (5) the polymer matrix used.

1. Excitation intensity: The amount of fluorescence enhancement measured for a given sample increases with increasing excitation intensity. A list of the percent fluorescence enhancement versus the relative excitation intensity for 12:56 DBA in two different matrices is shown in Table 8. For both matrices the amount of fluorescence enhancement increases with increasing intensity and begins to reach saturation at the highest intensities used.

TABLE 8.--Percent Fluorescence Increase for 0.1 M 12:56 Dibenanthracene in Various Polymers as a Function of the Relative Excitation Intensity.

Relative Excitation Intensity	% Fluorescence Increase	
	Pvac	Pst
100	27	7
40	17	4
20	5	0
10	1	-

2. Wavelength of excitation: The efficiency of the absorption of the exciting light by the solute is related to the spectral overlap of the solute's absorption spectrum and the exciting radiation. In general the molar absorptivities of the solutes used increases at shorter wavelengths and consequently even with a constant intensity, the number of electronically excited species generated will increase as the excitation is shifted to shorter wavelengths. Using this same consideration, if a fixed excitation source is used for a series of different solutes, part of the difference in the measured enhancement will be due to the difference in the efficiency of the absorption of the exciting light.

3. Relative positions of the excitation and detection systems: The measured amount of fluorescence enhancement is also dependent on the relative positions of the excitation source and

the detection system with the largest amount of fluorescence enhancement observed using the positions shown in Figure 2.

4. Partial pressure of oxygen: As the partial pressure of oxygen is reduced, the amount of fluorescence enhancement is also reduced. If pure nitrogen is used, no enhancement is observed.

5. Polymer matrix: The matrix used for a given solute also seemed to have an effect on the value of the enhancement measured with polyvinyl acetate giving the largest values. A quantitative comparison of all the matrices using a single solute was not made, but Table 9 shows the results for several solutes in four of the matrices.

In summary, those conditions which tend to maximize the triplet population (162), also maximize the measured oxygen induced fluorescence enhancement. Those solutes which have high triplet yields and long triplet lifetimes show the highest fluorescence enhancement.

### Pressure Studies

To determine more accurately the relationship between the partial pressure of oxygen and the amount of increase in the fluorescence, a series of experiments were undertaken. The results reported here are from the work with chrysene as the solute. A preliminary study was done with 12:56 DBA and is in qualitative agreement with the chrysene results.

The apparatus and procedures used in these experiments were the same as those discussed earlier except that the sample was

TABLE 9.--Percent of Fluorescence Intensity Increase (1 atm vs  $10^{-6}$  atm air).

Fluorescing Molecule	Matrix			
	Pmma	Pst	Pvac	Pvc
Anthracene	8	-2	2	-2
12 Benzanthracene	14			
34 Benzpyrene	6			
Phenanthrene	5			
Chrysene	10	-5	10	5
12:34 Dibenanthracene	16	-2	8	10
Fluoranthene	9			
12:56 Dibenanthracene	34	5	17	12

given one hour to equilibrate at each pressure. The sample was first evacuated for a number of hours and its luminescence spectrum recorded and stored. The pressure was then increased in small increments and the emission spectrum determined at each pressure. After normalization by the usual procedure, the difference was taken and integrated. A plot from one such series of measurements is shown in Figure 4 for chrysene  $10^{-3}$ M in polystyrene. The upper curve (a) is the percent fluorescence enhancement and the lower curve (b) is the percent phosphorescence quenching. It will be noted that the phosphorescence is completely quenched at a pressure of  $10^{-3}$  atmospheres of air which is also the pressure corresponding to the maximum fluorescence enhancement. The phosphorescence of



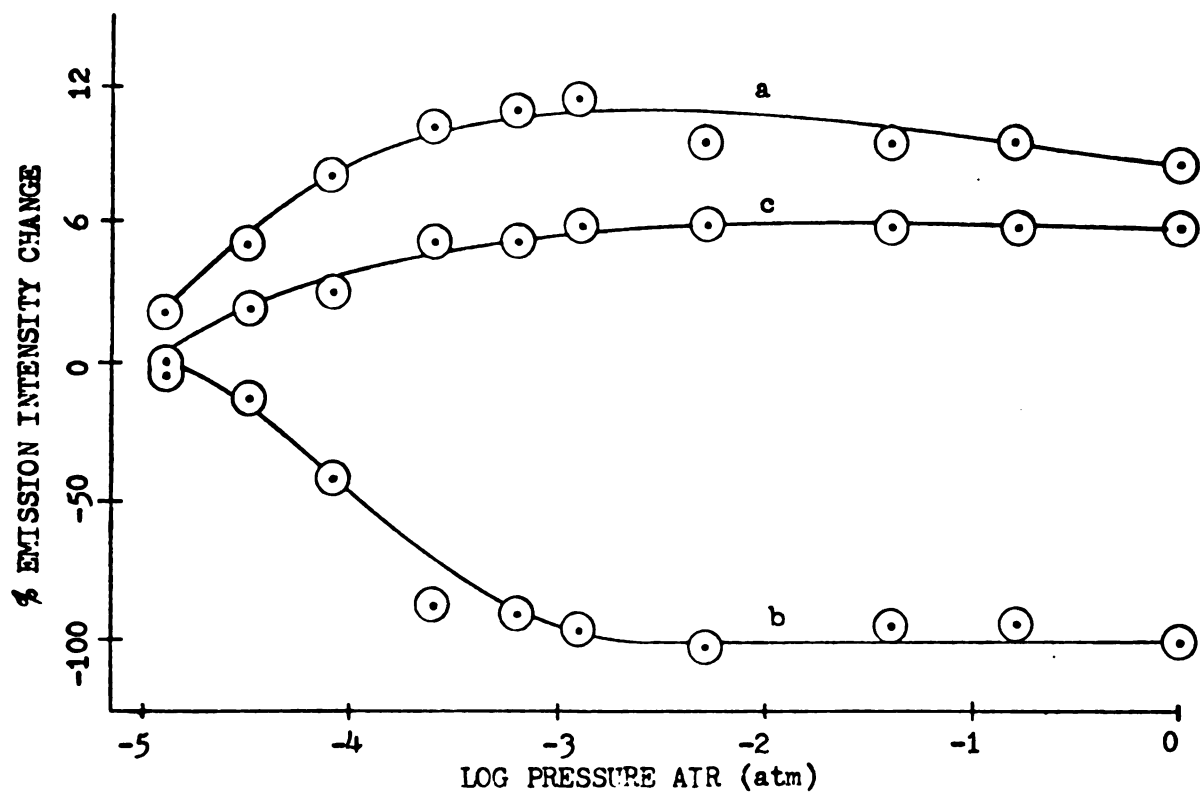


Figure 4.--Plot of % fluorescence enhancement and % phosphorescence quenching as a function of log (pressure of air), for chrysene  $5 \times 10^{-3}$  M in polystyrene. (a) % fluorescence enhancement (b) % phosphorescence quenching (c) relative change in the first two fluorescence vibronic bands.

course remains completely quenched as the pressure of air is increased while the fluorescence decreases slightly.

In Figure 5 is shown a similar plot of fluorescence enhancement versus pressure of air for pressures below  $10^{-2}$  atmospheres for chrysene  $10^{-2}$ M in polystyrene. In this plot it will be noted that the intensity of the fluorescence and phosphorescence remains approximately unchanged up to a pressure of  $10^{-5}$  atmospheres where the phosphorescence quenching and the fluorescence enhancement begins. All the pressure curves obtained for chrysene at different concentrations and excitation intensities are similar in shape to those shown.

The Franck-Condon envelope for the enhanced fluorescence is different from that of the fluorescence observed from the evacuated sample. An examination of Figure 3 shows that the red end of the fluorescence is increased relative to the blue end. If the relative change of the first two major vibronic bands for chrysene is plotted as a function of pressure, one gets a curve which parallels the fluorescence enhancement. An example of such a curve is included in Figure 4 (c). The Franck-Condon curves, however, do not show the decrease after reaching a maximum as is seen for the fluorescence enhancement curves.

#### Singlet Molecular Oxygen Feedback Mechanism

In view of the generality of quenching of luminescence by molecular oxygen, the observation by Geacintov, Oster and Cassen that the fluorescence of 12:56 DBA increases in the presence of

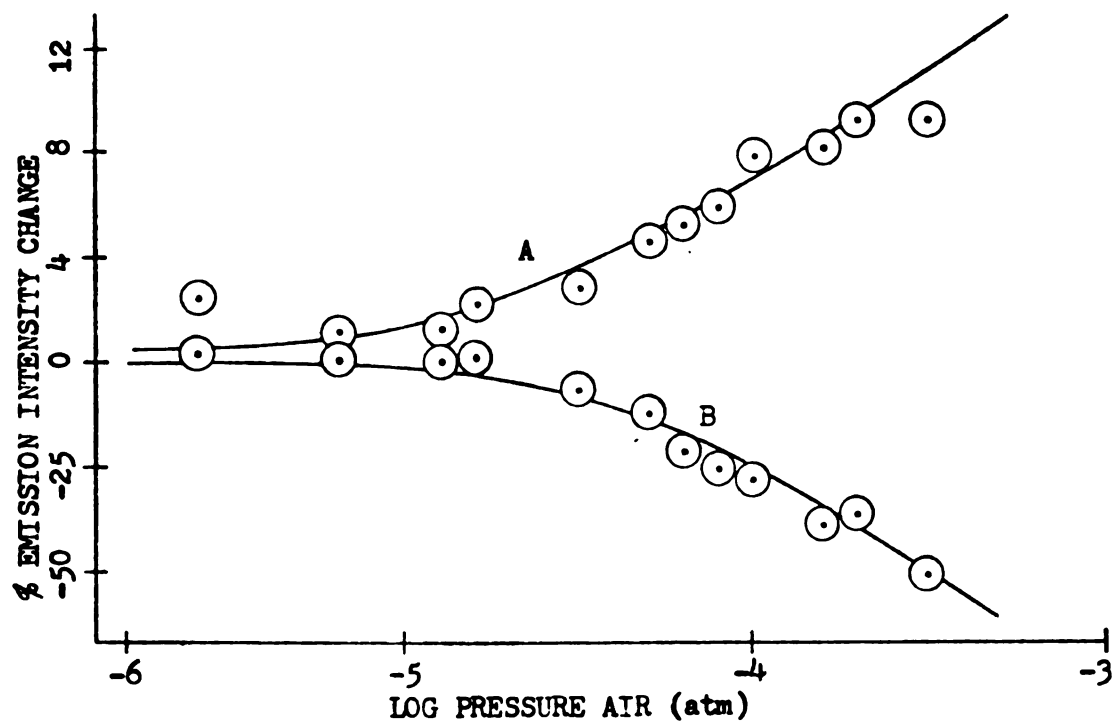


Figure 5.--Plot of % fluorescence enhancement and % phosphorescence quenching as a function of log (pressure of air), for chrysene 0.01 M in polystyrene. (a) % fluorescence enhancement (b) % phosphorescence quenching.

oxygen is most unusual. They attempted to explain the oxygen enhancement phenomenon and considered a ground state depopulation mechanism. This mechanism would account for at most 2% increase for their system while the observed increase was 10%. They were unable to explain the remaining part of the fluorescence enhancement (138).

In the absence of molecular oxygen, organic molecules dissolved in polymer matrices exhibit the normal luminescence properties of both fluorescence and phosphorescence (135). In the presence of ground state molecular oxygen the phosphorescence is quenched, returning the guest molecule to its ground state and producing singlet oxygen via electronic energy transfer from the quenched triplet state (61-64). The singlet states of molecular oxygen have long lifetimes (4-8) and are relatively resistant to collisional deactivation. It is proposed that, if the energetic requirements are met, electronic energy transfer from singlet molecular oxygen to the triplet state of the acceptor molecule can generate the excited singlet state of the acceptor molecule. This singlet oxygen mediated repopulation of the singlet manifold of the acceptor molecule contributes to the increase in the fluorescence intensity observed in the presence of molecular oxygen from organic molecules dissolved in polymer matrices and is the proposed singlet oxygen feedback mechanism (119) (Figure 6).

Since there are two low lying singlet states of interest in molecular oxygen, depending on the relative energy dispositions of the lowest excited singlet state and triplet state of the

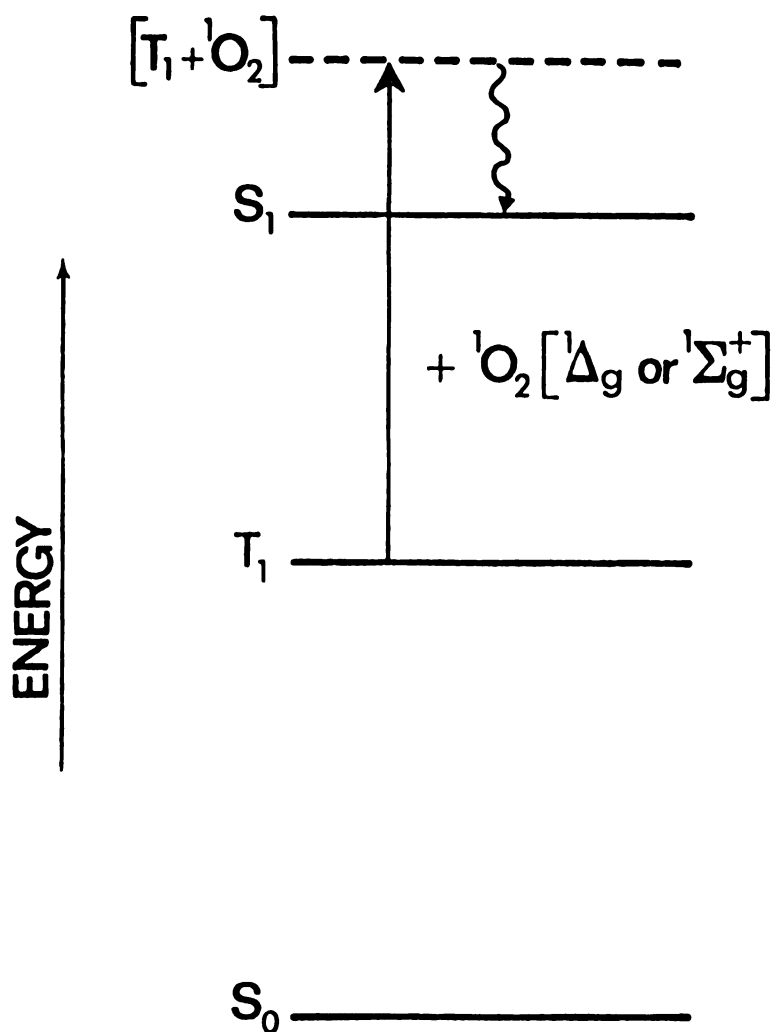
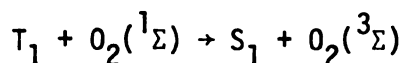


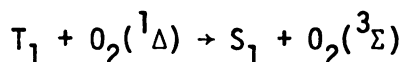
Figure 6. Schematic representation of the Singlet Molecular Oxygen Feedback Mechanism.

acceptor molecule, there are several pathways for the energy feed-back to take place.

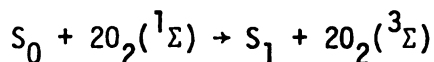
Mechanism 1



Mechanism 2



Mechanism 3



Mechanism 1 requires that the energy difference between the lowest excited singlet state and the lowest triplet state in the organic molecule be less than the excitation energy of the  $O_2(^1\Sigma)$  state of molecular oxygen,  $13,121\text{ cm}^{-1}$ . Mechanism 2 requires that this energy difference be less than  $7882\text{ cm}^{-1}$ . Mechanism 3 is a termolecular reaction in which two  $O_2(^1\Sigma)$  pool their excitation energy and transfer it to a ground state acceptor to produce the acceptor in its first excited singlet state.<sup>10</sup> This requires that the energy difference between the first excited singlet state and the ground state of the acceptor be less than  $26,242\text{ cm}^{-1}$ . Other termolecular processes are possible but are not energetically feasible for the acceptors used in this work.

On the basis of these three mechanisms, the acceptor molecules studied can be divided into four groups. For molecules in Group 1, only Mechanism 1 is energetically possible and examples of molecules in this group are naphthalene and anthracene.

For molecules in Group 2, only Mechanism 1 and 3 are possible and examples are 12 benzanthracene (BA) and 34 benzpyrene (BP). In Group 3, Mechanisms 1 and 2 are feasible. Chrysene and 12:34 DBA are members of Group 3. Finally for those molecules in Group 4, all three mechanisms are possible with 12:56 DBA and fluoranthene being representatives of this group.

### Correlations of Observations with Predictions

The feedback mechanism predicts a correlation between the number of energy transfer mechanisms which are energetically feasible for a given acceptor and the relative amount of oxygen induced fluorescence enhancement which is observed for that solute (163). The data presented in Table 9 qualitatively support this prediction. For instance 12:56 DBA which is a member of Group 4 shows the largest amount of fluorescence enhancement, 12 BA and chrysene show intermediate amounts of enhancement and are members of Groups 2 and 3 respectively. Anthracene shows a relatively low fluorescence enhancement and is a member of Group 1. There are however exceptions, for instance 34 benzpyrene.

In the feedback mechanism the triplet population is important in determining the efficiency of the feedback process since two triplet acceptor molecules are involved. The triplet population is related to the triplet quantum yield and triplet lifetime. If one compares the relative amount of fluorescence enhancement with the triplet quantum yield and triplet lifetime, the results for most of the listed molecules can be explained, including

34 benzpyrene. This consideration however predicts a low value for 12 BA contrary to what is observed. Neither of the above explanations adequately accounts for all the results.

#### Microscopic Mechanism

The singlet molecular oxygen feedback mechanism raises a question when one considers the details of the electronic energy transfer processes taking place between the organic and oxygen molecules. The production of the singlet oxygen in the quenching of the organic triplet state is understood (61). The gaseous diffusion of the singlet oxygen from the site of its formation to the second triplet also raises no difficulties in understanding. Upon collision, the singlet oxygen forms a collision complex with the organic triplet. In this complex under the influence of the electron exchange interaction, the energy transfer is spin allowed (125). The problem arises at this point in understanding the mechanism, in that the final state in this complex is an excited singlet state in close proximity to a ground state oxygen molecule. This is precisely the condition proposed for the efficient quenching of the excited singlet states of organic molecules by molecular oxygen (217). However, the singlet oxygen feedback mechanism proposes that the excited singlet state generated by energy transfer is not quenched but is capable of fluorescence. This aspect of the mechanism will be considered in a later chapter.



## CHAPTER IV

### A QUANTITATIVE COMPARISON OF GROUND STATE DEPOPULATION AND FLUORESCENCE ENHANCEMENT

#### Introduction

In the previous chapter, the singlet oxygen feedback mechanism was presented to provide a possible molecular basis to interpret the oxygen induced fluorescence increase observed for a number of polycyclic hydrocarbons in polymer matrices. This mechanism has been criticized by Jones and Nesbitt on the basis that the observed fluorescence enhancement can be accounted for by a trivial mechanism involving ground state depopulation (164). In this trivial mechanism the oxygen induced increase in the fluorescence intensity is attributed solely to the increase in the ground state population in the presence of molecular oxygen due to quenching of the triplet state of the organic molecule. This mechanism predicts that the maximum amount of fluorescence enhancement observed in a system is equal to the triplet population in that system in the absence of oxygen. Since the triplet population is dependent on the intensity of the exciting light, the triplet quantum yield, and the triplet lifetime, the amount of fluorescence enhancement should be related to these factors. As was noted in the last chapter, there is a correlation between these parameters and the amount of fluorescence enhancement observed. Since the

singlet molecular oxygen feedback mechanism predicts similar dependences, a decision between these two mechanisms cannot be made solely on the basis of the previous experimental results.

Since the trivial mechanism attributes the fluorescence enhancement solely to the increased ground state population in the presence of molecular oxygen, a comparison of the ground state depopulation to the amount of fluorescence enhancement is a critical test of the mechanism. To make this comparison, it is necessary to measure the change in the ground state population. This change in population can be determined by measuring the change in the  $S_0 - S_n$  absorption (165). In cases where the ground state depopulation is small this technique involves the measurement of a small change in a relatively large number. For the systems used in these experiments, it was found that the uncertainty in the measurement of the absorbance approached the value of the change in the absorbance. It was therefore necessary to use another method to obtain the desired information. The method used involved the measurement of the triplet concentration.

There are a number of ways to determine absolute triplet state populations. These include (i) ground state depopulation measurements (165), (ii) calculations from kinetic parameters (166,167) and (iii) measurements using the paramagnetism of the triplet state (168-171). In addition to these methods, if the molar absorptivity of the triplet-triplet transition is known, a Beer-Lambert Law experiment can be performed to find the triplet population (172).

In the experiments to follow the population of the lowest organic triplet state was determined from the triplet-triplet absorption and was compared to the amount of fluorescence enhancement measured under the same conditions. The results of these experiments show conclusively that the ground state depopulation in the absence of molecular oxygen is not sufficient to account for the magnitude of the fluorescence enhancement observed (119).

### Experimental

The apparatus used for these experiments is shown schematically in Figure 7. The samples were thin polymer films, the preparation of which was described in the previous chapter. The sample film was placed as shown against one face of the triangular quartz cell at 45° with respect to both the exciting light and the path of the absorption beam. The excitation source (a PEK 75 watt xenon lamp) was placed at right angles to the path of the reference beam with a 5 cm  $\text{NiSO}_4$  liquid filter and a Corning CS 7-54 glass filter for wavelength selection (173). The beam of the xenon lamp was focused to a spot approximately twice the diameter of the fiber optics used and its position was adjusted for each sample to maximize the measured triplet population. The absorption measurements were made by measuring the intensity of the radiation from a tungsten lamp with and without crossbeam excitation. To prevent scattered exciting light and sample luminescence from interfering with the absorption measurements, the light from the tungsten lamp was mechanically chopped before it entered the fiber optics and a PAR

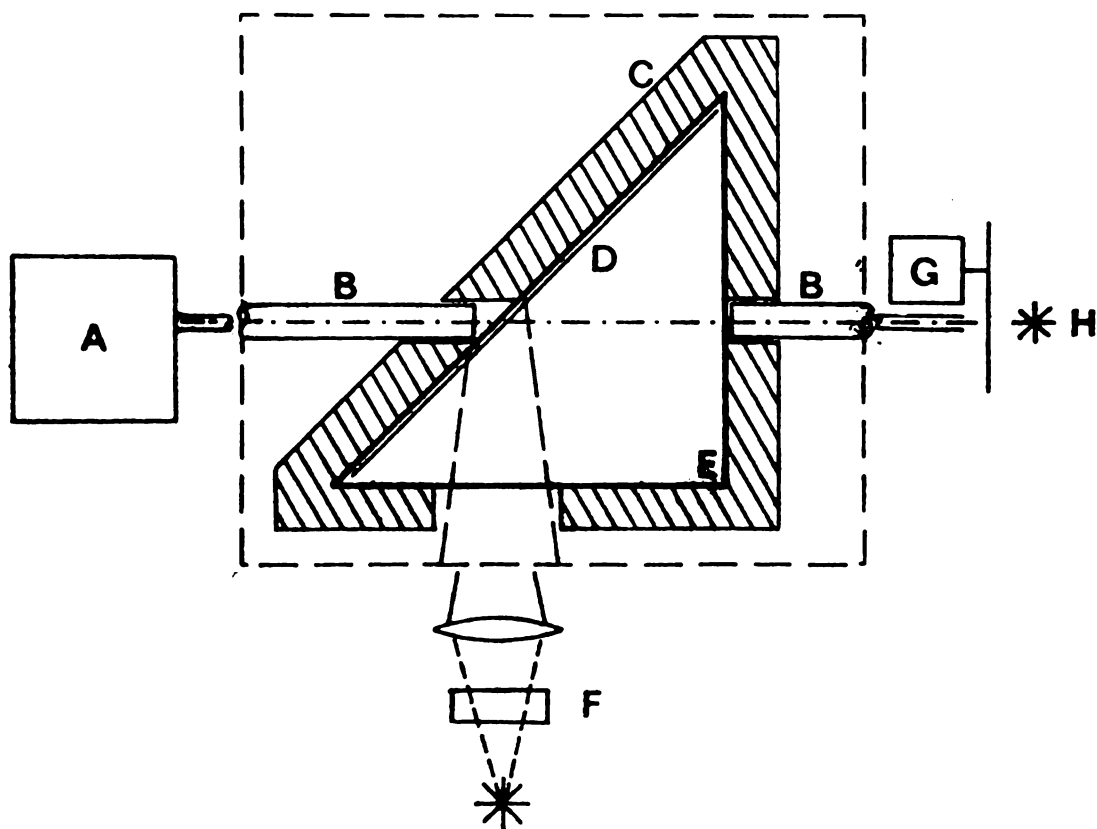


Figure 7.--Schematic of cross-beam apparatus: (A) detection system, (B) quartz fiber optics, (C) opaque cell covering, (D) sample, (E) cell, (F) excitation source, filter and lens, (G) mechanical light chopper, (H) light source for absorption measurements.

model 122 lock-in amplifier was used. By this technique, the contributions to the detected signal from scattered light and sample luminescence were electronically filtered out before the intensity was measured. A McPherson model 218 monochromator with an EMI 9558 QB photomultiplier was used to transduce the optical signal.

In a typical experiment, the sample film was placed in the cell and evacuated. The fiber optics were positioned to maximize the measured intensity of the tungsten lamp. The monochromator was set at the wavelength of the triplet-triplet absorption maximum for the solute used and the position and focus of the excitation source was optimized. The excitation beam was then alternately opened and blocked at approximately one minute intervals with the resulting signal intensity recorded on a strip-chart recorder. The zero intensity reading was checked frequently by blocking the light from both the light sources. These light intensity readings were converted to absorbances.

After the triplet-triplet absorbance had been measured, the wavelength of the monochromator was changed to the wavelength of the maximum in the fluorescence spectrum of the solute, the tungsten lamp output was blocked and a photometer substituted for the lock-in amplifier. The intensity of the fluorescence was then monitored on the strip chart recorder as the cell was opened to the atmosphere. The entire sequence was repeated a number of times to get a reliable average value.

In order to use the Beer-Lambert law to convert the absorbance to concentration, one needs to have values for both the molar absorptivity and the optical pathlength. Values of the molar absorptivities were obtained from the literature (174). Since the only information needed is the fraction of the molecules in the triplet state, pathlength can be eliminated from the equation by taking the ratio of the Beer's Law expressions for the triplet concentration and the ground state concentration. The fraction of molecules in the triplet state expressed as a percentage, can be calculated from the following equation:

$$\%T = (C_t/C_g) \times 100 = [(A_t \times a_s)/(A_s \times a_t)] \times 100$$

where  $C_t$  is the concentration of the triplet state during the excitation period and  $C_g$  is the ground state population in the absence of excitation.  $a_s$ ,  $a_t$ ,  $A_s$ , and  $A_t$  are the molar absorptivities and absorbances for the singlet and triplet transitions. The singlet absorbance was measured in a separate experiment using a Beckman DB with a blank polymer film for reference. The results for the solutes investigated are reported in Table 10 and are discussed below.

### Results and Discussion

An examination of the last two columns of Table 10 shows clearly that the amount of ground state depopulation (% triplets) is much less than the amount of fluorescence enhancement. Since the values of the % triplets are dependent on the values chosen for the molar absorptivities, a short discussion of this choice follows.

TABLE 10.--Comparison of the Amount of Ground State Depopulation to the Amount of Fluorescence Enhancement.

Guest Molecule	Matrix	Approximate Concentration	% Triplets	% Fluorescence Enhancement
Chrysene	Pst	$5 \times 10^{-4}$	2.1	17
Chrysene	Pst	$10^{-3}$	3.9	20
Chrysene	Pst	$5 \times 10^{-3}$	6.4	21
Chrysene	Pst	$10^{-2}$	3.2	45
Chrysene	Pst	$5 \times 10^{-2}$	1.4	35
Chrysene	Pst	$10^{-1}$	0.6	31
Chrysene	Pvc	$10^{-2}$	3.4(1.7)*	6.6
12:56 DBA	Pst	$10^{-3}$	9.3	71
12:56 DBA	Pst	$10^{-2}$	4.1	69
12:56 DBA	Pvc	$10^{-2}$	4.0(1.9)*	20

\*In atmospheric pressure of air.

The values for the singlet molar absorptivities,  $a_s$ , were obtained from Clar (175). These values were determined in heptane solution. It has been pointed out that the  $S_1$  absorption band of 12:56 DBA is more diffuse in the polymer matrix than in solution (138). This diffuseness would lower the value of  $a_s$  for the absorption maximum in the polymers as compared to solution. This means the value of the ground state population used in Table 1 is underestimated which would cause the fraction of molecules in the triplet state to be smaller than reported. If on the other hand, the value of  $a_t$  was also reduced due to the diffuseness of the

triplet-triplet absorption bands, this would result in at least a partial cancelation of this error.

The value of  $a_t$  was taken from the work of Brinen (174). He used 2-methyltetrahydrofuran as the solvent and worked at 77°K. The present experiments were done at room temperature in polymer matrices. A question may arise whether the value of  $a_t$  is the same for both systems. It is believed that the values for the molar absorptivities determined by Brinen should give results for the triplet population in the polymer system which are accurate to about ten percent or better for the following reasons. (i) Windsor and Novak found that the value of  $a_t$  for coronene, another polycyclic hydrocarbon, changed by less than ten percent comparing EPA at 77°K to polymethylmethacrylate at room temperature (176). (ii) The amount of ground state depopulation calculated using Brinen's values for  $a_t$  are in agreement with the upper limit set by the experiments performed using  $S_0 - S_n$  absorption to directly measure the change in the ground state population. (iii) The low resolution triplet-triplet absorption spectrum obtained for chrysene in polystyrene at room temperature (Figure 8) agrees qualitatively with that reported by Brinen for chrysene in 2-methyltetrahydrofuran at 77°K (174). By analogy with the effect of the polymer matrix on the singlet absorption spectrum, it may be expected that the triplet-triplet absorption bands may be more diffuse in the polymers which would lower the value of  $a_t$ . Even a ten percent uncertainty in the triplet population in no way affects the conclusions reached.



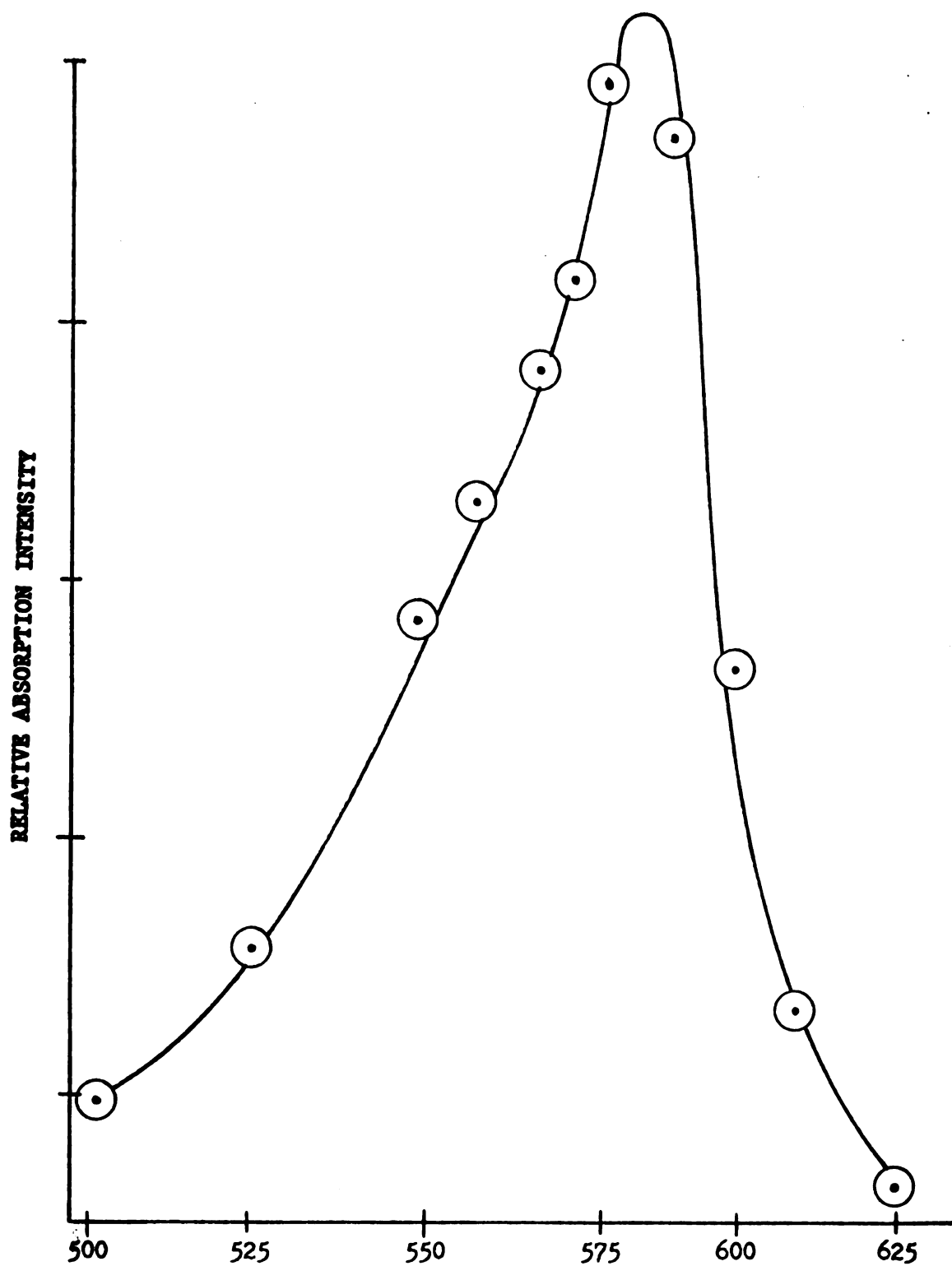


Figure 8.--Triplet-triplet absorption spectrum for chrysene in polystyrene at room temperature.

The low value for the enhancement in polyvinyl chloride as compared to polystyrene is striking and due at least in part to the low equilibrium oxygen concentration in this matrix (138) as evidenced by the observation of weak phosphorescence even after equilibration with air. The triplet concentration was determined for the samples in polyvinyl chloride, both at evacuation and equilibrated with air. For polystyrene, the triplet population in air was found to be negligible.

In summary, the amount of fluorescence enhancement far exceeds the amount of ground state depopulation for all the samples measured. Therefore some mechanism in addition to ground state depopulation must be operative. One possibility already presented is the singlet oxygen feedback mechanism. Several other mechanisms which do not actively involve molecular oxygen will be considered in the next chapter.

## CHAPTER V

### FLUORESCENCE ENHANCEMENT NOT ACTIVELY INVOLVING MOLECULAR OXYGEN

#### Introduction

The intensity of the fluorescence observed from a sample is dependent on (i) the intensity of the exciting light and (ii) its wavelength, (iii) the concentration of the absorbing molecules and (iv) the fluorescence quantum yield (177). Any process which affects one or more of these, will affect the observed intensity. For example, the concentration of the ground state molecules can be reduced by depopulation. The effective intensity of the exciting light can be reduced by a competitive absorption of the exciting light by states other than the solute ground state.

#### Processes Which Reduce the Fluorescence Intensity

The processes which lead to a reduction in the fluorescence intensity and do not actively involve molecular oxygen will be presented in this section. These processes all depend on the presence of a significant excited state population. They include (1) ground state depopulation, (2) the inner filter effect, (3) the trivial process of radiative energy transfer, i.e. reabsorption, and (4) non-radiative energy transfer which includes singlet-singlet and singlet-triplet energy transfer. These processes will be presented individually, then the total affect on the fluorescence

intensity will be compared with the results of experiments in which the organic triplet population was quenched in the absence of molecular oxygen.

1. Ground State Depopulation (164,165): In a system with an accessible metastable state the number of molecules in the ground state can be reduced under photostationary conditions by populating the metastable state. In the samples considered here the metastable state is the lowest triplet state. Since the fluorescence intensity is proportional to the ground state population, as this state is depopulated by populating the triplet state, the intensity of the fluorescence is reduced. This mechanism causes a reduction in the fluorescence which is equal to the amount of depopulation of the ground state.

2. Inner Filter Affect: The inner filter affect is a reduction in the intensity of the fluorescence observed due to a competitive absorption of the exciting light by species other than the electronic ground state of interest (171). In a system under photostationary excitation, there is a finite steady state population of the excited electronic states. Each of these states has its own absorption spectrum and if this spectrum has an appreciable strength at the wavelength of excitation, they can compete successfully with the solute ground state for the excitation photons. The amount of light absorbed by each species is proportional to its molar absorptivity and its population. The last consideration usually makes this process unimportant. For the systems which are of interest here, the triplet population is not negligible, and the

triplet-triplet absorption spectrum shows a strength which is comparable to that of the  $S_0 \rightarrow S_n$  absorption (178) so the effect can be significant.

3. Radiative Energy Transfer: Radiative energy transfer or reabsorption is the process to which the term, trivial effect was first applied (121). A photon emitted by one solute as fluorescence can be reabsorbed by another molecule in the sample before it can escape and be detected. The absorbing molecule could be (a) another ground state solute molecule (121), (b) an excited singlet state or (c) an excited triplet state of the solute (179-181). The magnitude of the affect will depend on the spectral overlap of the emission and absorption spectra involved. The  $S_1 \rightarrow S_n$  absorption of the fluorescence should not be important in these systems since the population of the first excited singlet state will be small.

The reabsorption of the fluorescence by another ground state solute molecule is important at high solute concentrations and leads to a reduction in the relative intensity of the first band of the fluorescence (121). Since the triplet-triplet absorption spectrum completely overlaps the fluorescence for the aromatic hydrocarbons (178), reabsorption by the triplet state can be important at high triplet populations.

4. Non-radiative Intermolecular Energy Transfer: For interacting molecules which are separated by distances greater than molecular diameters, the most important radiationless energy transfer mechanism is resonance dipole-dipole interaction (236).

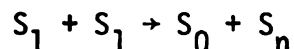
The theory for this interaction has been worked out in a form which is directly applicable to experiment by Forster (234). As a measure of the degree of interaction between the donor and acceptor molecules, he defined a reference distance  $R_0$  as the mean distance in angstroms between a donor and an acceptor where the probability for resonance energy transfer is fifty percent. The value of  $R_0$  is proportional to a spectral overlap integral which depends on the molar absorptivity of the acceptor and the spectral distribution of the fluorescence as well as other parameters. The rate of energy transfer  $K_{da}$  is related to the distance between the interacting molecules  $R$ , the value of  $R_0$  and the lifetime of the donor state:

$$K_{da} = 1/\tau \times (R_0/R)^6$$

The actual amount of energy transfer is then determined by a competition between the rates of the various processes leading to de-excitation of the first excited singlet state of the donor.

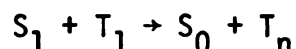
Two processes are of interest here (a) singlet-singlet and (b) singlet-triplet energy transfer. In a third process, excitation migration, the excitation energy of the first excited singlet is transferred to another unexcited molecule of the same kind, and leaves the overall populations unchanged.

(a) Singlet-Singlet Energy Transfer: This process is one in which the excitation energy of one excited singlet state is transferred by resonance energy transfer to a second molecule also in its first excited singlet state:



Under conditions of very high excitation intensities where the population of the  $S_1$  state is large, this process is important (181). Its effectiveness will depend on the average distance between the excited singlets and on the value of the spectral overlap integral. It would not be important at the intensities used in these experiments.

(b) Singlet-Triplet Energy Transfer: In the present experiments in the absence of oxygen an appreciable triplet population is produced and singlet-triplet energy transfer may be important. In this process the excitation energy of one molecule in its first excited singlet state is transferred to another molecule in its lowest triplet state and yields the second molecule in a higher triplet state and the first molecule in its ground state:



The excess energy of the higher triplet state can be lost rapidly to the environment as thermal energy. The efficiency of this process is dependent on the molar absorptivity of the  $T_1 \rightarrow T_n$  transition in the spectral region of overlap with the fluorescence emission of the donor. For most aromatic hydrocarbons the value of the spectral overlap is large (178) and singlet-triplet energy transfer is expected to be a relatively efficient process for many of these systems.

### Simulated Quenching Experiments

The characteristics which have been observed for the oxygen induced fluorescence enhancement in systems under photostationary conditions are (i) the spectral shift which enhances the lower energy end of the fluorescence more than the higher energy end, (ii) the amount of enhancement exceeds the amount of ground state depopulation. In the experiments which follow, the effect of the physical quenching of the organic triplet state by molecular oxygen is investigated using simulated quenching of the triplet state in the absence of oxygen and both the characteristics of oxygen induced fluorescence enhancement are observed in an evacuated sample.

The experiment involves the use of an auxiliary excitation source and a phosphoroscope to control the triplet population. The schematic diagram of the apparatus is shown in Figure 9. On one axis is the main excitation source, a PEK 100 watt high pressure mercury lamp with a monochromator to isolate the 331 nm mercury line. The intensity of this source was kept low to prevent the generation of a significant triplet population by this source. The fluorescence detection system was on the same axis and consisted of a McPherson 218 monochromator and an EMI photomultiplier. The auxiliary excitation source was a PEK 500 watt high pressure mercury lamp with 5 cm of a  $\text{NiSO}_4$  solution as a filter. The sample was an aromatic hydrocarbon dissolved in a thin polymer film and placed diagonally in a one centimeter quartz cell at the center of the phosphoroscope.



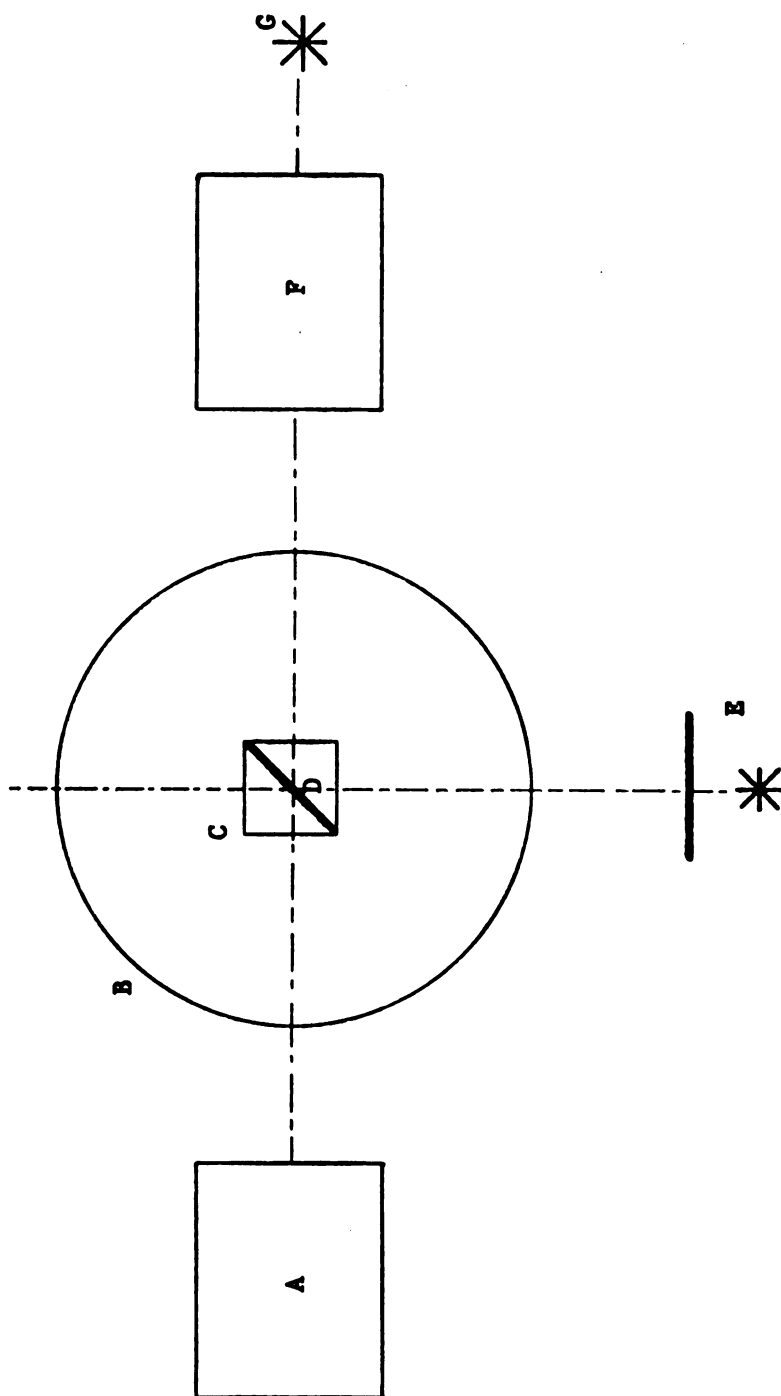


Figure 9.--Apparatus for simulated quenching experiments: (a) detection system, (b) phosphoroscope, (c) cell, (d) sample, (e) auxiliary excitation source and filter, (f) excitation monochromator, (g) main excitation source.

When the phosphoroscope was rotated the fluorescence from the solute excited by the low intensity primary source could be scanned with the detection monochromator. By varying the intensity of the light from the auxiliary source, the steady state triplet population can be varied. By this technique the triplet population can be varied from about zero to several percent of the total solute concentration without changing the intensity of the primary source.

In Table 11 are shown results for chrysene at a concentration of  $5 \times 10^{-3}$  M in polystyrene. One can see that at the highest intensities used for the auxiliary excitation source, there are approximately 2% of the solute molecules in the triplet state and a corresponding enhancement of the fluorescence of 5-11% depending

TABLE 11.--% Fluorescence Enhancement as a Function of % Triplets for Chrysene  $5 \times 10^{-3}$  M in Pst.

Relative Intensity of Auxiliary Source	% Triplets	% Fluorescence Enhancement		
		365nm	385nm	406nm
10	--	1	0.5	5
20	1.2	0.7	2	5
40	2	4	5	11

on the wavelength of observation. The uncertainty in these numbers could be a percent or two, but it is clear that the highest intensities used leads to an amount of fluorescence enhancement which is larger than the amount of ground state depopulation. The triplet populations reached in these experiments are significantly lower

than those reached in the experiments reported in the last chapter. The difference between the amount of ground state depopulation and the measured fluorescence enhancement may increase with the triplet population. The amount of fluorescence increase is strongly dependent on the wavelength at which it is measured.

The effect of the triplet population on the spectral intensity shift was investigated for several solutes in a separate series of experiments. The results are recorded in Table 12. It is found that the experimental conditions can be divided into two groups depending on the relative spectral distribution of the fluorescence. These two groups are shown in the table. It will be noted that the first group of conditions leads to a high steady state triplet population and in the second group there is only a low triplet population.

The correlation between the presence of a high triplet population and the blue shifted fluorescence intensity leads to the conclusion that the shift in the intensity is due to the presence of the triplet population which preferentially reduces the intensity of the red end of the fluorescence.

#### Interpretation of the Simulated Quenching Experiments

The triplet-triplet absorption spectrum for chrysene has been reported by several workers (174,182,183). The singlet-singlet absorption spectrum has also been reported (183). Using these spectra and the mechanisms discussed earlier the results of the simulated quenching experiments with chrysene can be explained.

TABLE 12.--Relative Spectral Intensity as a Function of Experimental Conditions.

Pressure	Temperature	Intensity
Group 1 - Blue shifted intensity		
evac	77°K	high
atm	77°K	high
evac	300°K	high
Group 2 - Red shifted intensity		
atm	300°K	high
evac	300°K	low
atm	300°K	low

In a  $5 \times 10^{-3}M$  chrysene in polystyrene sample, a 2% triplet concentration leads to a 5-11% decrease in the fluorescence intensity. The excitation source was of low intensity and therefore interactions involving the excited singlet states would not be important in explaining this reduction.

The ground state depopulation immediately accounts for a 2% decrease. Also since the triplet-triplet absorption spectrum is of a similar magnitude to the  $S_0 \rightarrow S_n$  absorption at the wavelengths used for excitation (182), the inner filter effect should account for 1.5 - 2% more.

By using the average value of the molar absorptivity of the  $T_1 \rightarrow T_n$  (174,182) transition in the region of the fluorescence band, and the values of  $R_0$  calculated by Berlman for chrysene as the donor and with a number of different acceptors (221), the value of  $R_0$  for

the singlet-triplet energy transfer for chrysene is estimated to be between 20 and 25 angstroms. Quantitative calculations cannot be made because of the lack of an accurate triplet-triplet absorption spectrum in the spectral region of the overlap with the fluorescence.

In the  $5 \times 10^{-3}$  M sample assuming a homogeneous distribution of the solute, the average intermolecular distance should be on order of 70 Å. Since there is an inverse sixth power dependence on the intermolecular distance (234), the singlet-triplet energy transfer is expected to be negligible unless there is a significant non-homogeneous distribution of the solute.

It is known that the loss of intensity in the first band of the fluorescence with increasing concentration of the solute is due to the reabsorption phenomenon (217). Since this reduction is observed even in the thin polymer films used in this study, it may be that the light is scattered around inside the heterogeneous interior of the film giving an effective pathlength which is much greater than the film thickness. It is expected that even a few percent triplet molecules could cause a noticeable change in the observed fluorescence intensity.

The average value of the molar absorptivity for the  $S_0 \rightarrow S_1$  absorption of chrysene is about 400 (175) whereas the average value for the  $T_1 \rightarrow T_n$  absorption in the same region is about 5000 (174, 182). Since the efficiency of the reabsorption is proportional to the molar absorptivity, the absorption by the triplet manifold should be more important than that of the singlet manifold by about an order of magnitude at equal concentrations. However, the

triplet population measured in the experiments in question was only a few percent of the total solute concentration. Therefore the triplet-triplet reabsorption should be somewhat smaller than for the ground state.

The wavelength dependence which is observed for the percent fluorescence enhancement can be explained by the reabsorption mechanism if the triplet-triplet absorption spectrum were more intense at the longer wavelengths of the chrysene fluorescence band. There is some difference in the intensity of the triplet-triplet absorption in the published spectra (174,182,183), but less than predicted by the fluorescence enhancement. The attempts made by this writer to determine the relative triplet-triplet absorption in this spectral region were foiled by the intense fluorescence and the weak absorption of the samples used.

In summary, the mechanisms presented in this chapter collectively account for a fluorescence enhancement in a photostationary system which is several times larger than the measured triplet population. They also account for the apparent Franck-Condon shift in the enhanced spectrum. They do not however explain the fate of the singlet oxygen generated in the quenching of the organic triplet states. An approximate calculation shows that in a photostationary experiment with reasonable values chosen for excitation and de-excitation processes, essentially all the ground state oxygen present in the polymer film is converted to singlet oxygen via the quenching of the organic triplet state. Efficient deactivation must occur at a rate which greatly exceeds that expected for

collisional quenching of singlet oxygen if there are to be sufficient ground state oxygen molecules to explain the continued quenching of the organic triplets. The singlet oxygen feedback mechanism does provide an efficient deactivation process for singlet oxygen and experiments conclusively demonstrating the feedback mechanism will be presented in the next chapter.

## CHAPTER VI

### SINGLET OXYGEN-TRIPLET ORGANIC MOLECULE ANNIHILATION LUMINESCENCE

#### Introduction

Based on the results of the photostationary experiments, it has been proposed that if energetically feasible, singlet molecular oxygen can transfer its excitation energy to an organic molecule in its first excited triplet state. In all the previous experiments, the expected fluorescence was detectable only as a difference between the sample luminescence in the presence and absence of oxygen. The other enhancement mechanisms discussed earlier also contribute to that difference. It is therefore not possible to make an unambiguous interpretation of the results. In the experiments presented in this chapter, the expected fluorescence is generated in the absence of both the normal prompt fluorescence and the excitation beam. These conditions eliminate all contributions from other enhancement mechanisms, allowing an unequivocal conclusion to be drawn regarding the feedback mechanism.

In this chapter the experimental apparatus developed for these experiments and the experimental procedure are explained. Then the results for a series of aromatic hydrocarbons with different energy dispositions will be discussed.



### Experimental

The general procedure of the experiment is to add oxygen to a phosphorescing sample and to observe the resulting emission. The apparatus designed for these experiments had to meet a number of requirements. (1) It had to have a minimum dead time, the time between the cut-off of the excitation and the start of the observation period. The dead time could not be eliminated completely because of the large amount of scattered light and the high intensity of the prompt fluorescence would reduce the detection sensitivity which could be used without saturating the electronics. (2) There had to be a minimum delay between the start of the observation period and the admission of the oxygen. The sum of the two delays (1 + 2) set a lower limit on the triplet lifetime of the acceptor which could be used in these experiments. (3) A method of normalizing the results from one experiment to those of another for accurate comparison and (4) a method of wavelength selection were required. (5) The recycle time needed to be kept as short as possible and as it was mostly controlled by the time required to re-evacuate the sample after each experiment, the pumping speed needed to be high. Finally, (6) the entire apparatus had to be constructed from the equipment already available in this laboratory.

The final version of the burst apparatus developed to meet the above requirements is shown in Figures 10 and 11. Figure 10 shows the mechanical and optical systems. The excitation source was a 1000 watt xenon lamp filtered with eight centimeters of  $\text{NiSO}_4$

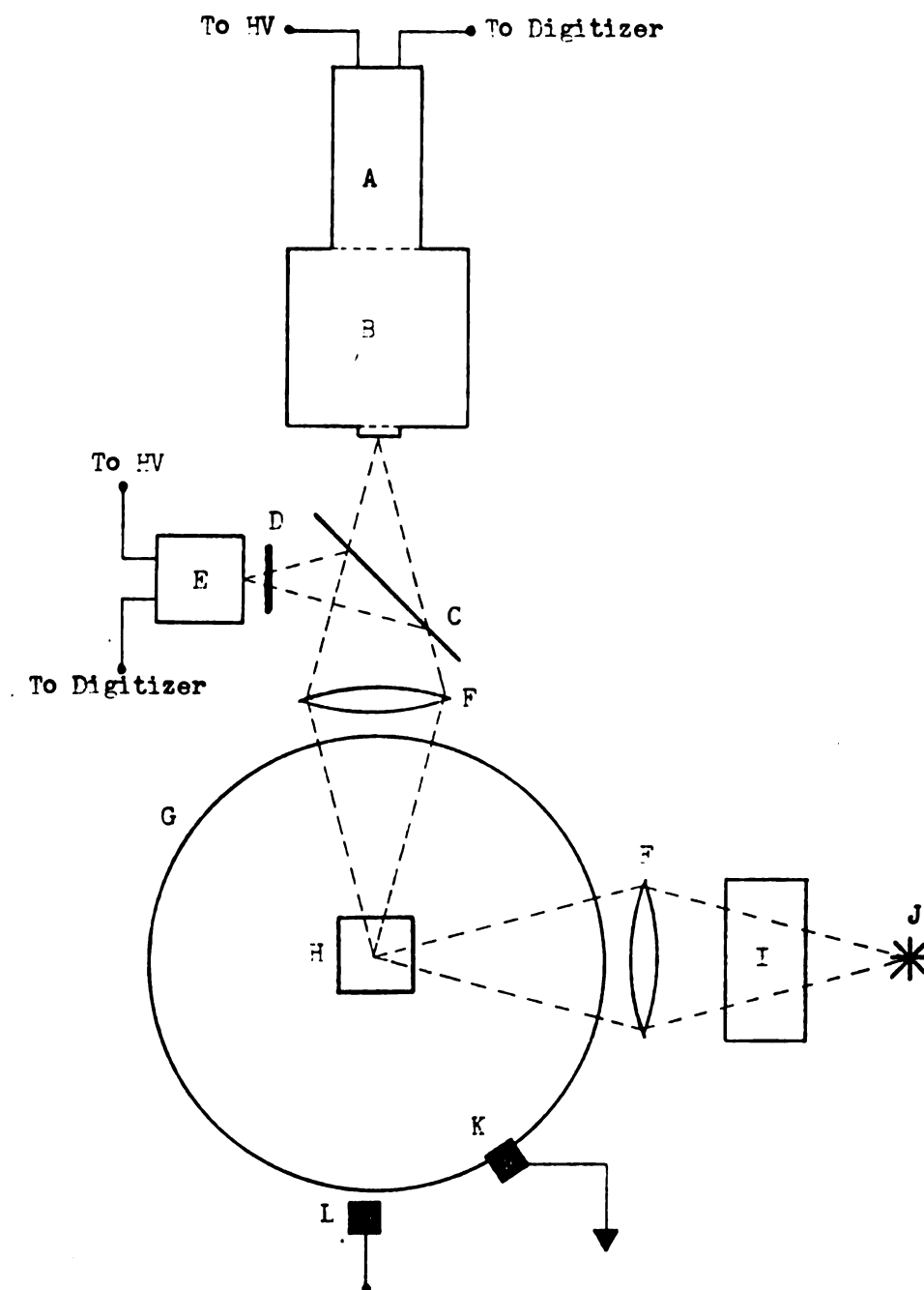


Figure 10.--Apparatus for detection of singlet oxygen-triplet organic molecule annihilation fluorescence: mechanical and optical systems. (A) EMI 9558 QB, (B) monochromator, (C) beam splitter, (D) filter, (E) RCA 1-P28, (F) lens, (G) phosphorometer, (H) sample cell, (I) filter, (J) 1000 watt xenon lamp, (K) electrical contact, (L) mechanical stop.

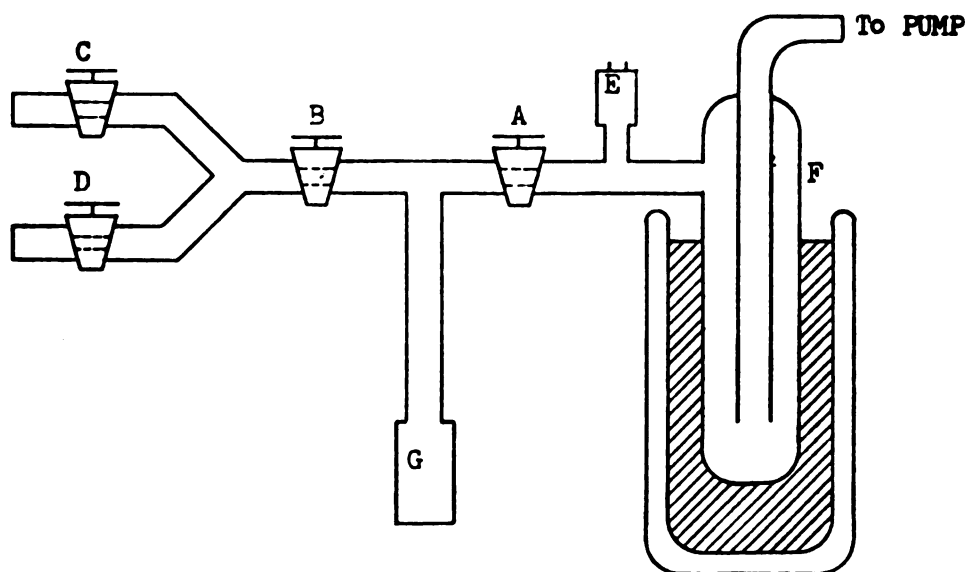


Figure 11.--Apparatus for detection of singlet oxygen-triplet organic molecule annihilation fluorescence: vacuum system. A, B, C, and D, vacuum valves; E thermocouple vacuum gauge, F liquid nitrogen trap, and G sample cell.

and a Corning 7-54 glass filter. This filter combination allows broad band excitation at wavelengths shorter than 350 nm (173). The phosphoroscope provided a convenient means to mechanically couple the shutters for the excitation and observation systems and allowed the dead time to be kept relatively short. The observation system consisted of quartz collection optics, a quartz plate used as a beam splitter and two photomultipliers. The photomultiplier at right angles to the main observation beam, was used for normalization purposes as explained below. It was an RCA 1-P28 with appropriate glass filters. The on beam photomultiplier with the monochromator was used for the main observation. The monochromator was a Bausch and Lomb quarter meter high intensity monochromator with appropriate grating, either visible (350-800 nm) or UV (200-400 nm), depending on the sample. The photomultiplier was an EMI 9558QB which has S-20 response.

The response of the photomultiplier as a function of time was digitized and stored in the memory of a Nicolet 1074 Instrument Computer, with dual channel input, one for each photomultiplier. The time sweep of the computer was triggered by the signal generated by a 1.5 volt battery upon contact between the two open connections in the trigger circuit, one attached to the phosphoroscope and the other to a mechanical stop as indicated. The contents of the computer memory could later be read out digitally on an oscilloscope screen or plotted with the aid of an X-Y recorder.

The vacuum system is shown in Figure 11. It consisted as indicated of a mechanical vacuum pump, liquid nitrogen trap, a

thermocouple vacuum gauge, a main shut off valve (A), the sample in a one centimeter square quartz cell, a valve to admit the quenching gas (B), and a chamber with choice of quenching gases. The quenching gas was usually air, either saturated with water vapor or dried over  $\text{CaCl}_2$ . Some synthetic atmospheres were also used, made by mixing tank nitrogen and tank oxygen in another vacuum line and were stored in glass bulbs until needed.

The usual experiment on this apparatus followed the procedure outlined below. The sample was first placed in the cell, attached to the vacuum line and evacuated by opening valves A and B, closing C and D. The appropriate filters and wavelengths were selected and the high voltage for each photomultiplier and the slit width on the monochromator adjusted to match the intensity of the observed results to the range of the digitizer. After a period of time long enough to assure good evacuation of the sample, valve B was closed and the quenching gas loaded into the quenching gas chamber through valve C or D. Valve A was then closed, isolating the sample from the vacuum pump. The phosphoroscope was rotated to illuminate the sample with the excitation beam. After an irradiation time sufficient to reach a steady state triplet population in the sample, the phosphoroscope was rapidly rotated by hand until the electrical contact hit the mechanical stop which triggered the sweep of the computer and stopped the phosphoroscope in the correct position to expose the luminescing sample to the detection system. Immediately after the sweep was triggered, valve B was opened admitting the quenching gas. After the completion of

the sweep, the results could be processed from the computer memory and the procedure repeated.

It was found that in most cases a sample could be reused a large number of times with no detectable deterioration of the sample. An exception was when pure oxygen at atmospheric pressure was used as the quenching gas. Under these conditions the sample showed significant photo-oxidation after several runs.

All the experiments reported here fall into two major groups, those using phosphorescence normalization and those using fluorescence normalization. For experiments in the first category, the light entering the off axis photomultiplier is filtered with a glass filter which transmits the phosphorescence of the solute molecule but not its fluorescence. The monochromator can be set to any wavelength, usually one in the fluorescence band of the solute. In this manner one part of the computer memory stores the phosphorescence intensity, showing the normal phosphorescence decay and the rapid quenching upon the admission of the oxygen. The second part of the computer memory stores the response of the second photomultiplier at the wavelength set on the monochromator. The intensity of the phosphorescence immediately prior to quenching is related to the triplet population at that moment and can be used to normalize the intensity of the response of the second photomultiplier. Actually since the intensity of the fluorescence produced in these experiments is not a linear function of the triplet population as will be shown later, only experiments with

equal phosphorescence intensities at the moment of quenching are compared.

For experiments in the second category, the light entering the off axis photomultiplier is filtered to transmit the fluorescence band of the solute and to block the phosphorescence. The monochromator is then set to any wavelength in this spectral region. The response of the second photomultiplier can then be expressed as the fraction of the total fluorescence occurring at that wavelength. The results from different runs on the same sample or on different samples of the same solute can be directly compared or averaged. In this way accurate spectra of the fluorescence can be determined.

#### Materials and Sample Preparation

The polymer used as the matrix for these investigations was polystyrene (both polystyrene- $h_8$  and polystyrene- $d_8$ ) as it is highly permeable to oxygen (138) and can be formed into fluffs (184). The polystyrene- $h_8$  (Pst) was prepared by thermal polymerization of styrene- $h_8$  (185). The styrene (Matheson, Colman and Bell) was first distilled under vacuum to remove the stabilizers, degassed by three successive freeze-pump-thaw cycles and then sealed under vacuum. The polymerization was accomplished by keeping the purified styrene at 124° C for 52 hours. The remaining unpolymerized monomer was removed by dissolving the product in benzene and precipitating it in methanol. To remove the solvent, the polystyrene was then dried under vacuum.

The polystyrene- $d_8$  was prepared similarly except the styrene- $d_8$  (Aldrich-Diaprep Inc., 98+%) was used as received, that is, polymerized directly in the shipping ampule. Thermal polymerization of styrene at 125° C for 24 hours leads to 90+% conversion of the monomer and gives an average molecular weight of about 150,000 (185).

The solutes used include 12:56 dibenzanthracene (DBA), recrystallized from glacial acetic acid; chrysene- $h_{12}$ , sublimed under vacuum; chrysene- $d_{12}$  Merck, Sharpe and Dohme; 12 benzanthracene (BA); pyrene; naphthalene; and carbazole, all Aldrich; and beta carotene, Nutritional Biochemical Corp.

The sample fluffs were prepared by dissolving the appropriate amount of polystyrene and solute in benzene to make a 1% solution of the polymer, freezing the solution with liquid nitrogen and evacuating it. The liquid nitrogen was removed after about half an hour and the pumping continued at room temperature for about 18 hours, until all the solvent had been removed. This procedure gives a fluff which has about twenty square meters of surface area per gram of the polymer (184).

### General Results

A typical result from a phosphorescence normalized experiment for chrysene 0.01 M in polystyrene is shown in Figure 12. The upper trace is the response of the on axis photomultiplier to the chrysene fluorescence at the wavelength indicated and the lower trace is the response of the off axis photomultiplier to the phosphorescence. The time scales are the same for both traces.



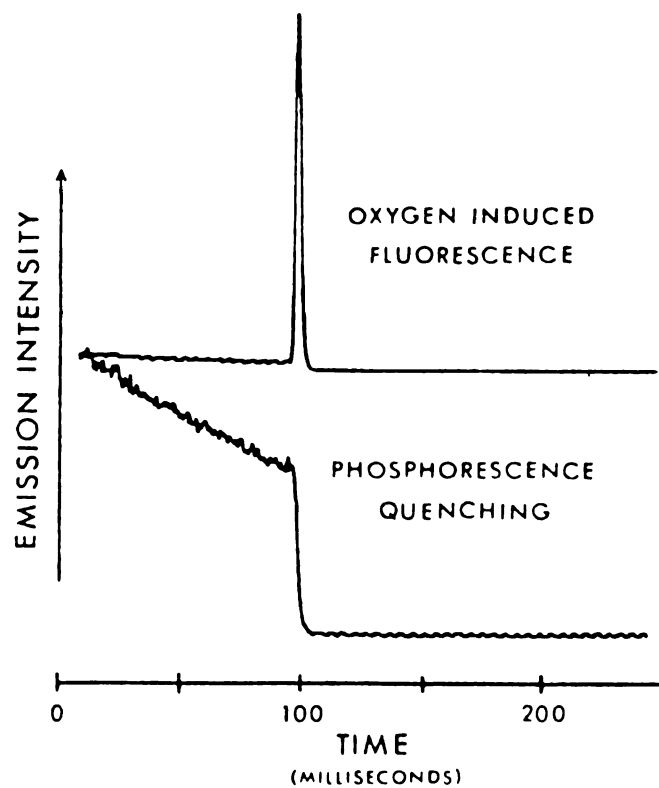
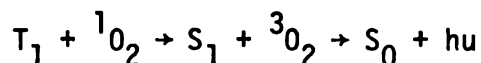


Figure 12.--Phosphorescence decay and oxygen induced fluorescence of chrysene ( $10^{-2}M$ ) in polystyrene fluffs.

The air was admitted at approximately 95 milliseconds after the trace began as is clearly indicated by the sudden rapid quenching of the phosphorescence. At the same time the phosphorescence is being quenched, there is a short burst of light at the wavelength indicated. This burst of light is the luminescence predicted by the feedback mechanism.



The reasons for this interpretation of the data are as follows. (1) The burst is coincident with the oxygen quenching of the phosphorescence. (2) Singlet oxygen will be produced in the quenching of the chrysene triplet state (61-64). (3) The  $S_1 - T_1$  energy difference in chrysene is such that the energy transfer is possible for both  ${}^1\Delta$  and  ${}^1\Sigma$ , but is too large for vibrationally excited ground state oxygen to be important. (4) Oxygen is required to observe the burst. (5) The burst is observed in the spectral region of chrysene fluorescence.

The first two conditions imply that the burst is seen only when both chrysene triplets and singlet oxygen are present. Due to the third condition, the proposed mechanism is energetically feasible unambiguously ruling out the participation of vibrationally excited ground state oxygen. Finally the fourth condition rules out triplet-triplet annihilation fluorescence which is known to occur in these samples in the absence of oxygen. The slight initial decay of the fluorescence in the upper trace prior to the admission of oxygen is due to this fluorescence.

As early as 1947 Kautsky and Muller reported the visual observation of a similar oxygen stimulated fluorescence burst by exposing phosphorescing dye molecules absorbed on silica gel to a sudden inflow of oxygen (186). They interpreted their results invoking the intermediacy of singlet oxygen. Subsequent attempts were made by Rosenberg and coworkers to understand the phenomenon, and they suggested that it resulted from energy transfer by vibrationally excited ground state oxygen (187-189). Because of the small singlet-triplet splitting in such dye molecules, this explanation is feasible. The fluorescing molecule used in this work has a large enough singlet-triplet splitting to unambiguously eliminate the possibility that vibrationally excited ground state oxygen could stimulate the emission and for energetic reasons requires the interaction of the electronically excited singlet states of molecular oxygen.

The proposed mechanism makes a number of kinetic predictions which are susceptible to experimental verification. It is predicted that (1) there should be a marked dependence of the intensity of the burst on the partial pressure of the oxygen and (2) the rate of diffusion of the oxygen into the matrix, (3) a square dependence of the burst intensity on the triplet population since two triplets are involved for each photon emitted (one to generate the singlet oxygen and another in the feedback step), and (4) a reduction in the burst intensity in the presence of singlet molecular oxygen quenchers. In addition to these kinetic predictions, the spectrum of the burst should coincide with the normal fluorescence spectrum of the organic acceptor.

As the fraction of oxygen in the quenching gas at constant pressure, or the total pressure of the quenching gas is reduced, the rate of triplet quenching is slowed and the fluorescence burst becomes less intense and of longer duration.

The effect of the diffusion rate of oxygen can be observed by using different methods to prepare the sample. In Figure 13, both traces are for 12:56 DBA 0.01 M in Pst. The upper trace is for the sample prepared as a fluff and the lower trace for the sample prepared as a thin film. These curves have been taken from oscilloscope traces. Since the films are denser than the fluffs, the rate of diffusion is slower and the predicted results are obtained. The rate of oxygen diffusion in the matrix can be slowed by lowering the temperature and is essentially stopped at 77° K. No burst is observed from a sample which is cooled to 77° prior to the experiment.

In Figure 14 is plotted the log of the intensity of the fluorescence burst against the log of the phosphorescence intensity (immediately prior to the admission of the quenching gas), for chrysene- $d_{12}$  0.01 M in Pdpst. The least squares slope of the graph is 1.84 with a correlation coefficient of 0.89. A similar plot for 12 BA in pst gives a slope of 1.6. Both of these numbers are in approximate agreement with the value of two predicted for the involvement of two triplet molecules in the process leading to the light emission.

In an effort to determine the relative importance of the two singlet states of oxygen ( $^1\Delta$  and  $^1\Sigma$ ) in the feedback process,

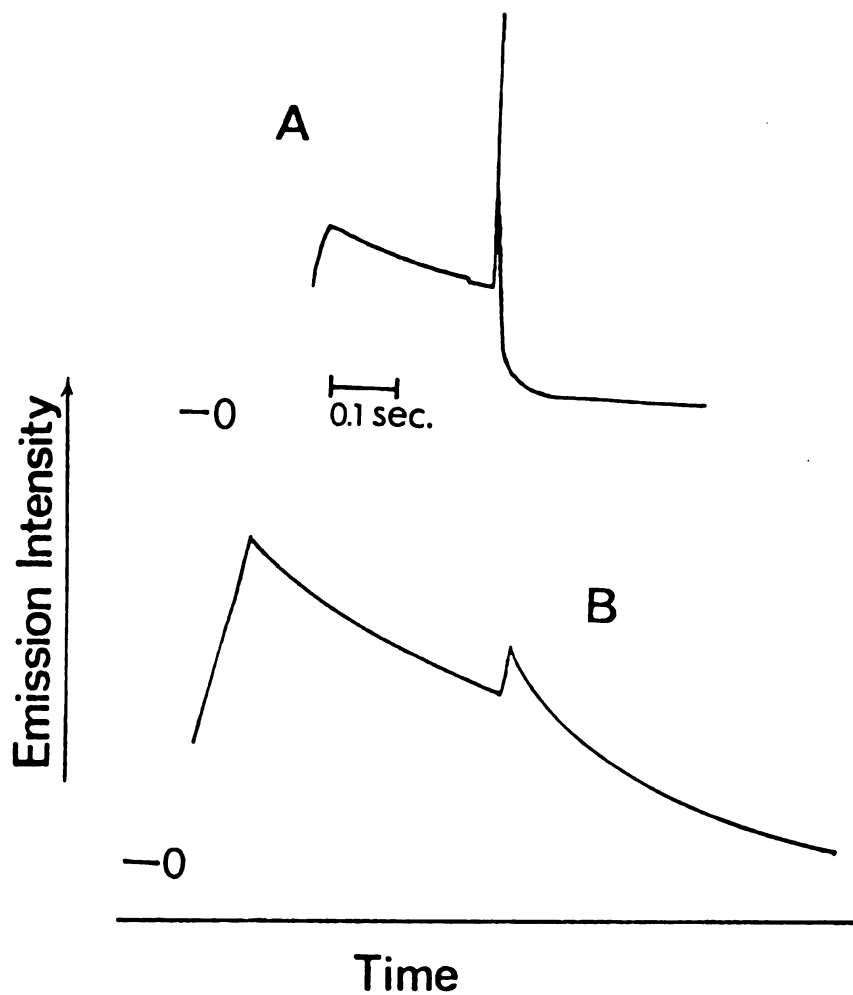


Figure 13.--Total emission showing oxygen induced fluorescence burst for 12:56 DBA ( $10^{-2}\text{M}$ ). (A) polystyrene fluffs, (B) thin polystyrene film.

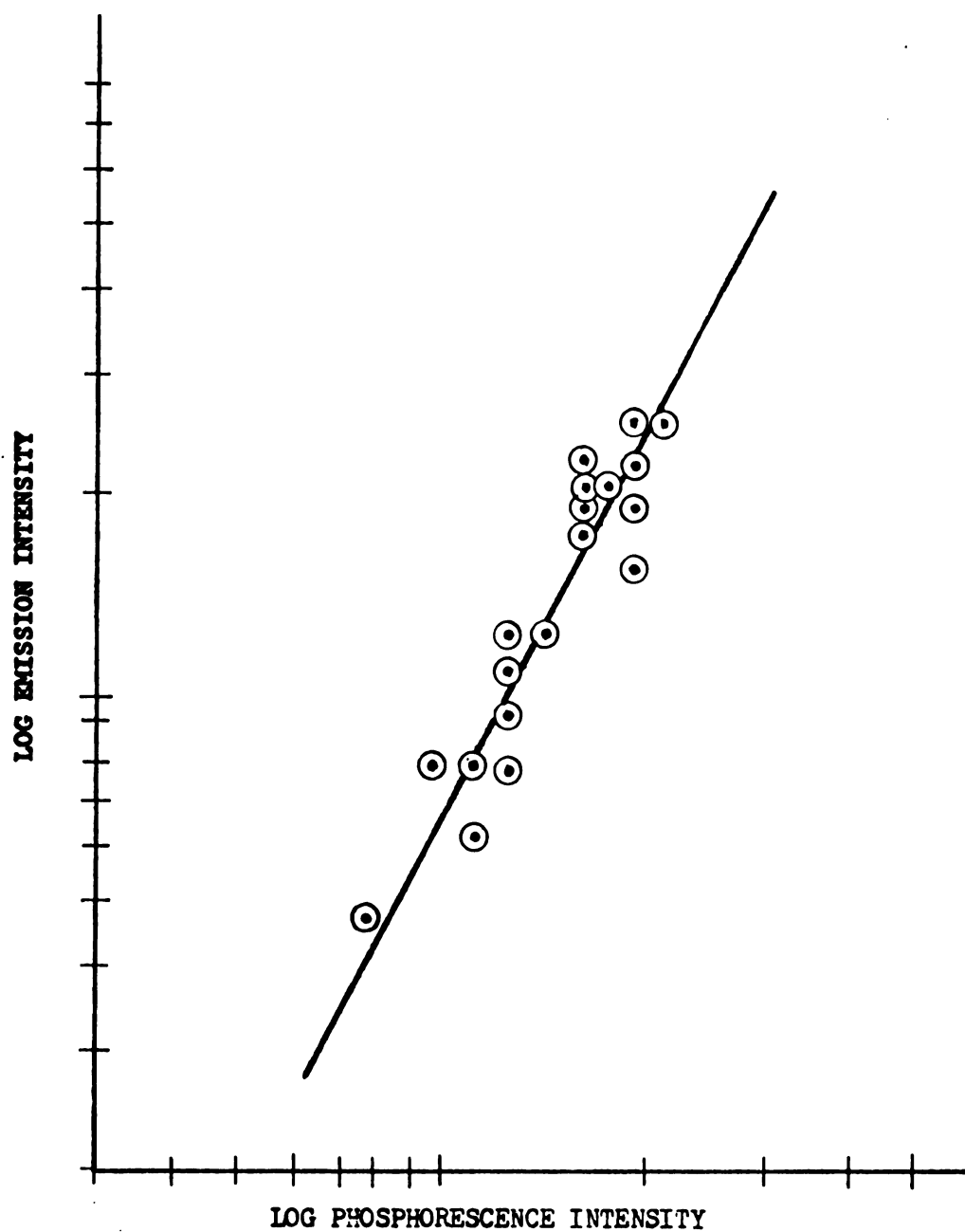


Figure 14.--Plot of log (singlet oxygen-triplet organic molecule annihilation fluorescence intensity) vs log (phosphorescence intensity) for chrysene-d<sub>12</sub> 0.01 M in deuterated polystyrene.

specific quenching experiments have been performed. It is known that  $O_2(^1\Sigma)$  is efficiently quenched by water (32,33) and that  $O_2(^1\Delta)$  is quenched much less efficiently (31). By comparing the burst intensity obtained using dry air with that obtained using air saturated with water vapor, the relative importance of the  $O_2(^1\Sigma)$  can be determined. Some possible problems with these experiments will be discussed later.

The water quenching experiments were performed by alternating between air saturated with water vapor at room temperature and air dried over  $CaCl_2$  and comparing the burst intensities for results with the same phosphorescence intensities. To be sure the water was removed from the sample after the wet run, two dry runs were done between each wet one.

The contribution from  $O_2(^1\Delta)$  can be determined by using beta carotene (36,41,56). Unfortunately it is a solid with a low vapor pressure at room temperature and must be incorporated directly into the matrix with the solute. This makes the accurate comparison of the intensity of the burst with and without beta carotene very difficult. The amount of quenching seems to be dependent on the sample preparation.

The experiments performed with the burst apparatus to investigate the feedback luminescence are: (1) observation of the burst for a number of different solute molecules, (2) determination of the spectrum of the burst for the different solutes, (3) water and (4) beta carotene quenching experiments, and (5) studies of the intensity dependence. The results of these experiments

for the solutes studied are summarized in Table 13 and discussed below.

### Chrysene

The most extensive set of experiments into the nature of the feedback luminescence have been performed with chrysene. The reasons for this are varied, it is non-carcinogenic (190), shows a large steady state fluorescence enhancement, is easily purified through vacuum sublimation (191), has a long triplet lifetime (165) which is required by the constraints of the apparatus used, and is available in deuterated form.

Chrysene is a member of group three in the feedback scheme. That is the energy difference between the first excited singlet state and the lowest triplet state is less than the excitation energy of either singlet oxygen state (See Figure 15).

The results presented in Figure 12 and discussed earlier show that for chrysene, a strong oxygen induced burst is observed. Using the fluorescence normalization procedure explained previously, a spectrum of the feedback luminescence for chrysene has been determined (Figure 16). The points define the burst spectrum; the normal prompt fluorescence spectrum for chrysene in Pst is shown for comparison. Each point in the spectrum is the average normalized intensity of several bursts on each of several samples and the error bars are the 90% confidence limits. These error bars are increased at several wavelengths due to the lack of precise resetability of the monochromator used and the tendency of the monochromator to



TABLE 13.--Summary of Results for Singlet Oxygen-Triplet Organic  
Molecule Annihilation Luminescence.

Acceptor	Emitting State	% Quenching Water	$\beta$ -Carotene	Slope Log-Log Plot
Chrysene-h <sub>12</sub>	S <sub>1</sub>	8 $\pm$ 5	90 - 99+	
Chrysene-d <sub>12</sub>	S <sub>1</sub>	10 $\pm$ 4		1.84
12:56 Dibenz- anthracene	S <sub>1</sub>	0 $\pm$ 6		
12 Benzanthracene	S <sub>1</sub>	7 $\pm$ 4	100	1.6
Pyrene	S <sub>1</sub>	8 $\pm$ 9		
	(S <sub>1</sub> •S <sub>0</sub> )	9 $\pm$ 8		
Napthalene	S <sub>1</sub>	100		
	(T <sub>1</sub> • <sup>1</sup> $\Delta$ )	4 $\pm$ 17		
Octafluoro- napthalene	none observed			
Carbazole	burst observed			

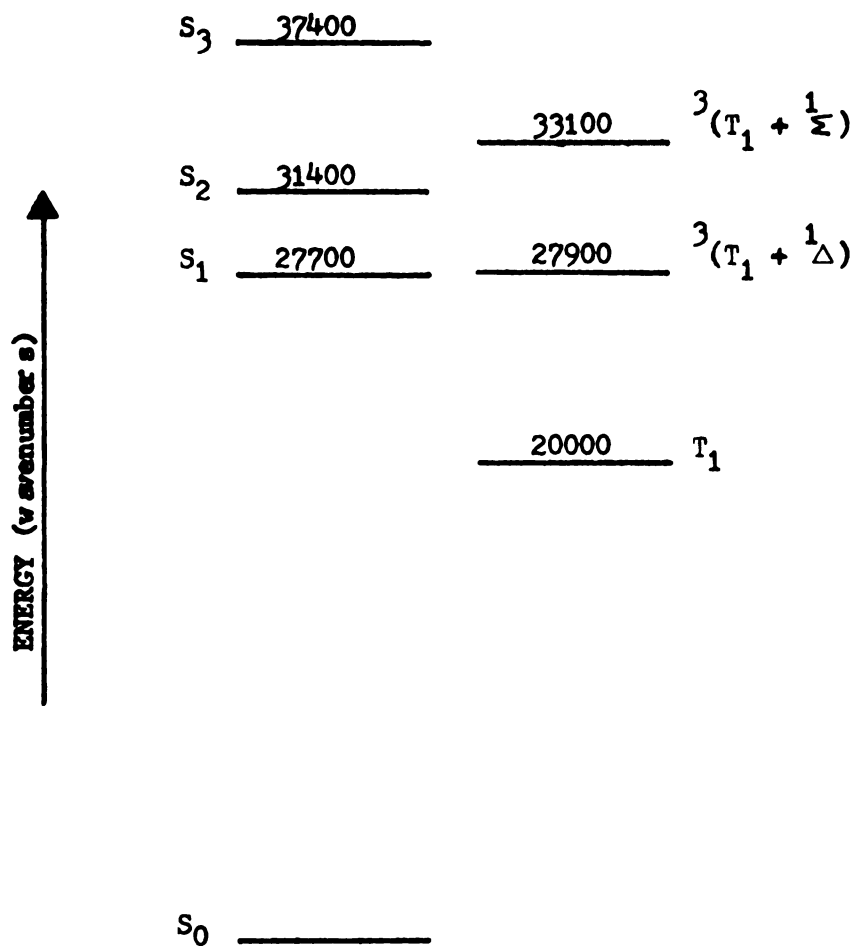


Figure 15.--Electronic Energy Level Diagram for Chrysene, including possible singlet oxygen feedback states.

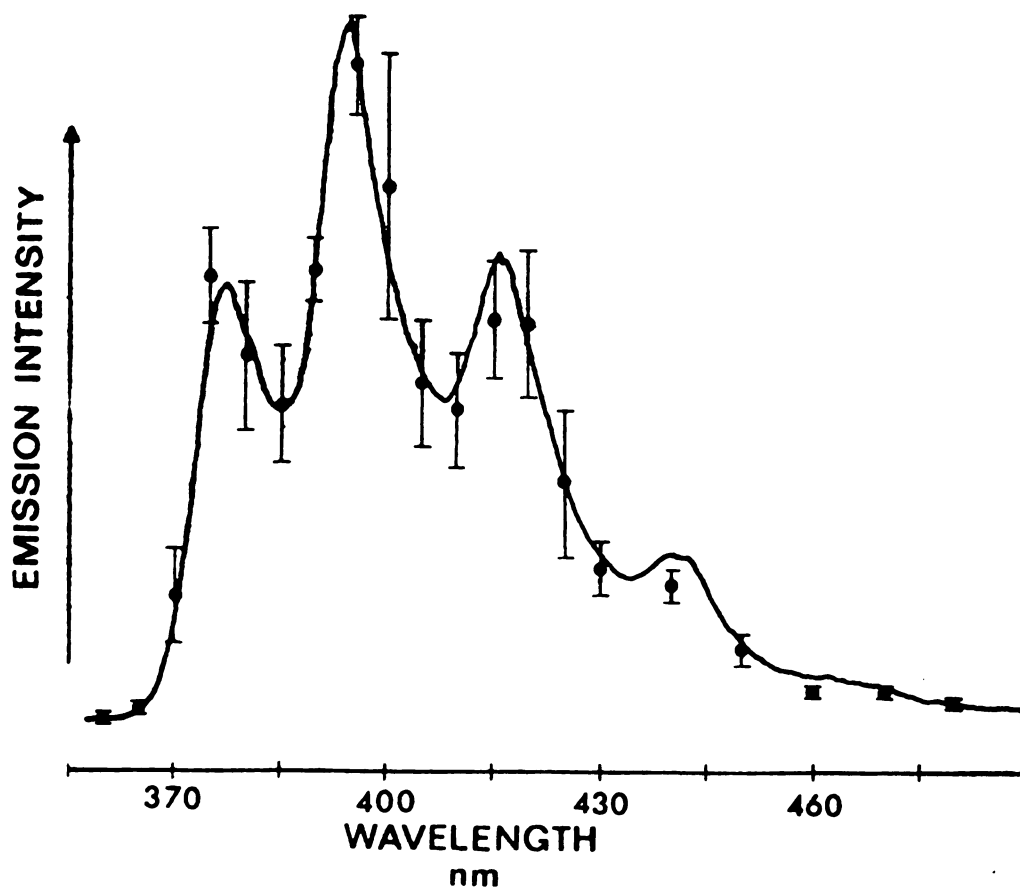


Figure 16.--Spectrum of oxygen induced fluorescence of chrysene  $10^{-2}M$  in polystyrene fluffs. The points define the oxygen induced fluorescence and the curve is the normal prompt fluorescence spectrum for the same sample recorded with the same detection system.

drift from the wavelength set during the measurements. The reference spectrum is recorded with the same monochromator and photomultiplier system for one of the samples used for the burst spectrum. The relative intensities of the two spectra are normalized to facilitate comparison.

It is clear from the close correspondence of the two spectra that they both arise from the same excited state, the first excited singlet state of chrysene and this confirms the prediction of the singlet oxygen feedback mechanism.

The water quenching experiments were performed for both chrysene- $\text{h}_{12}$  and chrysene- $\text{d}_{12}$ . The chrysene- $\text{h}_{12}$  0.01 M in Pst gave a  $8 \pm 5\%$  quenching by water and chrysene- $\text{d}_{12}$  0.01 M in Pspst gave  $10 \pm 4\%$  quenching. The uncertainty given is the 90% confidence limits and are relatively large due to the difficulty in obtaining quantitatively reproducible results. These results show that for chrysene there is a small reduction in the burst intensity due to water vapor. The interpretation of this observation is not entirely straight forward and will be discussed later.

The results of the beta carotene quenching experiments for chrysene depend on both the intensity and the preparation of the sample. For one sample with 0.01 M chrysene and 0.05 M beta carotene using the normal fluff preparation technique, the burst intensity was reduced by a factor of about ten. The reduction factor varied from ten at low phosphorescence intensities to seven at the highest intensities observed.

In another sample at the same concentration in which the fluff was partially redissolved during preparation, a quenching factor of 100 or more was measured. The lack of an identically prepared sample without beta carotene makes this number very uncertain and almost definitely too high.

Water quenching experiments on the sample containing the beta carotene did not show any appreciable effect, although the weaker intensity of the burst from this sample made the results much more uncertain.

Since the beta carotene is incorporated into the matrix in the same manner as the chrysene, it should occupy similar positions in the matrix. Also since a collision is required for the beta carotene to quench singlet oxygen (36), the singlet oxygen must be physically diffusing from the site where it is formed to the site where it is quenched.

In summary for chrysene, both states of singlet oxygen are energetically able to undergo feedback, the feedback luminescence is due to emission from the first chrysene excited singlet state, the presence of water vapor in the quenching gas reduces the burst intensity approximately 10%. Beta carotene at five times the chrysene concentration decreases the burst intensity by about 90% and the slope of the plot of the log of the burst intensity versus the log of the phosphorescence intensity of chrysene- $d_{12}$  is 1.84.

#### 12:56 Dibenzanthracene

This molecule is a member of group four in the feedback classification (Figure 17), and shows the largest steady state

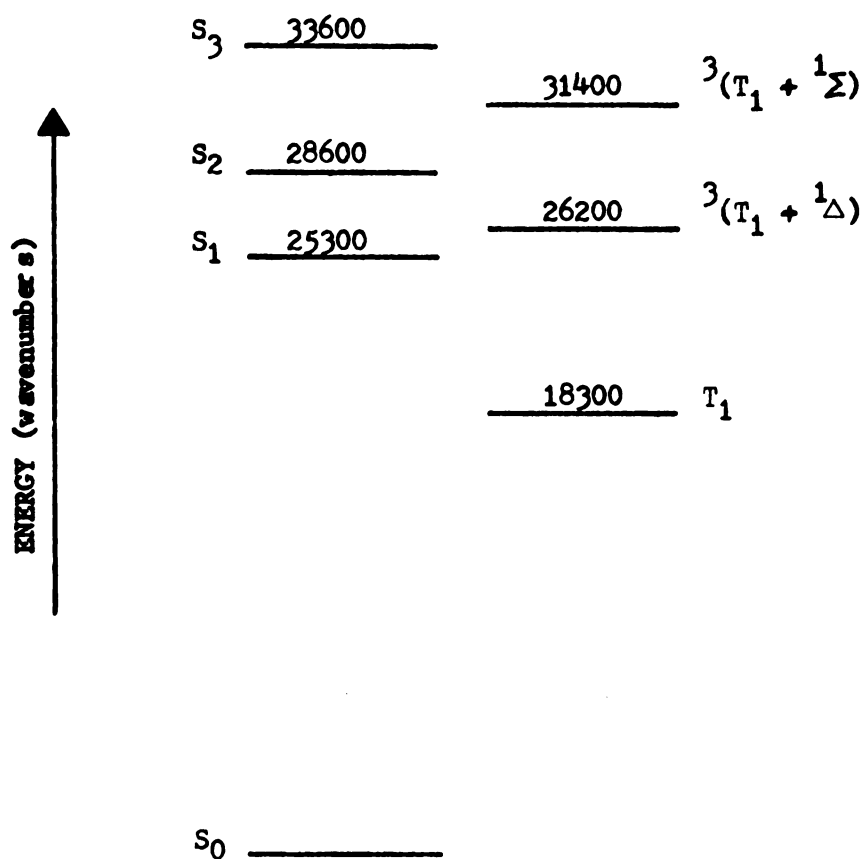


Figure 17.--Electronic Energy Level Diagram for 12:56  
Dibenzanthracene, including possible singlet oxygen  
feedback complex states.

fluorescence enhancement of all the molecules investigated. It is expected to show a strong feedback luminescence burst. As was shown earlier a strong burst is observed for 12:56 DBA in Pst fluffs.

The spectrum of the burst is shown in Figure 18. The points are the average intensity of several bursts at the indicated wavelengths recorded on a storage oscilloscope without the benefit of normalization. The error bars are an optimistic estimate of the uncertainty. The solid line is the normal fluorescence for the same sample recorded with the same detection system. It is clear that the spectrum of the burst is identical to the normal fluorescence and arises from emission from the first excited singlet state of 12:56 DBA.

Water quenching experiments on 12:56 DBA 0.01 M in Pst gives a value of  $0 \pm 6\%$  quenching. The uncertainty is the 90% confidence limit.

### 12 Benzanthrane

12 benzanthrane is a group two molecule in the feedback scheme (Figure 19). Only the  $^1\Sigma$  and the  $2(^1\Sigma) + S_0$  transitions of the proposed steps are energetically feasible. In this case a weak water sensitive burst would be expected. The feedback burst is observed for this molecule and is of only moderate intensity. Because it is not strong, it was not possible to obtain a spectrum of a quality comparable to those presented earlier with the instrumentation available. A rough spectrum has been obtained and is shown in Figure 20. The bars represent the approximate relative

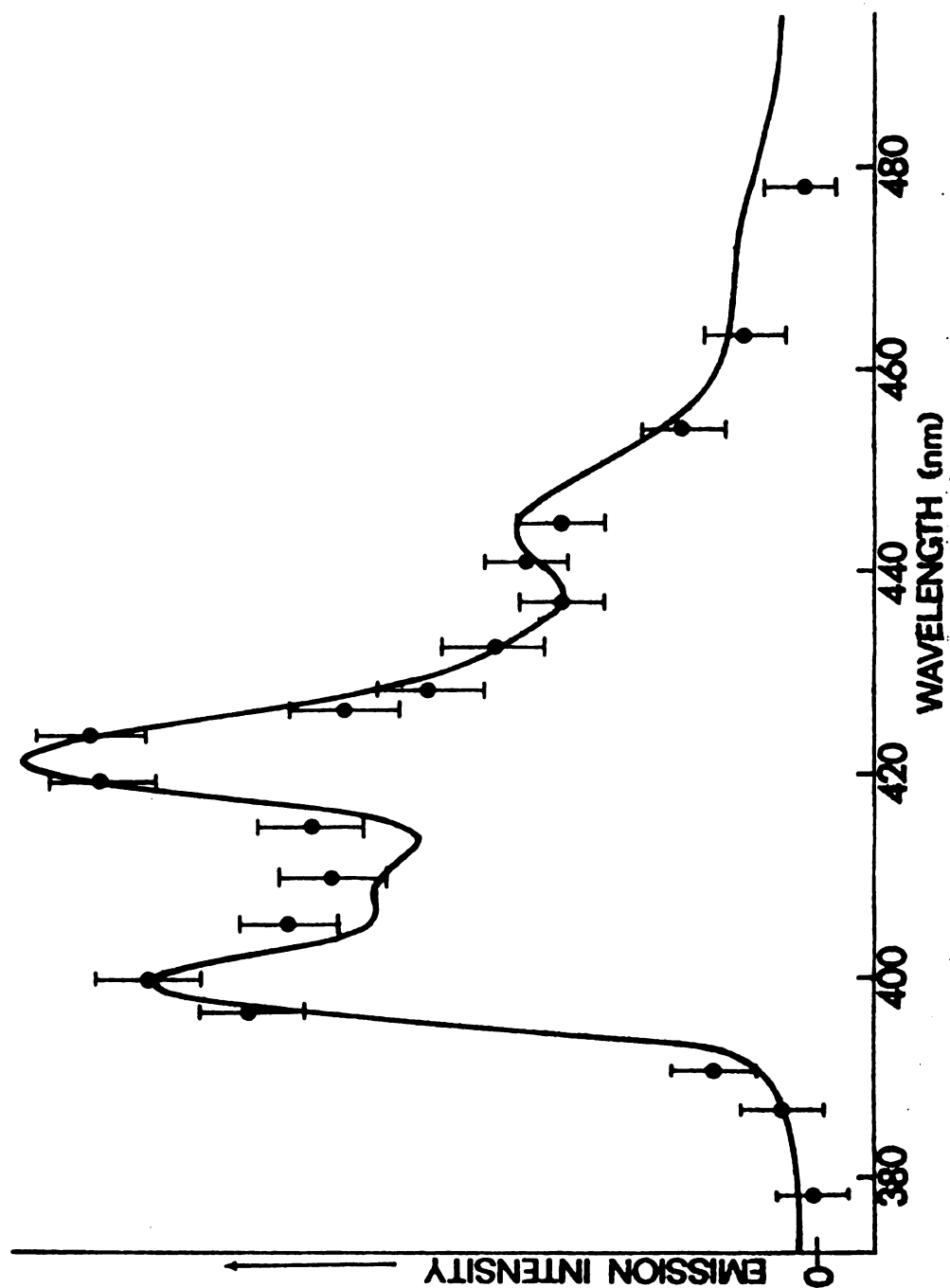


Figure 18.--Spectrum of oxygen induced fluorescence of 12:56 DBA  $10^{-2}M$  in polystyrene fluffs. The points define the spectrum of the oxygen induced fluorescence and the curve is the normal prompt fluorescence spectrum for the same sample recorded with the same detection system.



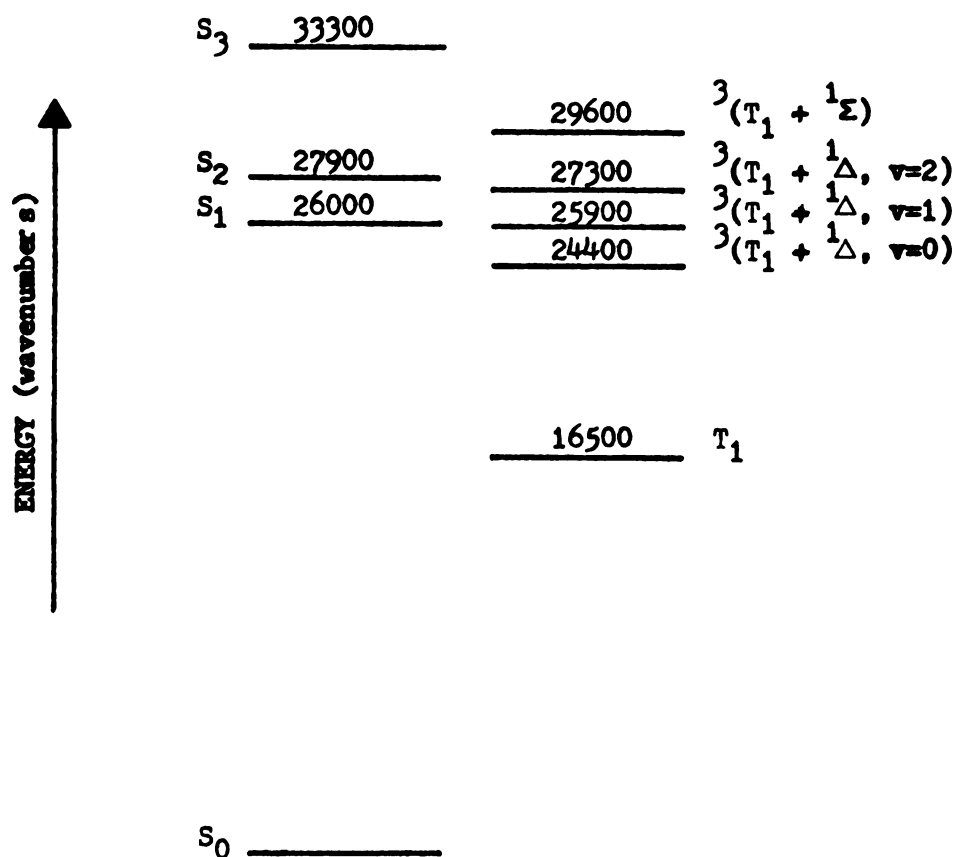


Figure 19.--Electronic Energy Level Diagram for 12 Benzanthracene, including possible singlet oxygen feedback complex states.

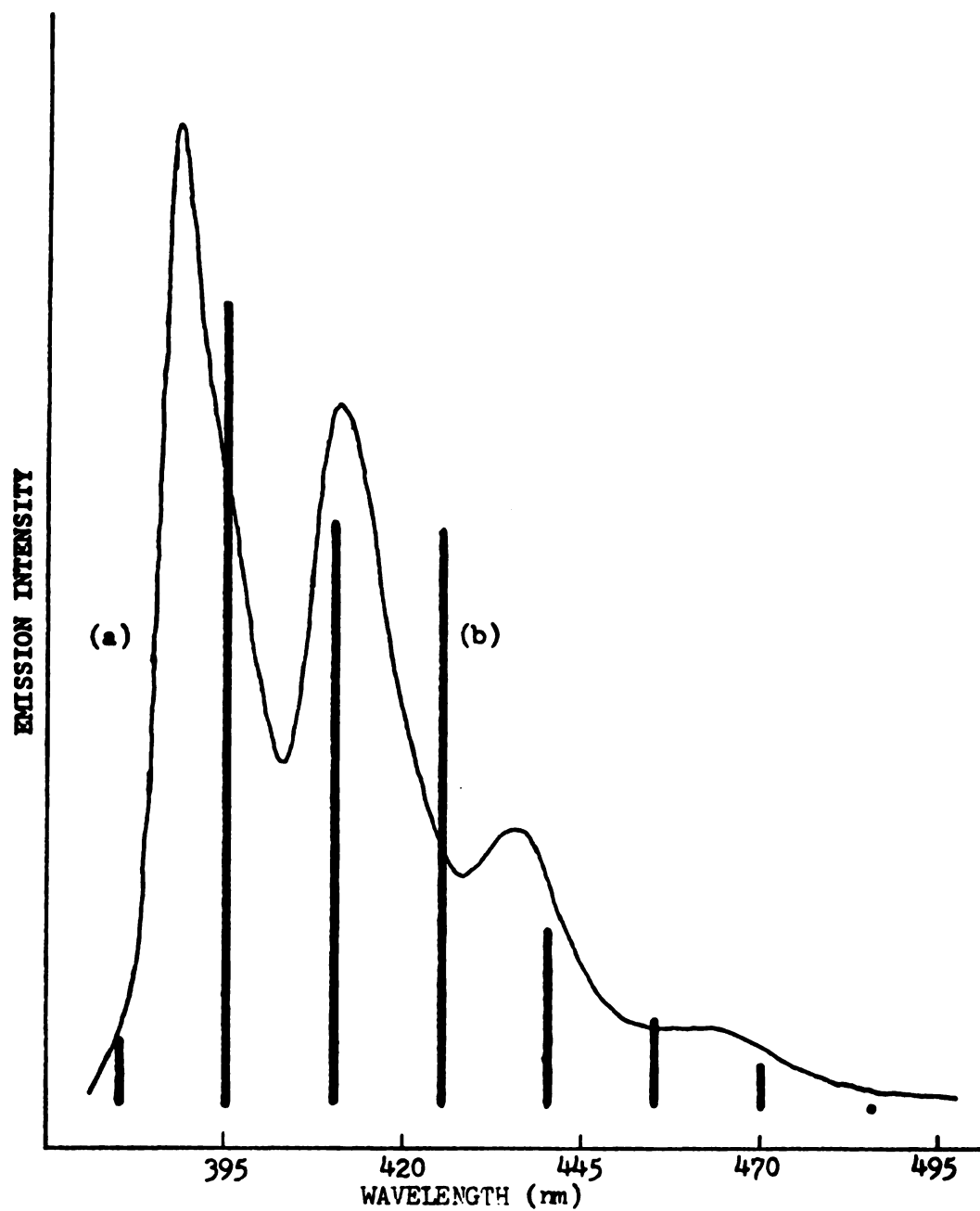


Figure 20. — Fluorescence spectrum of 12 Benzanthracene 0.01 M in polystyrene. (a) prompt fluorescence spectrum, (b) normalized intensity of singlet oxygen-triplet organic molecule annihilation fluorescence.

intensity of the burst at the indicated wavelengths. The reference spectrum was obtained at much higher resolution than the burst spectrum using a Heath monochromator and an RCA C31034 photomultiplier. The spectral correspondence for the two spectra is good and it is concluded that the emitting state in the feedback burst is the  $S_1$  of 12 BA.

The water quenching experiments on 12 BA 0.01 M in Pst gave a value of  $7 \pm 4\%$  quenching with water vapor where the uncertainty is the 90% confidence limits. The interpretation of this result is complicated by several factors and a brief discussion of these will now be given.

In all the previous measurements of the quenching of  $O_2(^1\Delta$  and  $^1\Sigma)$  by water were performed in steady state flow experiments (31-33). Under these conditions the sample is homogeneous and there is time for equilibrium to be reached. In the quenching in the fluffs, the situation is quite different. The generation and quenching of the singlet oxygen takes place over a short period of time in the advancing pressure front and is not an equilibrium situation. It is uncertain if the efficiency of quenching of  $^1\Sigma$  by water in this situation is the same as in the steady state experiments.

In addition the concentration of the oxygen in the air is six times larger than that of the water vapor. Calculations using the steady state quenching rate constants in Table 3 show that the water present in air saturated with water vapor at room temperature should reduce the lifetime of  $^1\Sigma$  by a factor of about one hundred.

The effective concentration of the water in the advancing pressure front may be different than that of the macroscopic system and change this result.

A final factor which complicates the interpretation of the water quenching results is the product of water quenching of  $^1\Sigma$  are not known. It has been suggested that  $^1\Sigma$  is quenched to a vibrationally excited level of  $^1\Delta$  (232). If this is true, and both singlet state of molecular oxygen are capable of the singlet oxygen feedback step, the water may not effect the burst intensity even though the  $^1\Sigma$  is quenched.

It is assumed here that the  $^1\Sigma$  is quenched efficiently by water and that the immediate product of the quenching is a vibrationally excited level of  $O_2(^1\Delta)$ . These assumptions lead to the following conclusions. For chrysene the burst intensity was reduced by 10% and both  $^1\Delta$  and  $^1\Sigma$  are energetically able to undergo the feedback transition. This indicates that the feedback via  $^1\Sigma$  is more efficient than the  $^1\Delta$  in this case. This is reasonable because the rate of energy transfer is known to decrease as the electronic energy of the final state approaches closer than  $1000\text{ cm}^{-1}$  to the initial state (192,193). For  $^1\Delta + T_1 \rightarrow S_1 + ^3\Sigma$  for chrysene the energy difference is about  $200\text{ cm}^{-1}$  whereas  $^1\Sigma + T_1 \rightarrow S_1 + ^3\Sigma$  the difference is  $5400\text{ cm}^{-1}$ .

For 12:56 DBA it is concluded that  $2(^1\Sigma) + S_0 \rightarrow S_1 + 2(^3\Sigma)$  is not an important feedback step since there was no reduction in the burst intensity due to water quenching. Also it is concluded that either both  $^1\Delta$  and  $^1\Sigma$  are equally efficient in the feedback step or  $^1\Sigma + T_1 \rightarrow S_1 + ^3\Sigma$  is not an important step.

For 12 BA the assumptions listed above lead to an interesting conclusion. Since the effect of the water quenching is small,  $^1\Sigma$  cannot be the major energy transfer species. The  $S_1 \rightarrow T_1$  energy difference for 12 BA is  $9500 \text{ cm}^{-1}$  (Figure 19), and the excitation energy of the  $^1\Delta$  state is only  $7882 \text{ cm}^{-1}$ . The remaining energy difference could be made up by vibrational energy of the molecular oxygen. The first vibrationally excited level of  $^1\Delta$  should be approximately degenerate with the  $S_1 - T_1$  energy gap of 12 BA (1).

The lifetime of the first vibrational level of  $^1\Delta$  in a high pressure oxygen system is found to be longer than that of the zeroth vibrational level of the same state (35,39,40). It is also found that helium is very efficient in quenching the vibrational energy of  $^1\Delta_{(v=1)}$  without changing the lifetime of the zeroth level (35). The involvement of vibrationally excited singlet oxygen could be tested using a quenching gas containing large amounts of helium.

Since no information is available to ascertain the quenching efficiency of  $^1\Sigma$  by beta carotene (36,41,55-57), the beta carotene quenching studies in which no burst at all was detected from a sample 0.01 M in 12 BA and 0.05 M in beta carotene is suggestive of the involvement of  $^1\Delta$ .

A plot of the log of the burst intensity versus the log of the phosphorescence intensity for 12 BA was made and the slope of the line was 1.6. This may indicate a lower efficiency for the feedback process than was observed in chrysene, slope 1.84, although these slopes are each determined from a single sample and the actual value is probably somewhat dependent on the sample preparation.

### Pyrene

Pyrene is a member of group one in the feedback scheme, that is only the  $^1\Sigma$  state is energetic enough to undergo feedback. Since the  $S_1 - T_1$  energy difference is  $10,000\text{ cm}^{-1}$  even the  $^1\Delta_{(v=1)}$  state has insufficient energy. The feedback luminescence would therefore be expected to be weak and water sensitive.

The feedback luminescence for pyrene 0.01 M in Pst is observed to be weak as expected but its spectrum does not correspond to the normal fluorescence of pyrene (Figure 21). It is obvious that the burst spectrum (indicated by the bars) is red shifted and has lost the vibrational structure apparent in the pyrene fluorescence.

The feedback luminescence spectrum for pyrene 0.1 M in Pst is shown in Figure 22 with the prompt fluorescence spectra for 0.1 and 1.0 M pyrene. The structureless and redshifted band in the 1.0 M pyrene fluorescence spectrum is due to the emission by the pyrene excimer (148).

It is evident that the feedback luminescence observed for pyrene 0.1 and 0.01 M is similar to the emission of the pyrene excimer, even though the contribution of the excimer to the prompt emission for these samples is small in both cases (148). It would appear that there is specific sensitization of the pyrene excimer in the triplet pyrene-oxygen system. No feedback luminescence has been observed from the 1.0 M pyrene system. This may be due to the shorter triplet lifetime observed for this system which is below the lower limit set by the design of the burst apparatus.

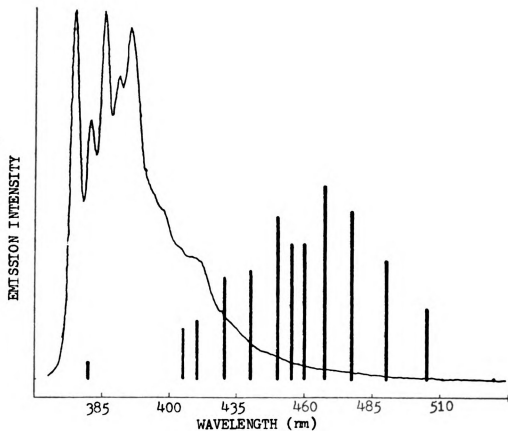


Figure 21.--Spectrum of oxygen induced luminescence of pyrene  $10^{-2}M$  in polystyrene fluffs. The bars define the spectrum of the oxygen induced luminescence and the curve is the normal prompt fluorescence for the same sample.

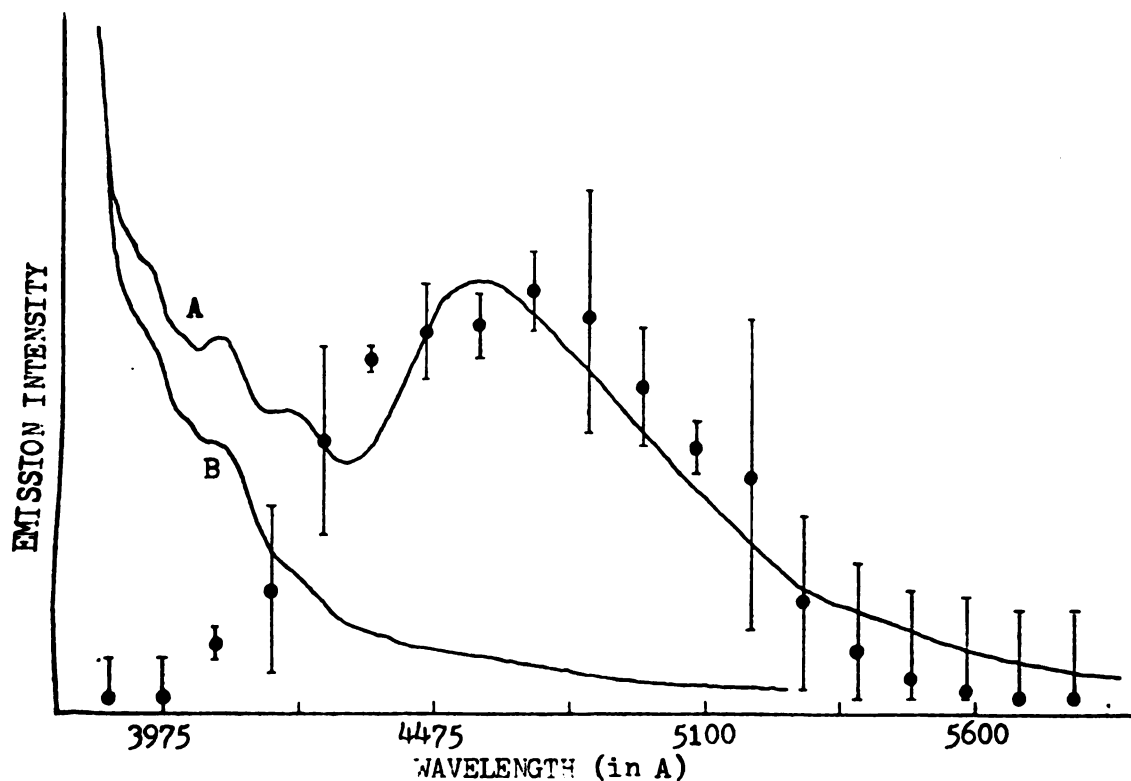


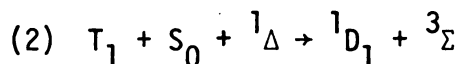
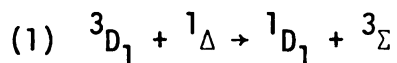
Figure 22.--Spectrum of oxygen induced luminescence for pyrene  $10^{-1}M$  in polystyrene fluffs. The points define the spectrum of the oxygen induced luminescence. Curve A is the prompt fluorescence spectrum for the same sample. Curve B is the prompt fluorescence and excimer emission of pyrene 1.0 M in polystyrene fluffs.



In addition to the excimer band just discussed, the 0.01 M pyrene sample showed a weak feedback luminescence burst at about 380 nm which is in the envelope of the normal pyrene monomer fluorescence. It was not observed in every burst for the 0.01 M sample and was never observed in a sample with a higher pyrene concentration.

Water quenching experiments on pyrene were performed on both bands observed for the 0.01 M sample. At 390 nm the intensity was reduced by  $8 \pm 9\%$  and at 470 nm the reduction was  $9 \pm 8\%$ .

In Figure 23 the energy levels for both the monomer and excimer states in pyrene are shown. Since the apparent emitting state is the  $^1D_1$  state, the first excited singlet state of the excimer, it is necessary to examine mechanisms which will sensitize this state by energy transfer from singlet molecular oxygen. Excluding the participation of the  $^1\Sigma$  state based on the results of the water quenching experiments, there are two possible ways of sensitizing the  $^1D_1$  state:



The first energy transfer pathway would imply the existence of the triplet excimer state of pyrene some 100 milliseconds after the excitation had been extinguished, the usual time lapse before the oxygen is admitted. In crystals where the triplet excimer state of pyrene has been directly observed, the lifetime of the state is on the order of a few milliseconds at low temperatures,

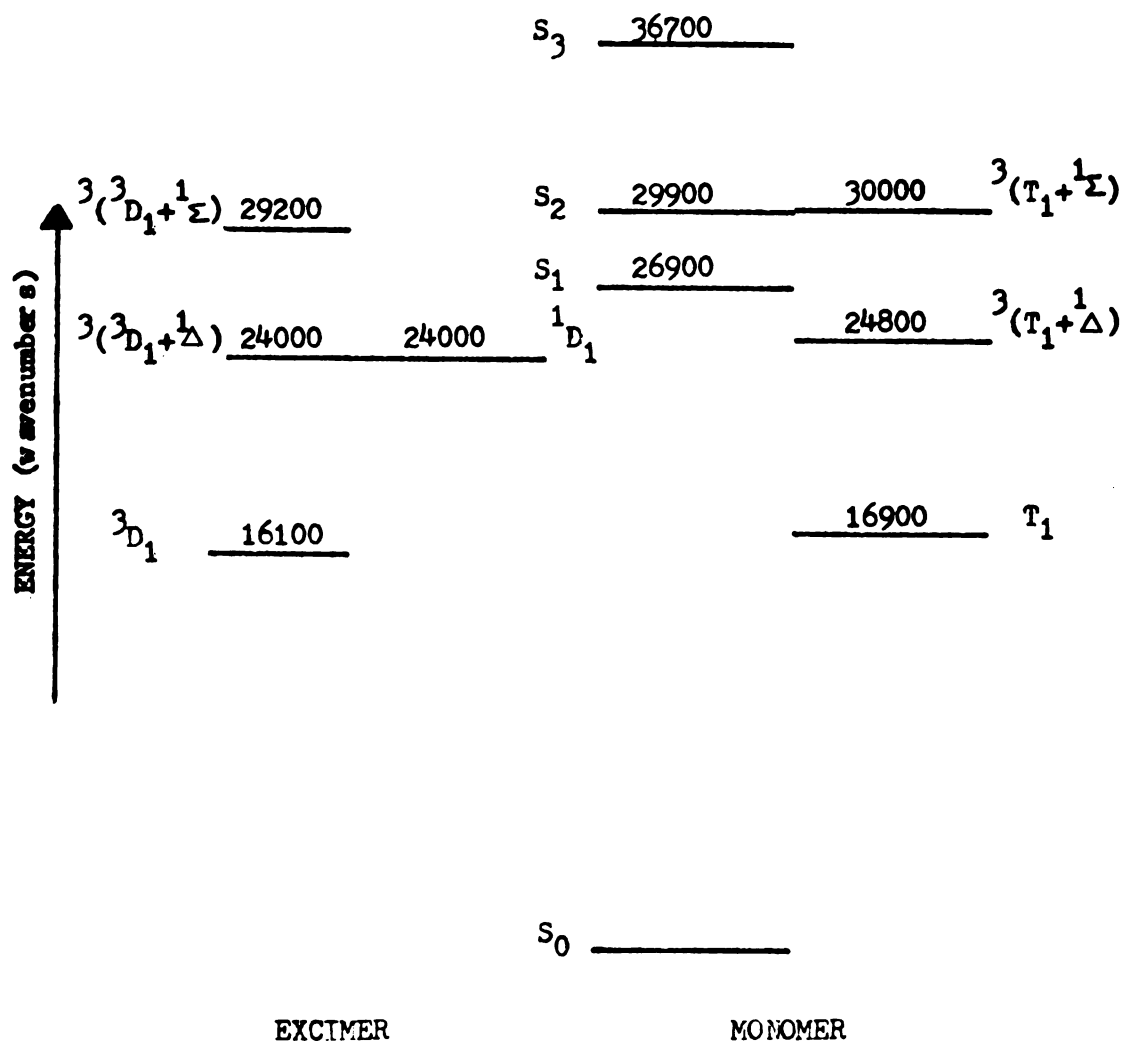


Figure 23.--Electronic Energy Level Diagram for Pyrene, including possible singlet oxygen feedback complex states.

and decreases as the temperature is increased (194,195). Also even though the triplet state excimers have been observed in concentrated solutions of 12 BA and 12:34 DBA they were not observed for pyrene (196). It therefore seems unlikely that a sufficiently high concentration of pyrene triplet excimers would be present under these conditions to account for the observed feedback luminescence.

The second pathway is singlet oxygen feedback to a latent excimer, two pyrene molecules close to the excimer geometry which accept the energy as a pair. It has been found that the excimer emission from pyrene in polymers is from pairs of pyrene molecules which interact in the ground state through Van der Waals forces (148). The pairs have both a broadened and red-shifted absorption spectrum and a different excitation spectrum from those pyrene molecules which emit the normal monomer fluorescence. Their absorption spectrum is also different from that for microcrystals. There is a time delay between the intensity maximum for the monomer and excimer emissions in polymers after a pulsed excitation, which is not found in microcrystals (148). This rules out the importance of microcrystals in the explanation of the excimer emission from pyrene in polymers.

Further evidence for the latent excimers in polymer matrices is found from the results of work at high pressures (149). In these experiments it was observed that the emission spectrum of 0.01 M in a plastic matrix can be converted from nearly pure monomer emission to nearly pure excimer emission by the application of 25

kilobars of pressure. This pressure compresses the matrix by less than 20%.

In summary it seems likely that the feedback luminescence is due to energy transfer to latent excimers with one of the partners initially in its triplet state. Though the exact oxygen state involved is not known, it would seem necessary to postulate one of the vibrationally excited levels of  $^1\Delta$  to be consistent with the water quenching results.

The weak emission at 380 nm observed for the 0.01 M pyrene sample is interpreted to be emission from the  $S_1$  state of the pyrene monomer in analogy with the results obtained for the last three solutes.

#### Napthalene

Napthalene like pyrene is a member of group one and again the feedback luminescence is expected to be weak and water sensitive.

In two experiments, both times using the napthalene sample for the first time, with careful drying of the entire vacuum line and the sample and using air dried over phosphorus pentoxide for eighteen hours, a very weak burst was observed at about 330 nm. This wavelength is in the spectral region of the napthalene fluorescence. The burst was of short duration, lasting only 0.1 millisecond as compared with 5 to 10 milliseconds for most other molecules. Repeated trials with each of these samples failed to yield another flash in this spectral region. No other sample gave a similar flash at all in this spectral region.

For all samples, in the spectral region around 375 nm, a flash of weak intensity (but much stronger and of longer duration than that just discussed) has been observed. A very rough spectrum of this band is shown in Figure 24. It is a structureless band at the resolution available, with an observed full width at half maximum equal to the spectral bandpass of the monochromator used. This implies that the actual bandwidth may be smaller than indicated by the experimental results. This band shows only a small quenching by water vapor,  $4 \pm 17\%$ .

The assignment of this band is not immediately clear. It does not energetically correspond to any transition of the isolated naphthalene molecule. If one rules out the active participation by the polymer matrix, the only transition which is energetically consistent is emission from the collision complex ( $^1\Delta \cdot T_1$ ), Figure 25. The absorption to this complex state taken from an absorption spectrum of naphthalene in solution under high pressure oxygen (114), is plotted in Figure 24. The mirror image relationship between the absorption and emission bands is good as expected for this assignment (197).

In the naphthalene-oxygen system, there are no lower states to which the ( $^1\Delta \cdot T_1$ ) complex state (oxciplex) can convert since all the excited singlet and triplet states of naphthalene are at higher energy. The oxciplex can emit, dissociate or internally convert to ( $^3\Sigma \cdot T_1$ ). In a photostationary experiment this emission would be completely masked by the normal naphthalene fluorescence and would not be detectable. Comparable transitions for most

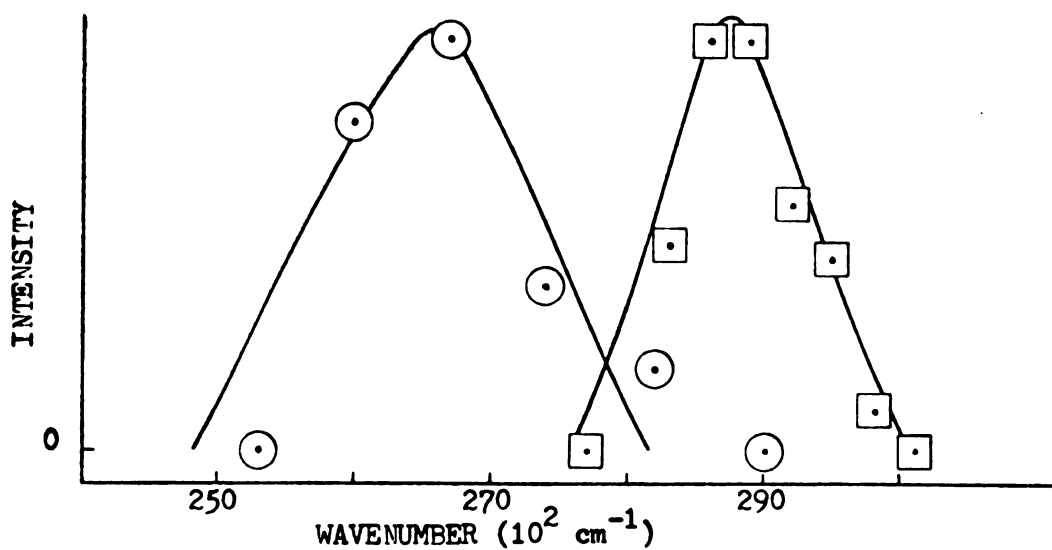


Figure 24.--Absorption and Emission spectra of naphthalene ( $T_1$ ) - molecular oxygen ( $^1\Delta$ ) oxciplx. (A) Oxciplx emission from oxygen induced luminescence of naphthalene, (B) Oxciplx absorption from absorption spectrum of naphthalene in solution under high pressure oxygen.

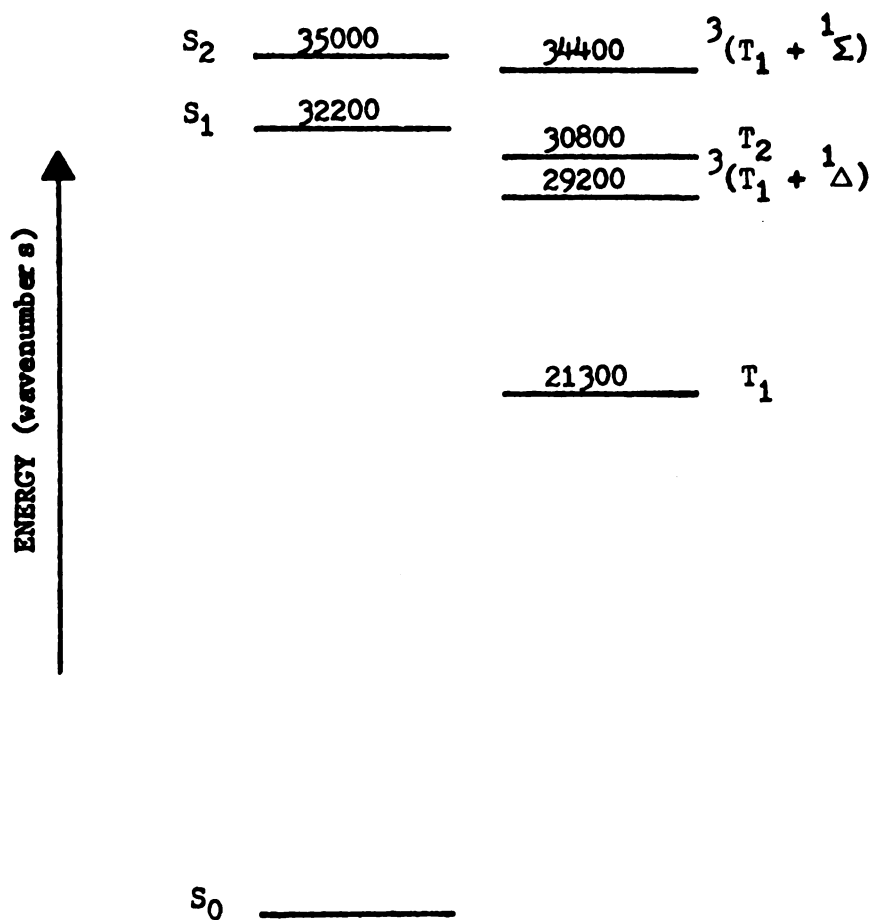


Figure 25.--Electronic Energy Level Diagram for Naphthalene, including possible singlet oxygen feedback complex states.

other aromatic hydrocarbons would not be observed since the complex state would be rapidly depopulated to yield a lower energy complex state.

#### Other Molecules

In addition to the above molecules, two other acceptors have been tested. First, carbazole which shows the burst. No spectrum or further investigations have been performed on this solute. Second, octafluoronaphthalene for which no burst was observed. It is probable that the failure to see a burst in this second case is due to the shortness of the triplet lifetime of the octafluoronaphthalene (198) which leads to the decay of the triplet population before the oxygen can be added to the sample. Many other molecules of potential interest, most notably anthracene also suffer from this restriction.

#### Discussion

The results of the singlet oxygen-triplet organic molecule annihilation experiments can be explained by the singlet oxygen feedback mechanism. (1) The emission intensity shows the correct dependence for the involvement of two triplet organic molecules and (2) shows the expected dependence on the rate of oxygen diffusion. (3) The emission intensity is reduced in the presence of beta carotene which is diagnostic for the participation of singlet molecular oxygen. (4) The spectrum of the emission for each molecule tested corresponds to the most highly luminescent state of



either the organic acceptor or the oxcipler which is energetically accessible.

In high resolution gas phase experiments Ishiwata, et al. (199) have found a triplet HNO- singlet oxygen annihilation fluorescence from the reaction  $\text{HNO} (^3\text{A}'') + \text{O}_2 (^1\Delta) \rightarrow \text{HNO} (^1\text{A}') + \text{O}_2 (^3\Sigma)$ . Giachardi, et al. (200) reacting electronically excited states of  $\text{NO}_2$  with molecular oxygen, have found evidence for the enrichment of the  $^1\Sigma$  population from the reaction  $\text{NO}_2^* + \text{O}_2 (^1\Delta) \rightarrow \text{NO}_2 + \text{O}_2 (^1\Sigma)$  in discharge experiments. These experiments illustrate the energy pooling options available by energy transfer to ground and excited state molecular oxygen.

## CHAPTER VII

### THEORETICAL ANALYSIS OF THE SINGLET OXYGEN

#### FEEDBACK MECHANISM

##### Theoretical Approach

The states of the collision complex between molecular oxygen and an organic molecule are shown in Figure 26. The complex states are labeled by the initial states of the oxygen and organic molecule. The total multiplicity of each complex state is indicated. The theoretical approach to understanding the effects of molecular oxygen on the photophysical processes in organic molecules consists of (1) defining the molecular complex between the oxygen molecule and the organic molecule and (2) evaluating the rates of transitions between the states of this complex under the influence of intermolecular perturbations or of a radiation field.

An approach to the calculation of the rates of radiationless transitions under the influence of an intermolecular perturbation which has been used for the oxygen-organic molecule complex system (61,201) is the use of the "Golden Rule" formula as adapted by Robinson and Frosch (202,203).

$$\omega(t)/t = (2\pi\rho)/(\hbar N) \beta_{el}^2 F$$

where  $\omega(t)/t$  is the rate of the transition from state  $\psi_i$  to a set of weakly coupled final states  $\psi_f$ .  $\rho$  is the density of the final

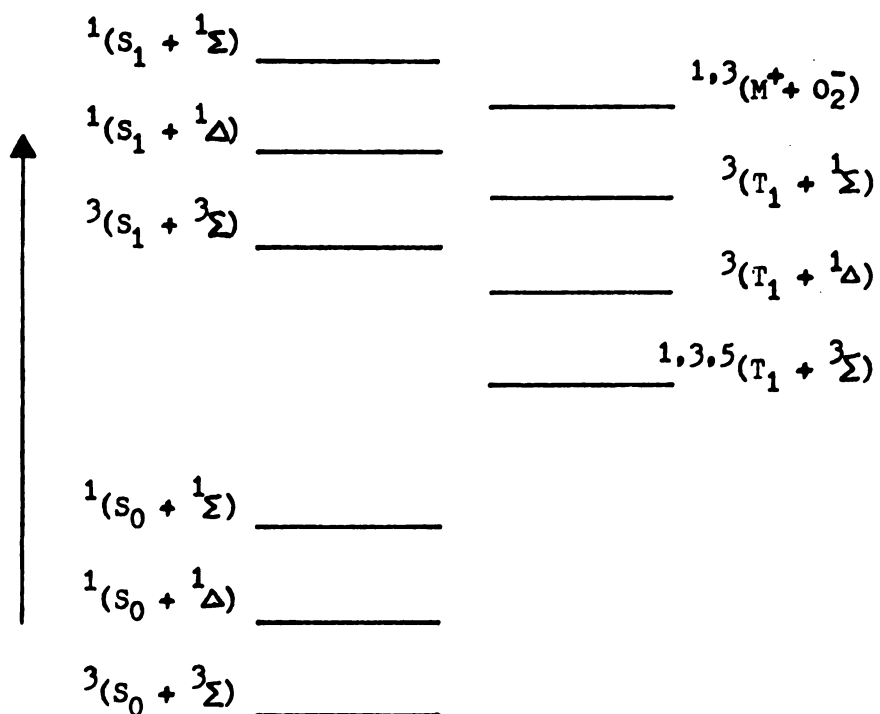


Figure 26.--Molecular Oxygen - Organic Molecule Complex States.

states which are nearly degenerate with the initial state.  $N$  is the number of molecules per cubic centimeter.

$$\beta_{e1} = (\psi_f | \hat{H} | \psi_i)$$

is the electronic matrix element and

$$F = \sum_N (\chi_f | \chi_i)^2$$

is the Franck-Condon factor with  $\psi$  and  $\chi$  being the electronic and nuclear parts of the total wavefunction separated using the Born-Oppenheimer approximation.

These equations show that the important quantities in determining the rates of the radiationless transitions are:

1. the density of final states,
2. the Franck-Condon factor, and
3. the electronic matrix element.

Of these three quantities, only the electronic matrix element can be directly calculated. The other two quantities must be estimated to evaluate the rate.

To calculate the electronic matrix elements one must first obtain the wavefunctions for the initial and final states. For intramolecular radiationless transitions the electron-electron repulsion act to directly couple the initial and final states and one can use first order perturbation theory to evaluate  $\beta_{e1}$  (125). If the value of this matrix element is small indirect mixing through

an intermediate state, usually considered to be the charge transfer state, may be important (109,113). Second order perturbation theory is necessary to evaluate the matrix element for indirect mixing. Thus to second order (201):

$$\beta_{el} = (\phi_f | \hat{H} | \phi_i) + \frac{(\phi_i | \hat{H} | \phi_{ct})(\phi_{ct} | \hat{H} | \phi_f)}{E_i - E_{ct}}$$

where  $\phi_i$ ,  $\phi_f$ ,  $\phi_{ct}$  are the electronic wavefunctions and  $E_i$  and  $E_{ct}$  are the energies of the initial and intermediate (charge transfer) states. The first term is referred to as the electron exchange mechanism (direct mixing) and the second term as the charge transfer mechanism (indirect mixing) (201).

#### Rates of the Singlet Oxygen Feedback

A calculation of the rates of the feedback processes and of the rate of quenching of the excited singlet state by molecular oxygen would determine the feasibility of the singlet oxygen feedback mechanism. These rates can be evaluated using the golden rule approach.

The electronic matrix elements were evaluated by using theoretically derived expressions given by Gijzeman (201) and shown in Table 14. The  $c_i$ 's and  $d_i$ 's are the coefficients for the atomic orbitals on the carbon atoms in the wavefunctions for the highest and second highest bonding molecular orbitals. The value of these coefficients were obtained from tables given by Coulson and Streitwieser (204). These values are shown in Table 15. The

TABLE 14.--Electronic Matrix Elements for Processes Involving Oxygen and Alternant Aromatic Hydrocarbons.

Process	Matrix Elements*	
	Exchange Mechanism ( $\text{cm}^{-1}$ )	Charge Transfer Mechanism ( $\text{cm}^{-2}$ )
$T_1 + {}^3\Sigma \rightarrow S_0 + {}^1\Delta$	$14.6 (c_1^2 - c_2^2)$	$\frac{1.5 \times 10^7 (c_1^2 - c_2^2)}{(E_{ct} - E_i)}$
$S_1 + {}^3\Sigma \rightarrow T_1 + {}^1\Delta$	$8.47 (c_1 d_1 + c_2 d_2)$	$\frac{4.3 \times 10^6 (c_1 + c_2)(d_1 + d_2)}{(E_{ct} - E_i)}$
$S_1 + {}^3\Sigma \rightarrow T_1 + {}^3\Sigma$	$13.9 (c_1 d_1 + c_2 d_2)$	$\frac{6.4 \times 10^6 (c_1 + c_2)(d_1 + d_2)}{(E_{ct} - E_i)}$

\* Calculated from the expressions given by Gijzeman, using  $4 \times 10^{-3}$  for the value of the  $2p - 2p \pi$  overlap integral.

TABLE 15.--Coefficients of Atomic Orbitals in the Wavefunction\* of the Highest and Second Highest Bonding Molecular Orbitals.

Naphthalene-D <sub>2h</sub>									
Carbon #	1	2	9						
c <sub>i</sub>	0.425	0.263	0.000						
d <sub>i</sub>	0.000	-0.408	0.408						
12 Benzanthracene (BA) - C <sub>1h</sub>									
Carbon #	1	2	3	4	5	6	7	8	9
c <sub>i</sub>	-0.003	0.203	0.095	-0.160	0.288	0.298	-0.445	0.324	0.194
d <sub>i</sub>	0.433	0.208	-0.285	-0.411	0.303	0.225	0.025	-0.111	-0.238
Carbon #	10	11	12	13	14	15	16	17	18
c <sub>i</sub>	-0.236	-0.300	0.393	0.078	-0.204	-0.167	-0.154	-0.047	0.100
d <sub>i</sub>	-0.060	0.196	-0.212	-0.351	0.102	-0.009	-0.141	0.159	0.199

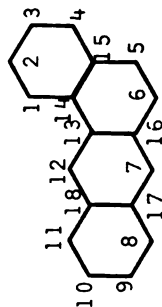
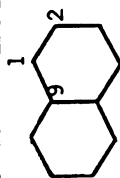
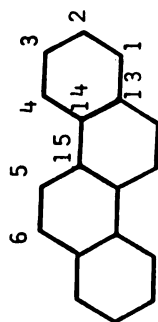


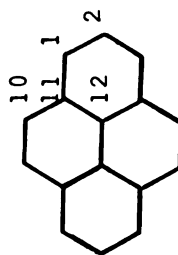
Table 15.--Continued.

Chrysene - C<sub>2h</sub>



Carbon #	1	2	3	4	5	6	13	14	15
c <sub>i</sub>	0.295	0.120	-0.233	-0.241	-0.234	-0.385	0.033	0.107	0.264
d <sub>i</sub>	-0.090	-0.337	-0.177	0.197	-0.292	-0.033	0.266	0.333	-0.200

Pyrene - D<sub>2h</sub>



Carbon #	1	2	10	11	12
c <sub>i</sub>	0.368	0.000	-0.295	0.164	0.000
d <sub>i</sub>	-0.186	-0.424	0.138	0.260	0.277



TABLE 15.--Continued.

12:56 Dibenzanthracene (DBA) - C<sub>2h</sub>

Carbon #	1	2	3	4	5	6	7	15	16
c <sub>i</sub>	0.056	0.216	0.046	-0.194	0.319	0.289	-0.368	-0.007	-0.190
d <sub>i</sub>	0.319	0.043	-0.289	-0.241	0.151	-0.020	0.231	-0.323	0.175
Carbon #	17	18							
c <sub>i</sub>	-0.139	-0.182							
d <sub>i</sub>	0.124	-0.165							

\* c<sub>i</sub> is for highest bonding orbital, d<sub>i</sub> is for second highest bonding orbital, values taken from Coulson and Streitwieser (204).

appropriate value of the term containing the  $c_i$ 's and  $d_i$ 's is not clearly defined since for each C-C bond a different value is obtained. The root-mean-square average of the values obtained for all the bonds around the perimeter of the molecule in question was computed and used to evaluate the electronic matrix elements for that molecule. The values of these terms for each hydrocarbon investigated are shown in Table 16.

TABLE 16.--Root-Mean Square Average of Terms in Atomic Orbital Coefficients for Aromatic Hydrocarbons of Interest.

Molecule	$(c_1 - c_2)$	$(c_1d_1 + c_2d_2)$	$(c_1 + c_2)(d_1 + d_2)$
Chrysene	0.04	0.099	0.08
12:56 DBA	0.065	0.04	0.06
12 BA	0.066	0.09	0.129
Pyrene	0.09	0.05	0.12
Napthalene	0.13	0.12	0.21

In the expression for the matrix elements evaluated using the charge transfer mechanism, the difference in the electronic energy of the charge transfer state and the initial state of the complex appears in the denominator. The energy of the charge transfer state is not known for the hydrocarbons of interest here but can be estimated in the following way. The energy of the charge transfer state is given by (109)

$$E_{ct} = I_p - E_a - W$$

where  $I_p$  is the ionization potential of the organic donor,  $E_a$  is the electron affinity of the molecular oxygen, and  $W$  is the electrostatic and other interaction energies of the charge transfer state. The oxygen charge transfer absorption has been reported for benzene in the gas phase at  $45,600 \text{ cm}^{-1}$ . Using this energy to evaluate  $W$  and assuming that  $W$  remains constant for all other aromatic hydrocarbons, the energy of the charge transfer state can be calculated from:  $E_{ct} = I_p - 3.5 \text{ eV}$ . This approximation places the charge transfer state above the first excited singlet state for all the aromatic hydrocarbons considered here.

The Franck-Condon factors were evaluated using the procedure suggested by Benson and Geacintov (140). It has been shown that the  $E_0$  term in the semi-empirical equation derived by Siebrand relating the magnitude of the Franck-Condon factor to the energy gap, corresponds to the part of the electronic energy which is not dissipated by the C-H stretching modes of the hydrocarbons (193, 206).  $E_0$  is found to decrease with decreasing  $E$  (the energy gap), and a plot of  $E_0$  versus  $E$  for chrysene is given by Shlag, et al. (193). The value of  $E_0$  for each  $E$  was determined from this graph and used for all the hydrocarbons considered. Siebrand's expression (207)

$$\log F(E) = -m (E - E_0)/\eta - 0.74$$

was then used to estimate the Franck-Condon factor.  $m = 10^{-4}$ ,

$$\eta = N_h(N_h + N_c)^{-1}.$$

The plot of Schlag, et al. (193) only extends down to an energy gap of approximately  $1500 \text{ cm}^{-1}$ . Many of the energy gaps of interest in the present calculations are smaller than this. To obtain an estimate of the Franck-Condon factor for energy gaps less than  $1500 \text{ cm}^{-1}$  the plot was extrapolated to zero and the same equation used. This procedure yields Franck-Condon factors which are about constant with energy gap below about  $1500 \text{ cm}^{-1}$ . The values of  $F$  and of the electronic matrix elements in  $\text{cm}^{-1}$  for both the exchange and charge transfer mechanism for each hydrocarbon of interest are given in Table 17.

Finally to calculate the values of the radiationless transition rates, one needs a value for the density of final states. According to Robinson and Frosch (203), the density of final states can be replaced by the vibrational relaxation time which they estimate should be about  $10^{-11}$  sec. Substituting this value and the appropriate values for the constants into the golden rule formula and multiplying by the spin statistical factor,  $g$ , one has

$$k = 0.71 \times 10^{12} g \beta_e^2 F$$

Using this equation and the values given in Table 17, the rates have been calculated and are given in Table 18. It will be seen that the singlet oxygen feedback rate is approximately an order of magnitude faster than the corresponding quenching of the excited singlet state. It will also be seen that the charge transfer interaction is more important in determining the rate of both processes than the direct mixing.

TABLE 17.--Values of Electronic Matrix Elements\* and Franck-Condon factors for Aromatic Hydrocarbons of Interest.

Process	Chrysene	12:56 DBA	12BA	Pyrene	Napthalene
$1(T_1 + {}^3\Sigma) \rightarrow$ ex	1.2	0.95	1.3	1.3	1.9
$1(S_0 + {}^1\Delta)$ e1 ct	82	59	85	83	124
$F (x10^3)$	1.8	4.2	11	7.8	1.5
-----					
$3(S_1 + {}^3\Sigma) \rightarrow$ ex	0.34	0.34	0.56	0.42	1.0
$3(T_1 + {}^1\Delta)$ e1 ct	63	30	71	63	117
$F$	0.22	0.23	0.23	0.17	0.15
-----					
$3(S_1 + {}^3\Sigma) \rightarrow$ ex	0.56	0.56	0.92	0.70	1.7
$3(T_1 + {}^3\Sigma)$ e1 ct	91	41	132	124	280
$F (x10^3)$	19.3	23	7.2	4.5	4.9

\* in  $\text{cm}^{-1}$ .

TABLE 18.--Rate of Intramolecular Radiationless Transitions Between the States of the Complex  
in  $\text{sec}^{-1}$ .

Molecule	$^1(T_1+^3\Sigma) \rightarrow$		$^1(S_0+^1\Delta)$		$^3(S_1+^3\Sigma) \rightarrow$		$^3(T_1+^1\Delta)$		$^3(S_1+^3\Sigma) \rightarrow$		$^3(T_1+^3\Sigma)$	
	Exchange	Charge Transfer	Exchange	Charge Transfer	Exchange	Charge Transfer	Exchange	Charge Transfer	Exchange	Charge Transfer	Exchange	Charge Transfer
Chrysene	$2 \times 10^8$	$9 \times 10^{11}$	$2 \times 10^{10}$	$6 \times 10^{14}$	$1 \times 10^9$	$3 \times 10^{13}$						
12:56 DBA	$3 \times 10^8$	$1 \times 10^{12}$	$2 \times 10^{10}$	$1 \times 10^{14}$	$2 \times 10^9$	$7 \times 10^{12}$						
12 BA	$1 \times 10^9$	$6 \times 10^{12}$	$5 \times 10^{10}$	$6 \times 10^{14}$	$1 \times 10^9$	$2 \times 10^{13}$						
Pyrene	$1 \times 10^9$	$4 \times 10^{12}$	$2 \times 10^{10}$	$5 \times 10^{14}$	$5 \times 10^8$	$2 \times 10^{13}$						
Napthalene	$4 \times 10^8$	$2 \times 10^{12}$	$1 \times 10^{11}$	$1 \times 10^{15}$	$3 \times 10^9$	$7 \times 10^{13}$						

### Oxciplex Emission

The electronic matrix element for the oxciplex transitions in naphthalene has been calculated using expressions similar to those above, also given by Gijzeman (201). A value of  $2.5 \text{ cm}^{-1}$  for mixing through  $S_3$  was obtained. The oscillator strength of an induced transition,  $f_b$  with a frequency of  $\nu_b$  can be estimated using (203):

$$f_b = f_e (\nu_b/\nu_e)(\beta^2/\Delta E)$$

where  $f_e$  is the oscillator strength of the mixing state with a frequency  $\nu_e$ ,  $\Delta E$  is the energy difference between B and E, and  $\beta$  is the electronic matrix element coupling the two states. Using this equation and assuming an oscillator strength of one for the  $S_3$  state in naphthalene, one gets a predicted oscillator strength of  $2 \times 10^{-8}$  for the simultaneous transition. This low value would be expected since it is a two electron transition.

If this oscillator strength is of the right order of magnitude, the oxciplex must be relatively stable since the predicted radiative lifetime is on the order of a tenth of a second (103) and emission from this state is observed.

### Conclusions

In conclusion even though these values are not expected to be very accurate as far as the absolute value is concerned, it is hoped that the relative rates of the processes are predicted correctly. These rates predict that the feedback rate should be

faster than the quenching of the triplet state by ground state oxygen and comparable to the rate of oxygen quenching of the excited singlet state.



## CHAPTER VIII

### SUMMARY

The investigation of the singular unexplained observation of increased fluorescence in the presence of molecular oxygen has lead to the proposal of the singlet oxygen feedback mechanism and the discovery of singlet oxygen-triplet organic molecule annihilation luminescence. The singlet oxygen feedback mechanism states: if the energetic requirements are met, electronic energy transfer from singlet molecular oxygen to the triplet state of the acceptor molecule can generate the excited singlet state of the acceptor molecule (119).

This mechanism has been verified by the observation of singlet oxygen-triplet organic molecule annihilation luminescence for a number of systems. It is found that the luminescence generated by the singlet oxygen feedback mechanism corresponds to the emission from the most highly luminescent state of either the free organic molecule or the oxygen organic molecule complex which is energetically accessible. The feedback mechanism can lead to:

- (1) emission from the first excited singlet state of the free organic molecule in for example chrysene, 12:56 DBA, and 12 BA;
- (2) emission from the excimer state of the organic acceptor in pyrene, even though the contribution of the excimer emission to

the prompt photoexcited emission is small for these samples; (3) emission from the oxciplex ( $T_1 \cdot {}^1\Delta$ ) for those molecules which do not have either singlet or triplet states other than  $T_1$ , which are of lower energy than the oxciplex. An example is naphthalene.

The photostationary experiments show that the amount of oxygen induced fluorescence enhancement for a given sample is dependent on (1) the intensity and wavelength of the exciting radiation, (2) the particular solute molecule and its concentration, (3) the organic polymer matrix, (4) the partial pressure of oxygen, and (5) the relative positions of the excitation and detection systems. In addition it was found that the spectral distribution of intensity of the oxygen enhanced fluorescence is shifted to the red in comparison to the prompt fluorescence spectrum of an evacuated sample.

Since the intensity shift and the enhanced fluorescence were observed in the simulated quenching experiments in the absence of molecular oxygen, a number of processes involving oxygen only as a triplet quencher which would lead to enhanced fluorescence were considered. These include (1) ground state depopulation, (2) the inner filter effect, (3) reabsorption, and (4) intermolecular electronic energy transfer. The magnitude of the ground state depopulation in the absence of oxygen was determined in cross beam experiments using triplet-triplet absorption measurements. It was found that the amount of depopulation of the ground state was smaller than the amount of enhancement of the fluorescence by oxygen.

Quantitative estimates of the importance of the other processes to the oxygen enhanced fluorescence in a photostationary experiment cannot be made. The reabsorption of the fluorescence by the triplet manifold of the organic acceptor in the absence of oxygen seems to account for the observed intensity shift in the enhanced fluorescence. The importance of the singlet oxygen feedback mechanism under photostationary conditions is not known.

Experiments have been conducted in attempts to observe the expected oxygen dependent fluorescence in a system equilibrated with oxygen. Nanosecond time resolved spectroscopy has been used to observe the decay of the fluorescence in the presence and absence of oxygen. The systems investigated include (1) biacetyl in the gas phase, (2) biacetyl in solution, (3) chrysene and 12:56 DBA in polystyrene, and (4) pyrene in polystyrene. No oxygen dependent fluorescence component was observed in the decay for any of these systems.

The "Golden Rule" formula has been used to estimate the rates of the competing processes in the singlet oxygen feedback mechanism. It was found that the rate of the singlet oxygen feedback is an order of magnitude faster than the competing quenching of the excited singlet state by ground state oxygen. The singlet oxygen feedback may be further favored by rapid dissociation of the complex after intramolecular energy transfer, due to excess vibrational energy of the complex after the transfer.

Several aspects of this work deserve further investigation.

(1) A determination of the spectroscopic properties of the

oxygen-organic molecule complex should be undertaken. This could perhaps be accomplished through the use of supersonic molecular beams in conjunction with a determination of the excitation spectrum.

(2) The importance of excess vibrational energy in the oxyciplex to the path of its deactivation should be determined. This could be investigated by using laser excited singlet oxygen (generated in various vibrationally excited levels) in a reaction with a beam of triplet acceptors. (3) An improved version of the burst apparatus should be built so a wider variety of molecules can be investigated. These improvements should include (1) a reduction in the time between the shut-off of the excitation and the admission of the oxygen, (2) a faster way to get the oxygen in contact with the solute, and (3) a matrix which would not limit one to nonpolar solutes. Systems of interest would include (1) other aromatic hydrocarbons such as anthracene, (2) heterocyclics and molecules with lowest  $n-\pi^*$  such as benzophenone, and (3) biomolecules such as chlorophyll.

In conclusion, the singlet oxygen-triplet organic molecule annihilation fluorescence may account for the weak chemiluminescence of many chemical systems which require molecular oxygen. The possibility of energy summation through the singlet oxygen feedback mechanism may be important in biological systems.

## APPENDIX

## APPENDIX

### NANOSECOND TIME RESOLVED SPECTROMETER

#### Theory of Statistical Sampling Method

In the statistical sampling technique, one detects not more than one photon per excitation pulse. The probability of detecting this photon per unit time is proportional to the number of excited species at that time which is proportional to the decay function of the sample. The time distribution of the detected photons will give the decay function of the sample (214).

#### Instrumentation

The instrument described here is similar to the Ortec 9200 Nanosecond Spectrometer, but with several important changes. Most of the electronics modules were obtained from Ortec and the operating manuals which come with them should be read for specific details about their operation and adjustment. In addition the Ortec Application Note AN 35 was found very useful.

1. Lamp: The excitation source used in this instrument was a Model 510A Nanosecond Lamp obtained from Photochemical Research Associates (PRA) and has several advantages over the standard Ortec Lamp. The model 510A is a gated lamp which allows variable frequency excitation and higher intensities than free running lamps. It has a built-in 1-P28 which is used to detect the time of the excitation pulse. Some problems were encountered

with this lamp. It is not known whether the problems encountered are characteristic of this type of lamp in general or of this one in particular. In addition to the main excitation pulse of several nanoseconds duration, there was a weak pulse beginning about two microseconds after the main pulse and lasting until after forty microseconds. This secondary pulse is only a tenth of a percent of the main pulse but is sufficient to obscure any weak luminescence from the sample which occurs in that time region. The time profile of the secondary pulse could be changed by changing the frequency of the lamp and the voltage applied across the electrodes. The optimum conditions for this lamp were found to be 30 KHz., 7KV, 1 cm gap, and 0.5 atm.  $N_2$ .

2. Start channel: The start channel is used to detect the time of the excitation pulse. In this instrument, it consisted of an 1-P28, an Ortec 417 Fast Discriminator and an Ortec 425 Nanosecond Delay for calibration purposes. Fifty ohm cable was used throughout.

3. Stop channel: The stop channel is used to detect the time of the arrival of the emitted photon. In this instrument, a Phillips 56 D DUVP photomultiplier was used with an Ortec 454 Timing Filter Amplifier and a 463 Constant Fraction Discriminator. Again fifty ohm cable was used throughout with a fifty ohm terminator at the input of the 454.

4. TAC and PHA: The TAC converts the time between the start and stop signals to a voltage pulse, the height of the pulse is proportional to the lapsed time. The pulse height

analyser then converts the pulse height to a channel number and stores the result. The TAC used here was an Ortec 457 Biased Time to Pulse Height Converter and the PHA was a Northern NS-600 Econ Series Pulse Height Analyzer. Ninety-three ohm cable was used to connect these two modules.

5. Time resolved spectra: To collect spectra as a function of time after the exciting pulse, several additions to the above equipment are necessary. Another single channel analyzer is needed. The output of the TAC is then run through the SCA and only those events which occur in the time region of interest are recorded. One can either connect the output of the SCA to a ratemeter and record the output of the ratemeter directly with a recorder or use a multichannel scalar to count the number of events per dwell time at the output of the SCA as the spectrum is scanned.

6. General Considerations: To give the maximum flexibility for sample size and to reduce the light leaks, the monochromator and photon counting PMT were placed inside a light tight box (2 x 2 x 3 feet) with the excitation source mounted on the outside.

### Systems Investigated

1. Biacetyl: The photochemical and photophysical processes in biacetyl have been well studied. It has a relatively high phosphorescence quantum yield ( $\phi_p = 0.145 \pm 0.03$ ) (208). The fluorescence quantum yield is low ( $\phi_f = 2.6 \times 10^{-3}$ ) (208-212).



The rate constants of nearly all the intramolecular processes have been determined (211) as well as those for triplet-triplet annihilation (212) and quenching of the triplet state by molecular oxygen (211).

The experiments performed on biacetyl involved determining the luminescence spectrum at various times after the nanosecond excitation pulse for mixtures containing varying amounts of biacetyl vapor and oxygen. The low signal to noise due to the weak fluorescence intensity, made these experiments difficult. The results of these experiments gives no clear evidence for the production of any feedback fluorescence.

The reason for the failure to detect the feedback fluorescence in the vapor phase biacetyl may be due in part to the relatively low intensity of the exciting pulse. Assuming a molar absorptivity of ten for biacetyl (213), a vapor pressure of 40 torr, a flash intensity of  $10^7$  photons per flash, and an absorbing path-length of ten centimeters, about  $5 \times 10^6$  photons are absorbed. Since the triplet quantum yield is almost unity (208), approximately this same number of triplets are formed. The volume of excitation is approximately twenty cubic centimeters which gives the triplet population as  $2 \times 10^5$  triplets per cc. With two torr oxygen there are  $3 \times 10^{11}$  times as many ground state oxygen molecules as triplet biacetyl so it may be expected that the triplet biacetyl molecules will be completely quenched before there is an appreciable chance for encountering a singlet oxygen.

2. Hydrocarbons in polymer matrices: Since the singlet oxygen-triplet organic molecule annihilation fluorescence has been observed for a number of aromatic hydrocarbons in polymer matrices, it was hoped that these systems would show some effect of oxygen on the luminescence other than normal quenching in a system which was equilibrated with oxygen before excitation. Chrysene, 12:56 DBA and pyrene were all studied both as a function of time and wavelength with no new observations.

In the burst experiments the oxygen comes in as a pressure wave. The singlet oxygen formed by quenching the most accessible triplets on the outer parts of the matrix are then pushed into the matrix where unquenched triplets are waiting. One does not have this sort of a situation in a system which is equilibrated with oxygen before the triplets are formed. In these systems, all the triplets are accessible to oxygen when initially formed and unless the triplet population is being constantly replaced or is larger than the oxygen concentration, nearly all the triplets will be quenched before there is an appreciable singlet oxygen concentration. If the triplet population is too high, triplet-triplet annihilation will become important. If photostationary conditions are used, the prompt fluorescence will interfere with the observations.

## **BIBLIOGRAPHY**

## BIBLIOGRAPHY

1. G. Herzberg, "Spectra of Diatomic Molecules", Van Nostrand, New York, 1950.
2. J. Slater, "Quantum Theory of Molecules and Solids. I. Electronic Structure of Molecules", McGraw-Hill Book Co., New York, 1963, cf. Appendix 11, p 294 ff.
3. W. Moffitt, Proc. Roy. Soc., Ser. A, 210, 224 (1951).
4. R. M. Badger, A. C. Wright, and R. F. Whitlock, J. Chem. Phys., 43, 4345 (1965).
5. R. W. Nicholls, Can. J. Chem., 47, 1847 (1969).
6. W. H. J. Childs and R. Mecke, Z. Phys., 68, 344 (1931).
7. D. Q. Wark and D. M. Mercer, Appl. Opt., 4, 839 (1965).
8. L. Wallace and D. M. Hunten, J. Geophys. Res., 73, 4813 (1968).
9. J. W. Ellis and H. O. Kneser, Z. Phys., 86, 583 (1933).
10. A. U. Khan and M. Kasha, J. Am. Chem. Soc., 92, 3293 (1970).
11. H. Salow and W. Steiner, Nature, 134, 463 (1934).
12. H. Salow and W. Steiner, Z. Phys., 99, 137 (1936).
13. V. I. Dianov-Klovov, Opt. Spectros., 16, 409 (1964).
14. C. W. Cho, E. J. Allin, and H. L. Welsh, Can. J. Phys., 41, 1991 (1963).
15. R. P. Blickenderfer and G. E. Ewing, J. Chem. Phys. 51, 5284 (1969).
16. D. F. Evans, Chem. Commun., 367 (1967).
17. I. B. C. Matheson and J. Lee, Chem. Phys. Lett., 8, 173 (1971).
18. A. U. Khan and M. Kasha, J. Am. Chem. Soc., 88, 1574 (1966).
19. S. J. Arnold, E. A. Ogryzlo, and H. Witzke, J. Chem. Phys., 40, 1769 (1964).

20. S. J. Arnold, R. J. Browne, and E. A. Ogryzlo, *Photochem. Photobiol.*, 4, 963 (1965).
21. E. W. Gray and E. A. Ogryzlo, *Chem. Phys. Lett.*, 3, 658 (1969).
22. G. W. Robinson, *J. Chem. Phys.*, 46, 572 (1967).
23. R. P. H. Rettschnick and G. J. Hoytink, *Chem. Phys. Lett.*, 1, 145 (1967).
24. V. G. Krishna, *J. Chem. Phys.*, 50, 792 (1969).
25. V. G. Krishna and T. Cassen, *J. Chem. Phys.*, 51, 2140 (1969).
26. S. C. Tsai and G. W. Robinson, *J. Chem. Phys.*, 51, 3559 (1969).
27. G. L. Zarur and Y. N. Chiu, *J. Chem. Phys.*, 56, 3278 (1972).
28. J. F. Noxon, *J. Chem. Phys.*, 52, 1852 (1970).
29. T. P. J. Izod and R. P. Wayne, *Proc. Roy. Soc., Ser. A*, 308, 81 (1968).
30. F. Stuhl and K. H. Welge, *Can. J. Chem.*, 47, 1870 (1969).
31. I. D. Clark and R. P. Wayne, *Chem. Phys. Lett.*, 3, 405 (1969).
32. S. V. Filseth, A. Zia, and K. H. Welge, *J. Chem. Phys.*, 52, 5502 (1970).
33. F. Stuhl and H. Niki, *Chem. Phys. Lett.*, 7, 473 (1970).
34. C. K. Duncan and D. R. Kearns, *Chem. Phys. Lett.*, 12, 306 (1971).
35. J. G. Parker and D. N. Ritke, *J. Chem. Phys.*, 59, 3713 (1973).
36. A. Farmilo and F. Wilkinson, *Photochem. Photobiol.*, 18, 447 (1973).
37. P. B. Merkel, R. N. Nilsson, and D. R. Kearns, *J. Am. Chem. Soc.*, 94, 1030 (1972).
38. P. B. Merkel and D. R. Kearns, *J. Am. Chem. Soc.*, 94, 7244 (1972).
39. J. G. Parker and D. N. Ritke, *J. Chem. Phys.*, 61, 3408 (1974).
40. J. G. Parker, *J. Chem. Phys.*, 62, 2235 (1975).
41. C. S. Foote and R. W. Denny, *J. Am. Chem. Soc.*, 90, 6233 (1968).

42. P. B. Merkel and D. R. Kearns, Chem. Phys. Lett., 12, 120 (1971).
43. D. R. Adams and F. Wilkinson, J. Chem. Soc., Faraday Trans. II, 4, 586 (1972).
44. I. B. C. Matheson and J. Lee, Chem. Phys. Lett., 14, 350 (1972).
45. R. H. Young, D. Brewer, and R. A. Keller, J. Am. Chem. Soc., 95, 375 (1973).
46. P. B. Merkel and D. R. Kearns, J. Am. Chem. Soc., 94, 1029 (1972).
47. C. S. Foote, E. R. Peterson, and K. W. Lee, J. Am. Chem. Soc., 94, 1032 (1972).
48. T. Kajiwarra and D. R. Kearns, J. Am. Chem. Soc., 95, 5886 (1973).
49. I. B. C. Matheson, R. D. Etheridge, N. R. Kratowich, and J. Lee, Photochem. Photobiol., 21, 165 (1975).
50. I. B. C. Matheson, J. Lee, B. S. Yamanashi, and M. L. Wolbarsht, J. Am. Chem. Soc., 96, 3343 (1974).
51. R. H. Young and R. L. Martin, J. Am. Chem. Soc., 94, 5183 (1972).
52. W. F. Smith, Jr., J. Am. Chem. Soc., 94, 186 (1972).
53. W. F. Smith, Jr., W. G. Herkstroeter, and K. L. Eddy, J. Am. Chem. Soc., 97, 2764 (1975).
54. D. J. Carlsson, G. D. Mendenhall, T. Suprunchuk, D. M. Wiles, J. Am. Chem. Soc., 94, 8960 (1972).
55. S. Mazur and C. S. Foote, J. Am. Chem. Soc., 92, 3225 (1970).
56. C. S. Foote, R. W. Denny, L. Weaver, Y. Chang, and J. Peters, Ann. N. Y. Acad. Sci., 171, 139 (1970).
57. C. S. Foote, Y. C. Chang, and R. Denny, J. Am. Chem. Soc., 92, 5216, 5218 (1970).
58. D. F. Evans, Chem. Commun., 367 (1969).
59. I. B. C. Matheson and J. Lee, Chem. Phys. Lett., 7, 475 (1970).
60. H. Kautsky, Trans. Faraday Soc., 35, 216 (1939).

61. K. Kowaoka, A. U. Khan, and D. R. Kearns, J. Chem. Phys., 46, 1842 (1967).
62. D. R. Snelling, Chem. Phys. Lett., 2, 346 (1968).
63. D. R. Kearns, A. U. Khan, C. K. Duncan, and A. H. Maki, J. Am. Chem. Soc., 91, 1039 (1969).
64. E. Wasserman, V. J. Kuck, W. M. Delevan, and W. A. Yager, J. Am. Chem. Soc., 91, 1040 (1969).
65. B. Stevens and J. A. Ors, Michael Kasha Symposium on Energy Transfer, Florida State University, Jan. 8-10, 1976, Abs. p 10.
66. I. T. N. Jones and K. D. Bayes, Chem. Phys. Lett., 11, 163 (1971).
67. T. Frankiewicz and R. S. Berry, Envir. Sci. Tech., 6, 365 (1972).
68. T. P. J. Izod and R. P. Wayne, Nature, 217, 947 (1968).
69. J. F. Noxon, Can. J. Phys., 39, 1110 (1961).
70. K. Furukawa, E. W. Gray, and E. A. Ogryzlo, Ann. N. Y. Acad. Sci., 171, 175 (1970).
71. A. U. Khan and M. Kasha, J. Chem. Phys., 39, 2105 (1963); 40, 605 (1964).
72. A. U. Khan and M. Kasha, Nature, 204, 241 (1964).
73. R. W. Murry and M. L. Kaplan, J. Am. Chem. Soc., 90, 537 (1968).
74. R. W. Murry and M. L. Kaplan, J. Am. Chem. Soc., 91, 4160 (1969).
75. E. Wasserman, R. W. Murry, M. L. Kaplan, and W. A. Yager, J. Am. Chem. Soc., 90, 4160 (1968).
76. W. Bergmann and M. J. McLean, Chem. Rev., 28, 367 (1941).
77. H. H. Wasserman and J. R. Scheffer, J. Am. Chem. Soc., 89, 3073 (1967).
78. A. U. Khan, Science, 168, 476 (1970).
79. E. A. Mayeda and A. J. Bard, J. Am. Chem. Soc., 95, 6223 (1973).

80. J. W. Peters, J. N. Pitts, Jr., I. Rosenthal, and H. Fuhr, *J. Am. Chem. Soc.*, 94, 4348 (1972).
81. J. W. Peters, P. J. Bekowies, A. M. Winer, and J. N. Pitts, Jr., *J. Am. Chem. Soc.*, 97, 3299 (1975).
82. R. P. Steer, K. R. Darnell, and J. N. Pitts, Jr., *Tetrahedron Lett.*, 3765 (1969).
83. T. C. Pederson and S. D. Aust, *Biochem. Biophys. Res. Comm.*, 52, 1071 (1973).
84. K. Goda, J. Chu, T. Kemura, and A. P. Schaap, *Biochem. Biophys. Res. Comm.*, 52, 1300 (1973).
85. O. F. Oliveier, D. L. Sanieto, and C. Cilento, *Biochem. Biophys. Res. Comm.*, 58, 391 (1974).
86. S. H. Whitlow and D. F. Findley, *Can. J. Chem.*, 45, 2087 (1967).
87. S. Ness and D. M. Hercules, *Anal. Chem.*, 41, 1467 (1969).
88. A. M. Falick, B. H. Mahan, and R. J. Myers, *J. Chem. Phys.*, 42, 1837 (1965).
89. A. M. Falick and B. H. Mahan, *J. Chem. Phys.*, 47, 4778 (1967).
90. R. L. Brown, *J. Phys. Chem.*, 71, 2492 (1967).
91. S. N. Foner and R. L. Hudson, *J. Chem. Phys.*, 25, 601 (1956).
92. J. T. Herron and H. I. Schiff, *Can. J. Chem.*, 36, 1159 (1958).
93. R. B. Cairns and J. A. R. Samson, *Phys. Rev.*, 139, A1403 (1965).
94. I. D. Clark and R. P. Wayne, *Mol. Phys.*, 18, 523 (1970).
95. R. J. McNeal and G. R. Cook, *J. Chem. Phys.*, 47, 5385 (1967).
96. S. J. Arnold, Ph.D. Thesis, University of British Columbia, 1966.
97. L. W. Bader and E. A. Ogryzlo, *Discuss. Faraday Soc.*, 37, 46 (1964).
98. C. S. Foote and S. Wexler, *J. Am. Chem. Soc.*, 86, 3879 (1964).
99. C. S. Foote, *Science*, 162, 963 (1968).
100. P. D. Bartlett, G. D. Mendenhall, and A. P. Schaap, *Ann. N. Y. Acad. Sci.*, 171, 79 (1970).



101. J. R. Platt, J. Chem. Phys., 17, 484 (1949).
102. M. Kasha, Radiation Res. Suppl. 2, 243 (1960).
103. M. Kasha, Proc. International Conf. on Lumin., 166 (1966).
104. J. N. Murrell and J. A. Pople, Proc. Phys. Soc. A, 69, 245 (1956).
105. B. Stevens and E. Hutton, Nature, 186, 1045 (1960).
106. J. B. Birks, in "The Exciplex", (M. Gordon and W. R. Ware, ed.), Academic Press, New York, 1975, p 39.
107. C. A. Parker, Adv. Photochem., Vol. 2 (W. A. Noyes, G. S. Hammond, and J. N. Pitts, ed.), Interscience, New York, 1964.
108. C. A. Parker and C. G. Hatchard, Proc. Chem. Soc., 147 (1962); Proc. Roy. Soc. A, 269, 574 (1962).
109. H. Tsubomura and R. S. Mulliken, J. Am. Chem. Soc., 82, 5966 (1960).
110. A. U. Munck and J. R. Scott, Nature, 177, 587 (1956).
111. D. F. Evans, J. Chem. Soc., 1351 (1957); J. Chem. Soc., 3885 (1957); J. Chem. Soc., 1987 (1961).
112. G. J. Hoijtink, Mol. Phys., 3, 67 (1960).
113. J. N. Murrell, Mol. Phys., 3, 319 (1960).
114. C. Dijkgraaf, R. Sitters, and G. J. Hoytink, Mol. Phys., 5, 643 (1962).
115. D. F. Evans, "Optische Anregung Organischer Systeme", Verlag Chemie, Berlin, 1966, p 586.
116. D. F. Evans and J. N. Tucker, J. Chem. Soc., Faraday Trans. II, 68, 174 (1972).
117. E. A. Ogryzlo and A. E. Pearson, J. Phys. Chem., 72, 2913 (1968).
118. T. Wilson, J. Am. Chem. Soc., 91, 2387 (1969).
119. R. D. Kenner and A. U. Khan, J. Chem. Phys., 64, 1877 (1976).
120. R. D. Kenner and A. U. Khan, Chem. Phys. Lett., 36, 643 (1975).

121. E. Graviola and P. Pringsheim, *Z. Phys.*, 24, 24 (1924).
122. C. A. Parker and W. T. Rees, *Analyst*, 87, 83 (1962).
123. T. Forster, *Ann. Phys.*, 2, 55 (1948).
124. D. L. Dexter, *J. Chem. Phys.*, 21, 836 (1953).
125. G. J. Hoytink, *Accounts Chem. Res.*, 2, 114 (1969).
126. D. L. Dexter, *Phys. Rev.*, 126, 1962 (1962).
127. J. P. Colpa and J. A. A. Ketelaar, *Mol. Phys.* 1, 14 (1958).
128. I. J. Fahrenfort and J. A. A. Ketelaar, *J. Chem. Phys.*, 22, 1631 (1954).
129. J. A. A. Ketelaar and F. N. Hooge, *J. Chem. Phys.*, 23, 749 (1955).
130. H. P. Gush, W. F. J. Ware, E. J. Allin, and H. L. Welsh, *Phys. Rev.*, 106, 1101 (1957).
131. F. Varsanyi and G. H. Dieke, *Phys. Rev. Lett.*, 7, 442 (1961).
132. J. M. Marrs and M. Kasha, *Chem. Phys. Lett.*, 6, 235 (1970).
133. E. Nakazawa and S. Shionoga, *Phys. Rev. Lett.*, 25, 1710 (1970).
134. W. E. Graves, R. H. Hofeldt, and S. P. McGlynn, *J. Chem. Phys.*, 56, 1309 (1972).
135. G. Oster, N. Geacintov, and A. U. Khan, *Nature*, 196, 1089 (1962).
136. G. Oster, N. Geacintov, and T. Cassen, *Acta. Phys. Popon.*, 26, 489 (1964).
137. S. K. Lower and M. A. El-Sayed, *Chem. Rev.*, 66, 199 (1966).
138. N. Geacintov, G. Oster, and T. Cassen, *J. Am. Opt. Soc.*, 58, 1217 (1968).
139. N. E. Geacintov and C. E. Swenberg, *J. Chem. Phys.*, 57, 378 (1972).
140. R. Benson and N. E. Geacintov, *J. Chem. Phys.*, 60, 3251 (1974).
141. P. F. Jones and A. R. Calloway, *J. Chem. Phys.*, 51, 1661 (1969).

142. J. L. Kropp and W. R. Dawson, in "Molecular Luminescence", (E. C. Lim, ed.), Benjamin, New York, 1969, p 39.
143. P. F. Jones and S. Siegel, J. Chem. Phys., 50, 1134 (1969).
144. S. Rodriguez and H. Offen, J. Chem. Phys., 52, 586 (1970).
145. H. W. Offen, J. Chem. Phys., 42, 2523 (1965).
146. H. W. Offen and B. A. Baldwin, J. Chem. Phys., 44, 3642 (1966).
147. F. B. Bramwell and M. E. Laterza, J. Chem. Phys., 60, 4265 (1974).
148. P. Avis and G. Porter, J. Chem. Soc., Faraday Trans. II, 70, 1057 (1974).
149. P. C. Johnson and H. W. Offen, J. Chem. Phys., 55, 2945 (1971).
150. H. W. Offen and R. R. Eliason, J. Chem. Phys., 43, 4096 (1965).
151. R. G. Bennett, J. Chem. Phys., 41, 3047 (1964).
152. R. G. Bennett, R. P. Schwenker, and R. E. Kellogg, J. Chem. Phys., 41, 3040 (1964).
153. R. E. Kellogg and R. G. Bennett, J. Chem. Phys., 41, 3042 (1964).
154. R. E. Kellogg, J. Chem. Phys., 41, 3046 (1964).
155. R. G. Bennett, J. Chem. Phys., 41, 3048 (1964).
156. N. Mataga, H. Obashi, and T. Okada, J. Phys. Chem., 73, 370 (1969).
157. N. J. Turro and H. C. Steinmetzer, J. Am. Chem. Soc., 96, 4677 (1974).
158. E. I. Hormats and F. C. Unterleitner, J. Phys. Chem., 69, 3677 (1965).
159. G. W. Cowell and J. N. Pitts, Jr., J. Am. Chem. Soc., 90, 1106 (1968).
160. A. P. Schaap, A. L. Thayer, E. C. Blossey, and D. C. Neckers, J. Am. Chem. Soc., 97, 3741 (1975).
161. S. A. Dolm, H. A. Kruegl, and C. J. Penzia, Appl. Opt., 6, 276 (1967).

162. B. R. Henry and M. Kasha, J. Mol. Spec., 26, 536 (1968).
163. P. H. Bolton, R. D. Kenner, and A. U. Khan, J. Chem. Phys., 57, 5604 (1972).
164. P. F. Jones and R. S. Nesbitt, J. Chem. Phys. 59, 6185 (1973).
165. D. P. Craig and I. G. Ross, J. Chem. Soc., 1589 (1954).
166. D. S. McClure, J. Chem. Phys., 19, 670 (1951).
167. R. A. Keller and S. G. Hadley, J. Chem. Phys., 42, 2382 (1965).
168. G. N. Lewis and M. J. Calvin, J. Am. Chem. Soc., 67, 1232 (1945).
169. G. N. Lewis, M. Calvin and M. Kasha, J. Chem. Phys., 17, 804 (1949).
170. J. S. Brinen and W. G. Hodgson, J. Chem. Phys., 47, 2946 (1969).
171. J. S. Brinen, J. Chem. Phys., 49, 586 (1968).
172. M. Kinoshita, B. N. Srinivasan, and S. P. McGlynn, J. Mol. Spec., 18, 606 (1965).
173. M. Kasha, J. Opt. Soc. Am., 38, 929 (1948).
174. J. S. Brinen, in "Molecular luminescence", (E. C. Lim, ed.), Benjamin, New York, 1969, p 333.
175. E. Clar, "Polycyclic Hydrocarbons", Academic Press, New York, 1964, p 250, 331.
176. M. W. Windsor and J. R. Novak, in "Molecular Luminescence", (E. C. Lim, ed.), Benjamin, New York, 1969, p 365.
177. G. Weber and F. W. J. Teale, Trans. Faraday Soc., 53, 646 (1957).
178. H. Labhart, Helv. Chim. Acta, 47, 2279 (1964).
179. S. D. Babenko, V. A. Benderskii, V. I. Gol'Danskii, A. G. Lavrushko, and V. P. Tychinskii, Chem. Phys. Lett., 8, 598 (1971).
180. V. M. Agranovitch, B. I. Doronina, and Y. V. Konobeev, Soviet Phys. Solid State, 11, 2103 (1970).

181. N. Nakashima, Y. Kume, and N. Mataga, J. Phys. Chem., 79, 1788 (1975).
182. W. Heinzelman and H. Labhart, Chem. Phys. Lett., 4, 20 (1969).
183. K. A. Hodgkinson and I. H. Munro, Chem. Phys. Lett., 12, 281 (1971).
184. J. Greyson, R. B. Ingalls, and R. T. Keen, J. Chem. Phys., 45, 3755 (1966).
185. W. R. Sorsenson and T. W. Campbell, "Preparative Methods of Polymer Chemistry", Interscience, New York, 1968, p 218.
186. H. Kautsky and G. Muller, Z. Naturforsch A 2, 167 (1947).
187. J. L. Rosenberg and D. J. Shombert, J. Am. Chem. Soc., 82, 3252 (1960).
188. J. L. Rosenberg and F. S. Humphries, Photochem. Photobiol., 4, 1185 (1965).
189. J. L. Rosenberg and F. S. Humphries, J. Phys. Chem., 71, 330 (1967).
190. E. Caralieri and M. Calvin, Photochem. Photobiol., 14, 641 (1971).
191. E. Clar, "Polycyclic Hydrocarbons, Vol. I", Academic Press, New York, 1964, p 249.
192. G. Porter and F. Wilkinson, Proc. Roy. Soc. (London), A 264, 1 (1961).
193. E. W. Schlag, S. Schneider and S. Fischer, Ann. Rev. Phys. Chem., 22, 465 (1971).
194. O. L. J. Gijzeman, J. Langelaar, and J. D. W. van Voorst, Chem. Phys. Lett., 5, 269 (1970); 11, 526 (1971).
195. O. L. Gijzeman, W. H. van Leeuwen, J. Langelaar, and J. D. W. van Voorst, Chem. Phys. Lett., 11, 528 (1971); 11, 532 (1971).
196. M. A. Slifkin and A. O. Al-Chalabi, Chem. Phys. Lett., 29, 110 (1974).
197. V. L. Levshin, Z. Physik, 72, 368, 382 (1931).
198. H. M. Rosenberg and S. D. Carson, J. Phys. Chem., 72, 3531 (1968).

199. T. Ishiwata, H. Akimoto, and I. Tanaka, VIII International Conference on Photochemistry, Edmonton, Canada, August, 1975, Abstracts p V-11.
200. P. J. Giachardi, G. W. Harris, and R. P. Wayne, *ibid*, p F-11.
201. O. L. J. Gijzeman, J. Chem. Soc., Faraday Trans. II, 70, 1143 (1974).
202. G. W. Robinson and R. P. Frosch, J. Chem. Phys., 37, 1962 (1962).
203. G. W. Robinson and R. P. Frosch, J. Chem. Phys., 38, 1187 (1963).
204. C. A. Coulson and A. Streitwieser, "Dictionary of  $\pi$ -Electron Calculations", Freeman and Co., San Francisco, 1965.
205. J. B. Birks, E. Pantos, and T. D. S. Hamilton, Chem. Phys. Lett., 20, 544 (1973).
206. S. Fischer, J. Chem. Phys., 53, 3195 (1970).
207. W. Siebrand and D. F. Williams, J. Chem. Phys., 46, 403 (1967).
208. W. A. Noyes, Jr., G. B. Porter, and J. E. Jolley, Chem. Rev., 56, 49 (1956).
209. N. Padnos and W. A. Noyes, Jr., J. Phys. Chem., 68, 464 (1964).
210. C. S. Parmenter and H. M. Poland, J. Chem. Phys., 51, 1551 (1969).
211. H. W. Sidebottom, C. C. Badcock, J. G. Calvert, B. R. Rabe, and E. K. Damon, J. Am. Chem. Soc., 94, 13 (1972).
212. C. C. Badcock, H. W. Sidebottom, J. G. Calvert, B. R. Rabe, and E. K. Damon, J. Am. Chem. Soc., 94, 19 (1972).
213. J. G. Calvert and J. N. Pitts, Jr., "Photochemistry", John Wiley and Sons, Inc., New York, 1967, p 422.
214. W. R. Ware, in "Creation and Detection of the Excited State", A. A. Lamola, ed., Vol. 1A, Dekker, New York, 1971.
215. P. Pringsheim, "Fluorescence and Phosphorescence", Interscience, New York, N. Y., 1949.
216. C. Reid, "Excited States in Chemistry and Biology", Butterworth, London, 1957.

217. J. B. Birks, "Photophysics of Aromatic Molecules", Wiley-Interscience, London, 1970.
218. J. N. Murrell, "The Theory of the Electronic Spectra of Organic Molecules", Methuen, New York, 1963.
219. S. P. McGlynn, T. Azumi, and M. Kinoshita, "Molecular Spectroscopy of the Triplet State", Prentice-Hall, Englewood Cliff, N. J., 1969.
220. I. B. Berlman, "Handbook of Fluorescence Spectra of Aromatic Molecules", Academic Press, New York, 1965.
221. I. B. Berlman, "Energy Transfer Parameters of Aromatic Compounds", Academic Press, New York, 1973.
222. C. A. Parker, "Photoluminescence of Solutions", Elsevier Publishing Co., Amsterdam, 1968.
223. "Creation and Detection of the Excited State", A. A. Lamola, ed., Dekker, New York, 1971.
224. "Molecular Luminescence", E. C. Lim, ed., Benjamin, New York, 1969.
225. "The Exciplex", M. Gordon and W. R. Ware, ed., Academic Press, New York, 1975.
226. "Organic Molecular Photophysics", J. B. Birks, ed., Wiley-Interscience, New York, 1973.
227. C. S. Foote, Accounts Chem. Res., 1, 104 (1968).
228. K. Gollnick, Advan. Photochem., 6, 1 (1968).
229. S. J. Arnold, M. Kubo, and E. A. Ogryzlo, Advan. Chem. Ser., 77, 133 (1968).
230. R. P. Wayne, Advan. Photochem., 7, 311 (1969).
231. M. Kasha and A. U. Khan, Ann. N. Y. Acad. Sci., 171, 5 (1970).
232. D. R. Kearns, Chem. Rev., 71, 395 (1971).
233. A. U. Khan, Michael Kasha Symposium on Energy Transfer, Florida State University, Jan. 8-10, 1976.
234. Th. Forster, Disc. Faraday Soc., 27, 7 (1959).
235. G. Porter and F. Wilkinson, Proc. Roy. Soc. (London), Ser. A, 264, 1 (1961).

236. A. A. Lamola in "Energy Transfer and Organic Photochemistry, Vol. XIV, Techniques of Organic Chemistry", (A Weissberger, ed.), p 17, Wiley, New York, 1969.



MICHIGAN STATE UNIVERSITY LIBRARIES



3 1293 03071 3824